Supporting Materials

A New Amino Acid for Improving Permeability and Solubility in Macrocyclic Peptides through Side Chain-to-Backbone Hydrogen Bonding

Jaru Taechalertpaisarn[†], Satoshi Ono[‡], Okimasa Okada[‡], Timothy C. Johnstone[†], R. Scott Lokey[*,†]

[†]Department of Chemistry and Biochemistry, University of California, Santa Cruz, 1156 High Street, Santa Cruz, California 95064, United States

[‡]Modality Laboratories, Innovative Research Division, Mitsubishi Tanabe Pharma Corporation, 1000 Kamoshida-cho, Aoba-ku, Yokohama, Kanagawa 227-0033, Japan

*Correspondence to slokey@ucsc.edu

Table of Contents

Syntheses of Model Structures 4

a

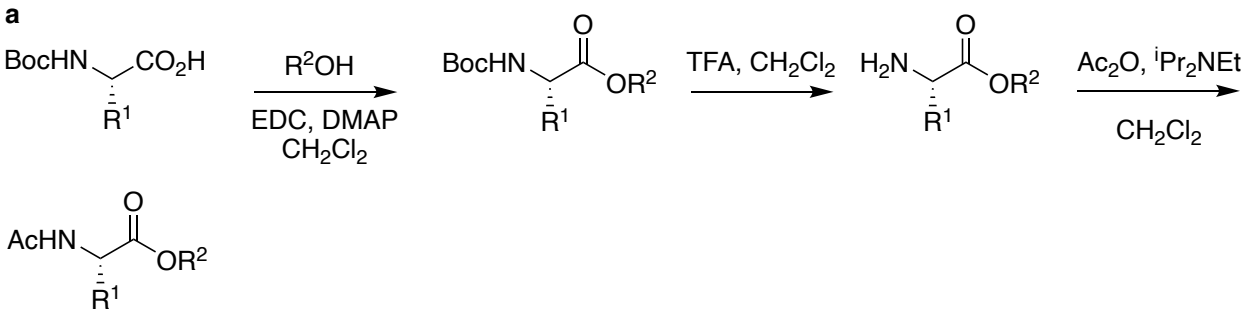

b

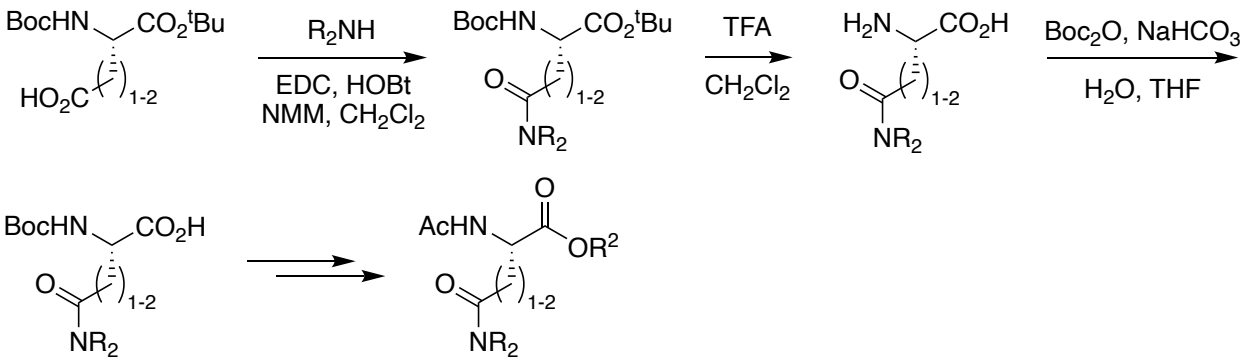

Scheme S1. Syntheses of model structures **4** with (**a**) accessible amino acids (R^1 = Me, -$CH(CH_3)_2$, -$CH_2CH(CH_3)_2$, -$CH(CH_3)CH_2CH_3$, -$CH_2CH_2CONH_2$, -$CH_2CH_2CO_2Me$) and (**b**) substituted amides. R^2OH = 4-phenyl-1-butanol; R_2NH = pyrrolidine or dimethylamine

General Synthesis of Model Compounds (Scheme S1a)

Boc-protected amino acids (1.5 eq), DMAP (1.5 eq) and 4-phenyl-1-butanol (1 eq) were dissolved in CH_2Cl_2 (0.1 M) at 0 ºC. EDC (1.5 eq) was added subsequently, and the reaction was stirred under Ar atmosphere at ambient temperature. Solution was diluted in CH_2Cl_2 and extracted with 10% citric acid (3x), saturated $NaHCO_3$ (3x) and brine. Organic layer was dried over $MgSO_4$ and reduced to obtain the product as an oil, which was used in the next step without further purification.

Boc-AA-OC_4H_8Ph (1 mmol) was dissolved in 3 mL CH_2Cl_2, then 3 mL of TFA was added and the reaction was stirred at room temperature for 3 h. Solution was completely dried, and the crude oil was used in the next step without further purification.

Crude material from previous step (0.5 mmol) was charged with 3 mL dry CH_2Cl_2 under Ar at 0 ºC. $^iPr_2NEt$ (2 eq) was added followed by Ac_2O (2 eq). The reaction was stirred overnight at ambient temperature. Organic solution was extracted with saturated NH_4Cl, $NaHCO_3$ and brine. After reducing the solution, product was purified by short column chromatography (50% EtOAc/hexanes then 5% MeOH/CH_2Cl_2) to obtain final product as oil.

General Synthesis of Substituted-amide Model Compounds (Scheme S1b)

Boc-Asp-O^{t}Bu or Boc-Glu-O^{t}Bu (1 mmol) and HOBt (1.5 eq) were dissolved in 10 mL CH_2Cl_2 at 0 ºC. EDC (1.5 eq) was added in one portion and the reaction was stirred at 0 ºC for 10 minutes followed by *N*-methylmorpholine (NMM, 3 eq) and secondary amine (pyrrolidine or dimethylamine, 1.5 eq). Reaction was allowed to stir at ambient temperature overnight under Ar. Solution was diluted in CH_2Cl_2 and extracted with 10% citric acid (3x), saturated $NaHCO_3$ (3x) and brine. Organic layer was dried over $MgSO_4$ and reduced to obtain product as solid. This solid compound was dissolved in 1:1 CH_2Cl_2/TFA solution to deprotect all acid-labile protecting groups. Once reaction was completed, solution was dried in vacuo, and the crude oil was azeotroped with diethyl ether and dried under vacuum overnight. This unprotected compound was then dissolved in 1:1 H_2O/THF and $NaHCO_3$ (2 eq) was added to the solution. Boc_2O (2 eq) was added, and the reaction was stirred overnight while pH was kept around 8. After reaction was completed, organic solvent was removed in vacuo, and the aqueous solution was extracted with diethyl ether (3x). The aqueous layer was acidified with citric acid until pH ~4 and extracted with EtOAc (5x). Organic layer was combined and reduced to obtain the Boc-protected amide-substituted amino acids. The remaining synthesis was done similar to the general synthesis described for Scheme S1a

General Synthesis of *N*-Fmoc-Amino Acids with Side-Chain Carboxamides.

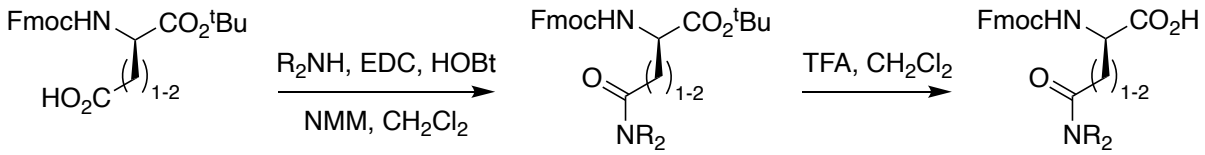

R_2NH = pyrrolidine, dimethylamine

Scheme S2. Synthesis scheme of Fmoc-amino acid building blocks.

A detail synthesis of D-Fmoc-Pye-OH was shown as an example. D-Fmoc-Glu-OtBu (10 g, 23.5 mmol) and hydroxybenzotriazole (HOBt; 4.76 g, 35.3 mmol) were dissolved in 200 mL CH_2Cl_2 at 0 ºC. 1-Ethyl-3-(3-dimethylaminopropyl) carbodiimide (EDC; 6.76 g, 35.3 mmol) was added in one portion, and the reaction was stirred for 10 minutes. *N*-Methylmorpholine (NMM; 7.8 mL, 70.5 mmol) was added followed by pyrrolidine (2.3 mL, 28.2 mmol). The reaction was stirred under argon overnight at the ambient temperature. The solution was extracted 3 times with 10% citric acid, 3 times with saturated sodium bicarbonate solution and brine. The organic layer was dried and reduced. The resulting colorless oil was treated with a solution of 1:1 TFA/CH_2Cl_2 (50 mL) and stirred until the reaction was completed monitored by TLC. The solution was removed under reduced pressure and successively evaporated remaining TFA residue with CH_2Cl_2. Approximately 150 mL of diethyl ether was added to the crude and the solution was stirred vigorously overnight until the white precipitate was formed. The white solid was filtered and rinsed with diethyl ether to obtain the final product, D-Pye, as white solid (8.92 g, 90%)

L-Fmoc-Pye-OH, D-Fmoc-Gln(NMe_2)-OH, D-Fmoc-Asn(Pyr)-OH and D-Fmoc-Asn(NMe_2)-OH were synthesized as described above.

(*R*)-2-((((9*H*-Fluoren-9-yl)methoxy)carbonyl)amino)-5-oxo-5-(pyrrolidin-1-yl)pentanoic acid (D-Fmoc-Pye-OH)

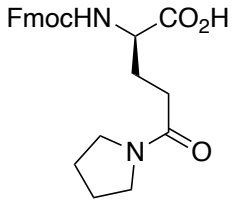

White solid, 90 % yield. ^{1}H NMR (500 MHz, $CDCl_3$) δ 7.77 (d, *J* = 7.5 Hz, 2H), 7.61 (t, *J* = 7.6 Hz, 2H), 7.41 (t, *J* = 7.5 Hz, 2H), 7.32 (t, *J* = 7.5 Hz, 2H), 6.19 (d, *J* = 5.9 Hz, 1H), 4.47 – 4.26 (m, 3H), 4.23 (t, *J* = 7.2 Hz, 1H), 3.58 – 3.35 (m, 4H), 2.86 (m, 1H), 2.53 (m, 1H), 2.36 – 2.23 (m, 1H), 2.10-1.94 (m, 3H), 1.94-1.82 (m, 2H). ^{13}C NMR (126 MHz, $CDCl_3$) δ 172.99, 172.50, 156.12, 143.87, 143.66, 141.28, 141.27, 127.73, 127.08, 127.06, 125.16, 125.08, 119.99, 67.13, 53.81, 47.08, 46.93, 46.31, 32.06, 29.39, 25.87, 24.27. HRMS (ESI) m/z calcd for $C_{24}H_{27}N_2O_5^+$ (M+H$^+$) 423.1914; found 423.1909

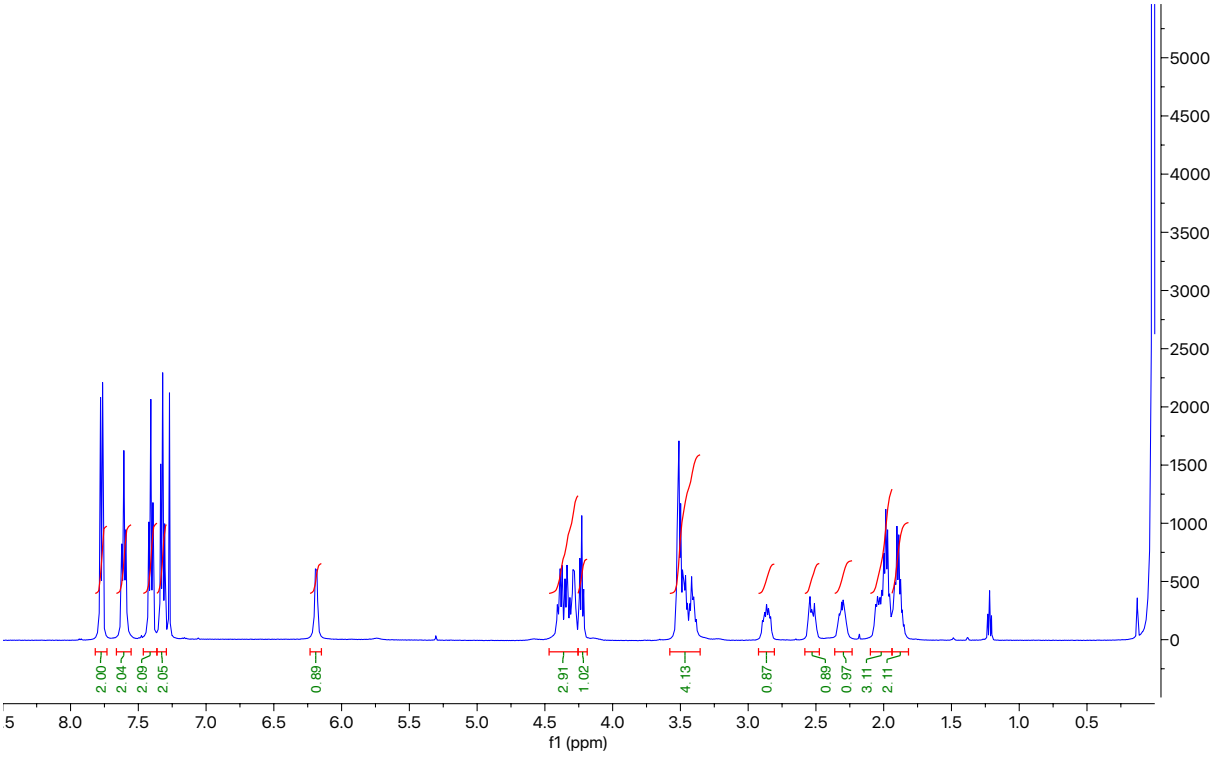

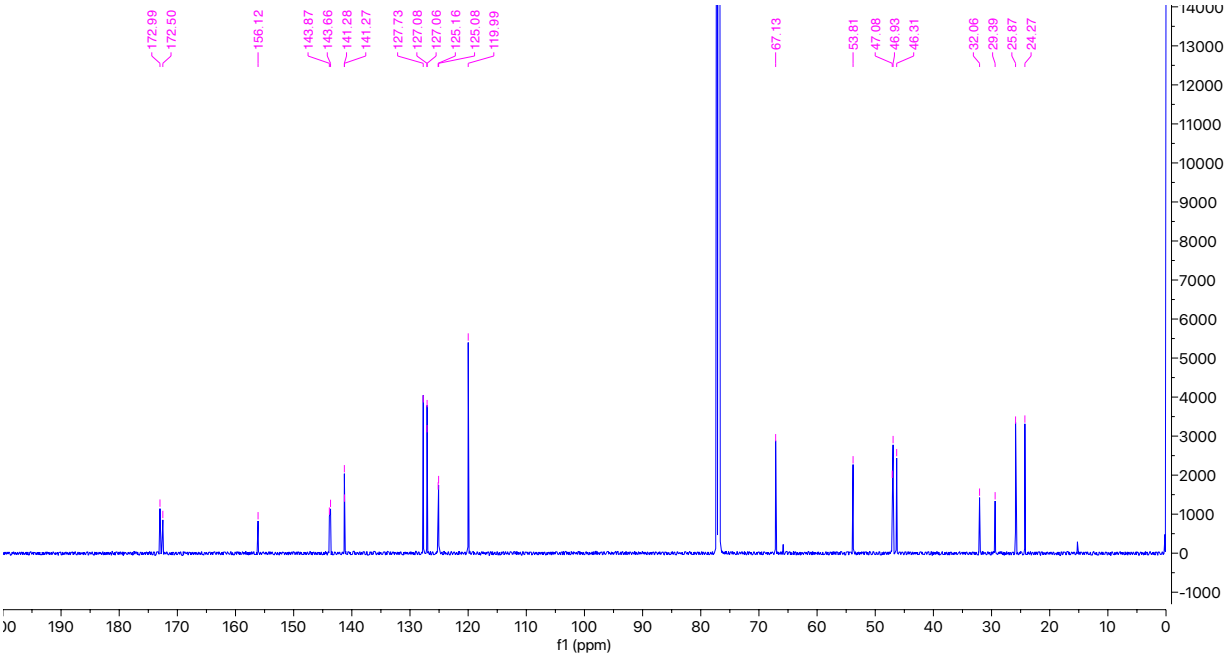

(*S*)-2-((((9*H*-Fluoren-9-yl)methoxy)carbonyl)amino)-5-oxo-5-(pyrrolidin-1-yl)pentanoic acid (L-Fmoc-Pye-OH)

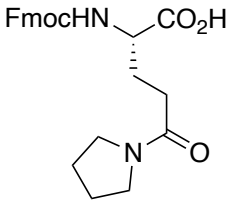

White solid, 88 % yield. ^{1}H NMR (500 MHz, $CDCl_3$) δ 7.76 (d, *J* = 7.6 Hz, 2H), 7.60 (t, *J* = 8.6 Hz, 2H), 7.40 (t, *J* = 7.5 Hz, 2H), 7.31 (t, *J* = 7.5 Hz, 2H), 6.18 (d, *J* = 6.2 Hz, 1H), 4.42-4.36 (m, 1H), 4.36-4.28 (m, 2H), 4.22 (t, *J* = 7.2 Hz, 1H), 3.58 – 3.32 (m, 4H), 2.78 (m, 1H), 2.50 (m, 1H), 2.30 (m, 1H), 2.05 (m, 1H), 1.99-1.91 (m, 2H), 1.88 (m, 2H). ^{13}C NMR (126 MHz, $CDCl_3$) δ 173.20, 172.37, 156.17, 143.86, 143.64, 141.25, 141.24, 127.71, 127.70, 127.06, 127.04, 125.16, 125.07, 119.96, 67.14, 53.74, 47.06, 46.96, 46.31, 31.67, 28.91, 25.84, 24.25. HRMS (ESI) m/z calcd for $C_{24}H_{27}N_2O_5^+$ ($M+H^+$) 423.1914; found 423.1913

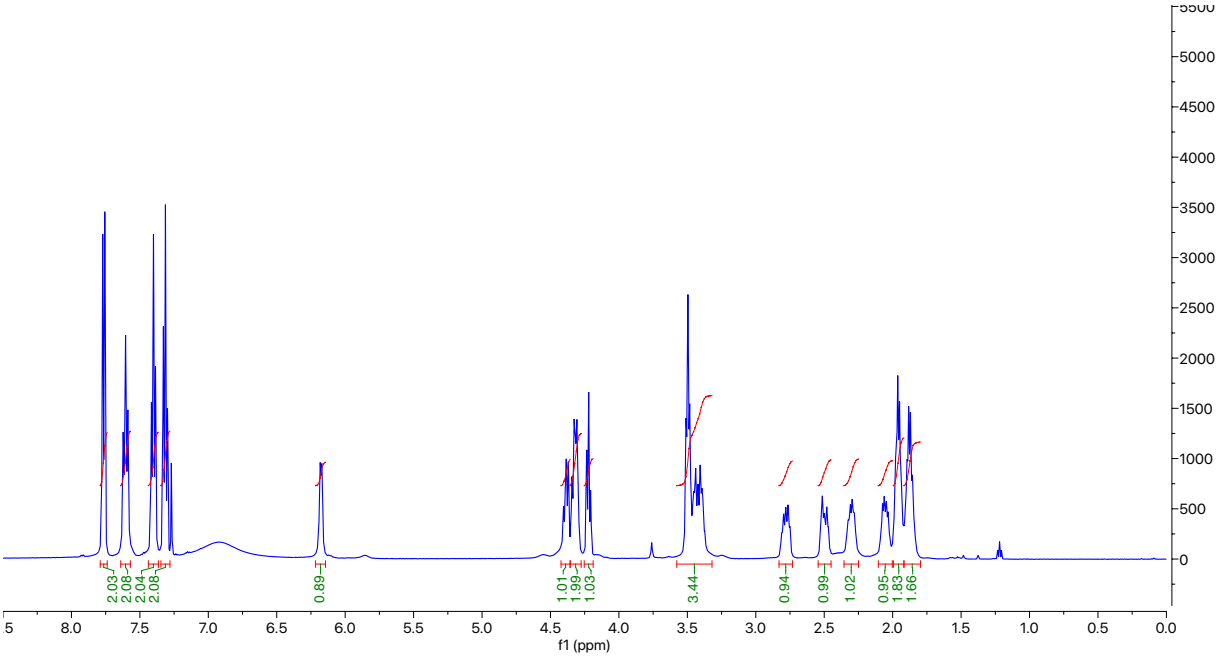

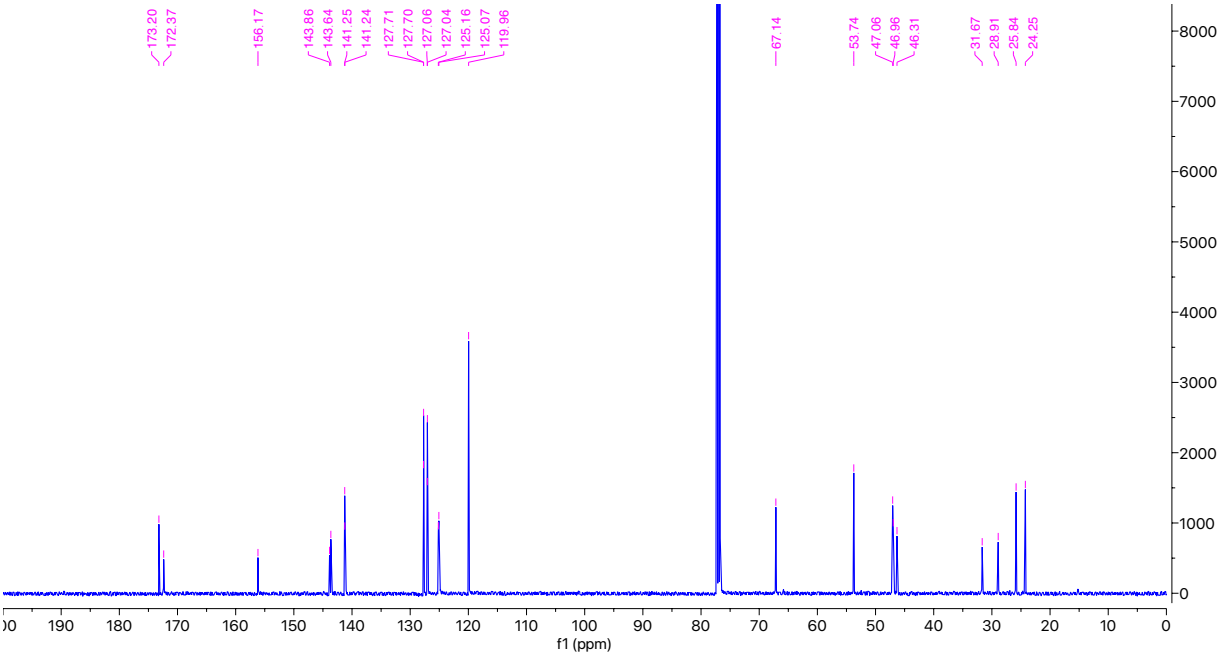

N^{2}-(((9*H*-Fluoren-9-yl)methoxy)carbonyl)-*N*^{5},*N*^{5}-dimethyl-*D*-glutamine {D-Fmoc-Gln(NMe$_2$)-OH}

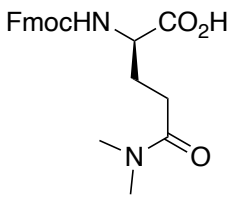

white solid, 85 % yield. ^{1}H NMR (500 MHz, $CDCl_3$) δ 7.77 (d, *J* = 7.3 Hz, 2H), 7.61 (t, *J* = 8.0 Hz, 2H), 7.41 (t, *J* = 7.6 Hz, 2H), 7.32 (t, *J* = 7.7 Hz, 2H), 6.15 (br, 1H), 4.43-4.30 (m, 2H), 4.30-4.25 (m, 1H), 4.22 (t, *J* = 7.4 Hz, 1H), 3.03 (s, 3H), 3.01, (s, 3H), 2.89 (m, 1H), 2.55 (m, 1H), 2.31 (m, 1H), 2.03 (m, 1H). ^{13}C NMR (126 MHz, $CDCl_3$) δ 174.05, 173.08, 156.17, 143.84, 143.64, 141.27, 141.25, 127.71, 127.07, 127.05, 125.14, 125.06, 119.97, 67.11, 53.74, 47.06, 37.49, 35.97, 30.64, 29.31. HRMS (ESI) m/z calcd for $C_{22}H_{25}N_2O_5^+$ ($M+H^+$) 397.1758; found 397.1756

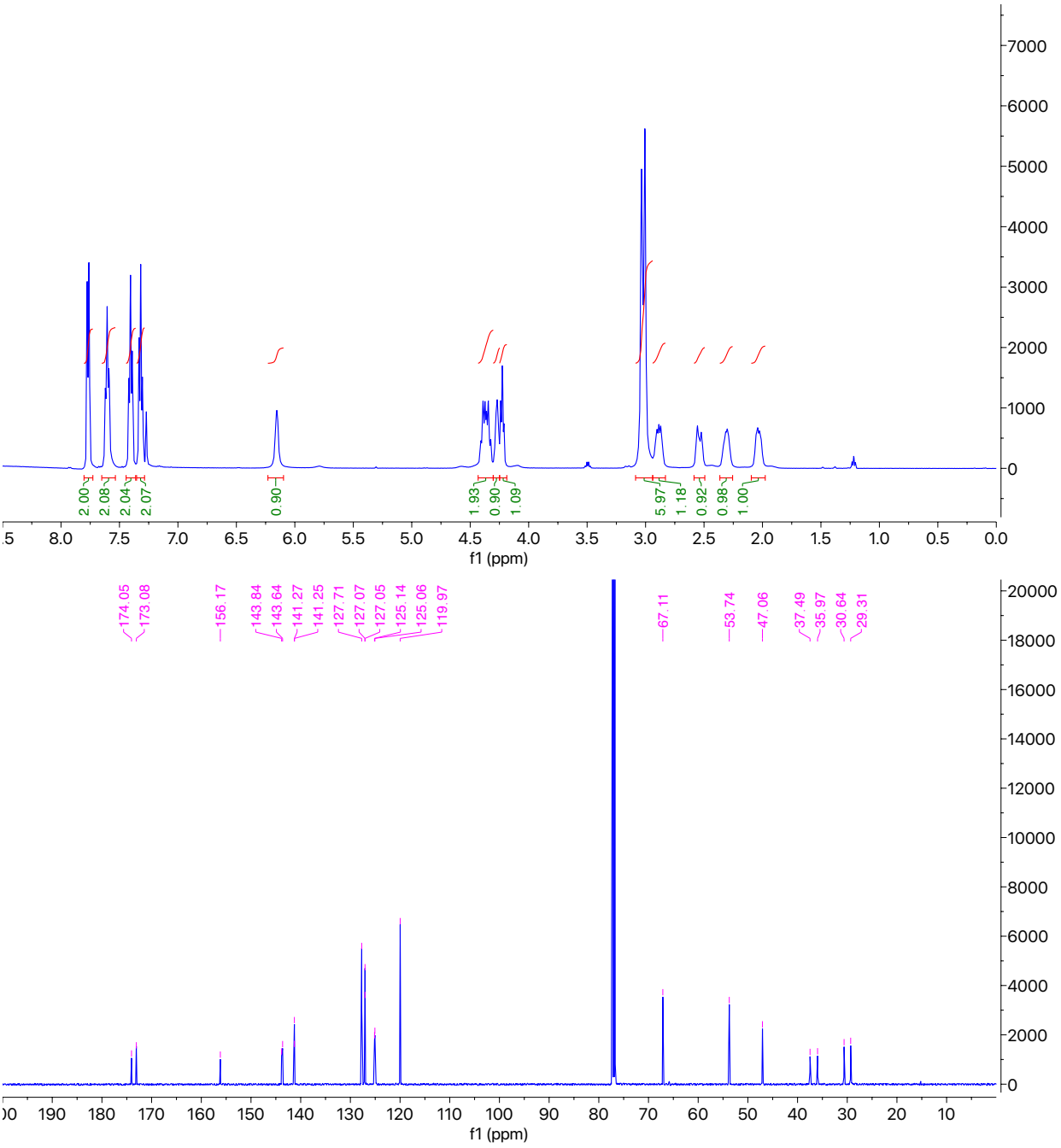

(*R*)-2-((((9*H*-Fluoren-9-yl)methoxy)carbonyl)amino)-4-oxo-4-(pyrrolidin-1-yl)butanoic acid {D-Fmoc-Asn(Pyr)-OH}

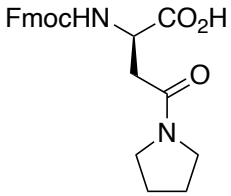

White solid, 84 % yield. ^{1}H NMR (500 MHz, $CDCl_3$) δ 7.77 (d, *J* = 7.6 Hz, 2H), 7.61 (t, *J* = 7.4 Hz, 2H), 7.41 (t, *J* = 7.5 Hz, 2H), 7.33 (t, *J* = 7.5, 2.1 Hz, 2H), 6.16 (br, 1H), 4.58-4.49 (m, 1H), 4.42 (t, *J* = 8.2 Hz, 1H), 4.34 (t, *J* = 8.6 Hz, 1H), 4.23 (t, *J* = 7.5 Hz, 1H), 3.62-3.45 (m, 3H), 3.42 (m, 1H), 3.21 (d, *J* = 16.7 Hz, 1H), 2.68 (dd, *J* = 17.0, 9.6 Hz, 1H), 2.11-1.97 (m, 2H), 1.97-1.87 (m, 2H). ^{13}C NMR (126 MHz, $CDCl_3$) δ 171.81, 170.58, 155.64, 143.81, 143.58, 141.30, 141.27, 127.75, 127.07, 127.05, 125.16, 125.07, 120.01, 67.20, 50.15, 47.38, 47.05, 46.49, 36.66, 25.79, 24.28. HRMS (ESI) m/z calcd for $C_{23}H_{25}N_2O_5^+$ ($M+H^+$) 409.1758; found 409.1755

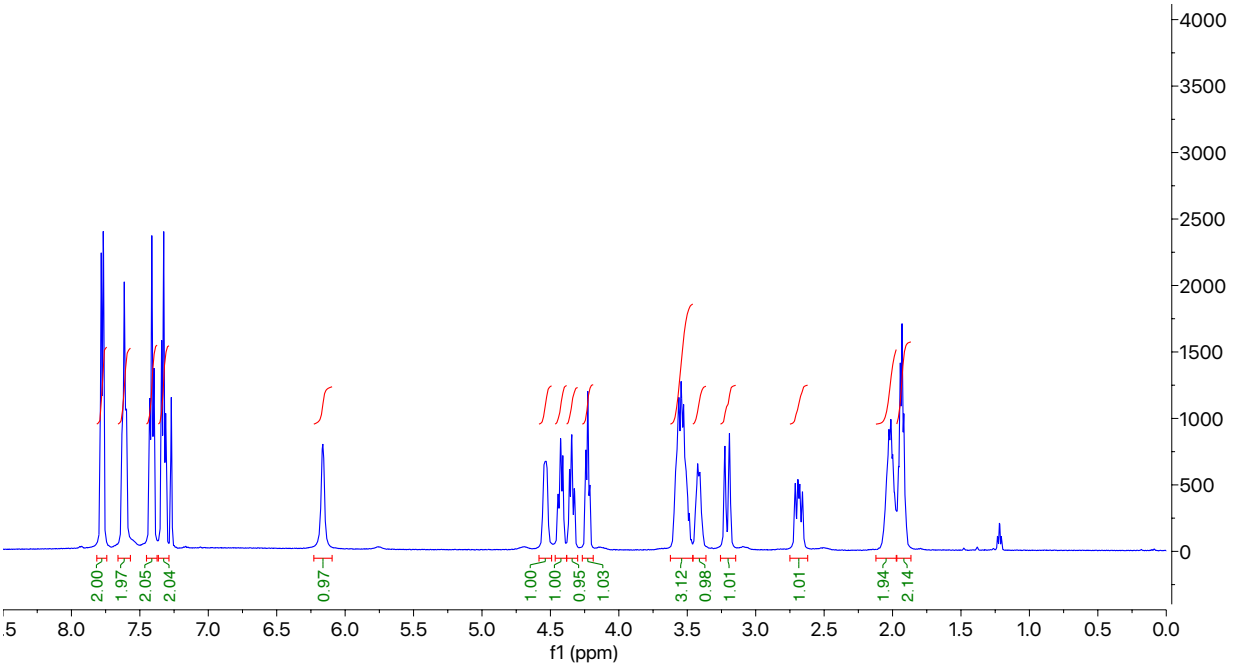

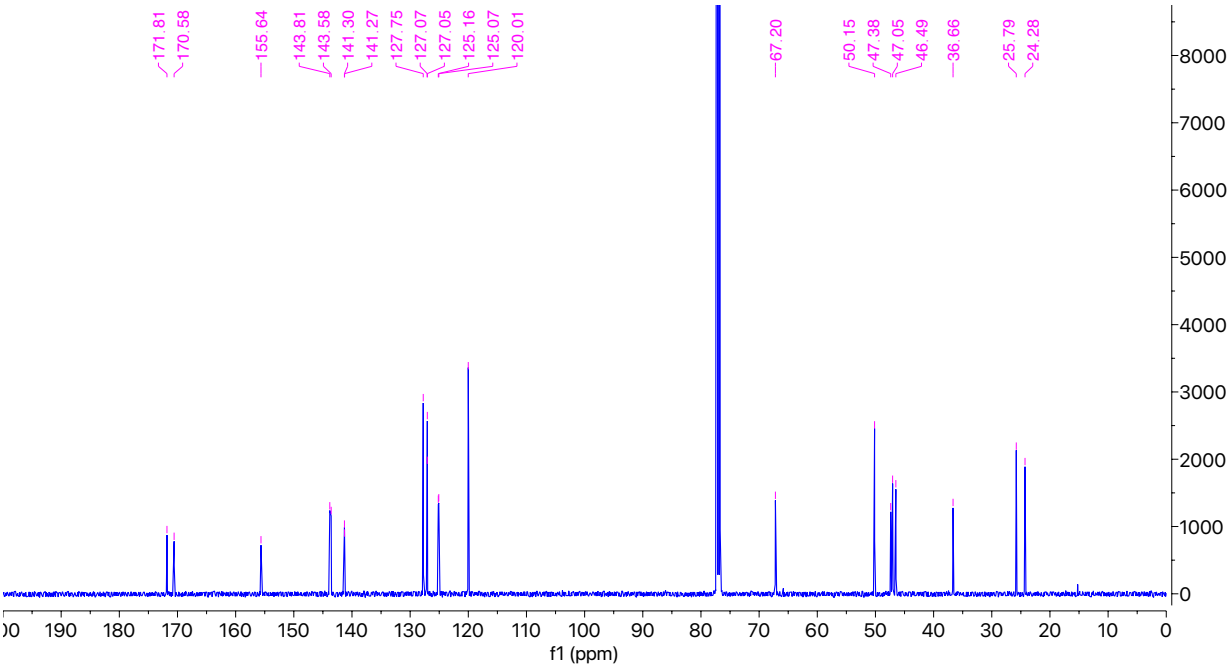

N^2-(((9*H*-Fluoren-9-yl)methoxy)carbonyl)-*N*^{4},*N*^{4}-dimethyl-*D*-asparagine {D-Fmoc-Asn(NMe$_2$)-OH}

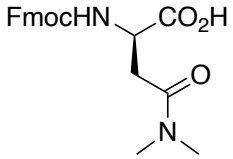

White solid, 79 % yield. ^{1}H NMR (500 MHz, $CDCl_3$) δ 7.77 (d, *J* = 7.2 Hz, 2H), 7.61 (t, *J* = 7.3 Hz, 2H), 7.40 (t, *J* = 7.7 Hz, 2H), 7.32 (t, *J* = 7.6 Hz, 2H), 6.20 (br, 1H), 4.65-4.55 (m, 1H), 4.42 (t, *J* = 8.3 Hz, 1H), 4.34 (t, *J* = 9.4 Hz, 1H), 4.26-4.19 (m, 1H), 3.27 (d, *J* = 16.7 Hz, 1H), 3.05 (s, 3H), 3.02 (s, 3H), 2.74 (dd, *J* = 17.2, 7.7 Hz, 1H). ^{13}C NMR (126 MHz, $CDCl_3$) δ 172.68, 171.88, 155.91, 143.89, 143.67, 141.32, 141.29, 127.76, 127.11, 127.09, 125.24, 125.16, 120.01, 67.26, 50.35, 47.10, 37.68, 35.97, 35.85. HRMS (ESI) m/z calcd for $C_{21}H_{23}N_2O_5^+$ (M+H$^+$) 383.1601; found 383.1600

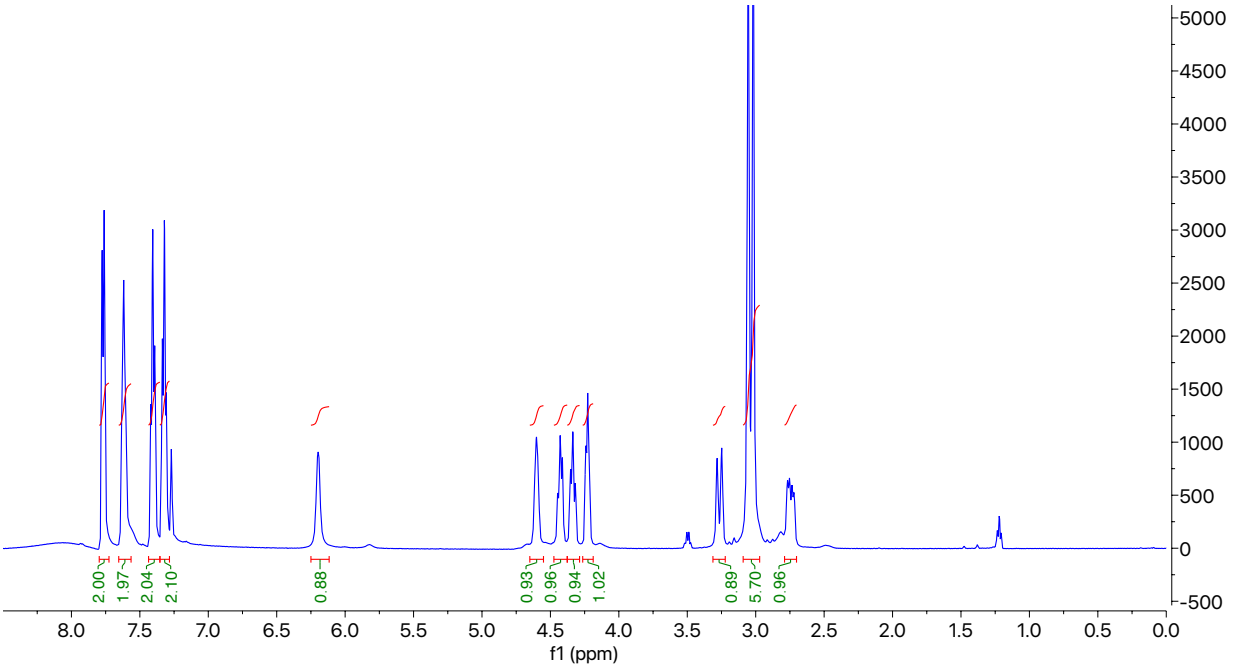

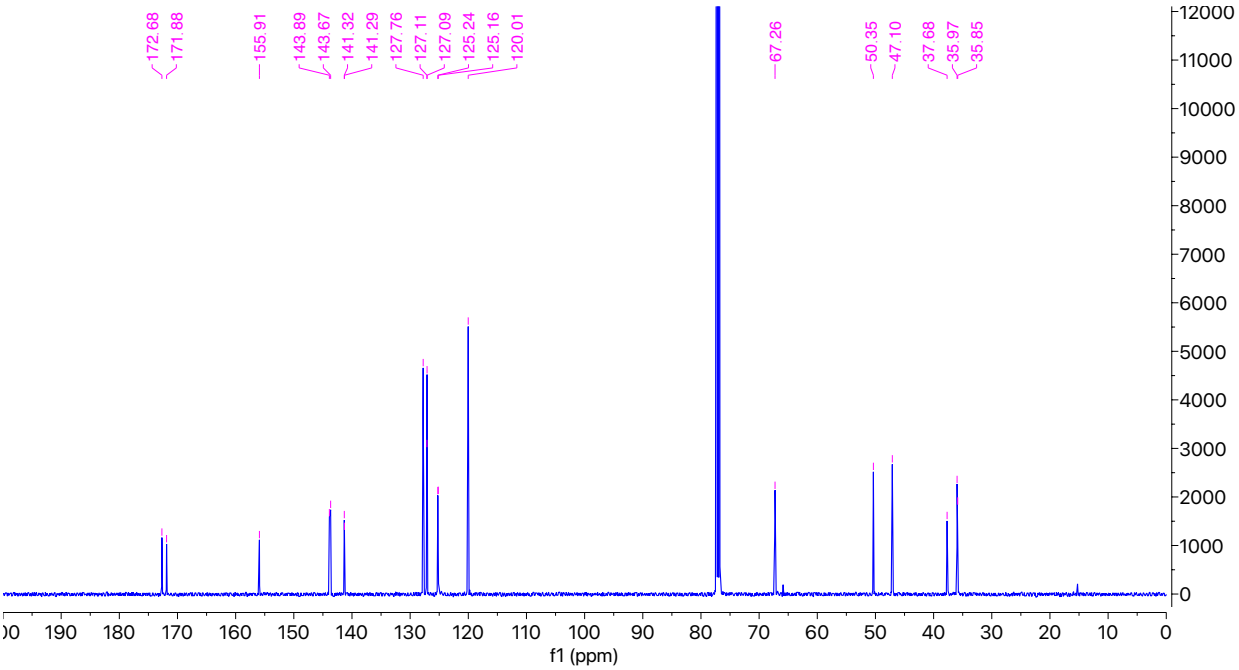

Synthesis of 3-Amino-1-(pyrrolidin-1-yl)propan-1-one

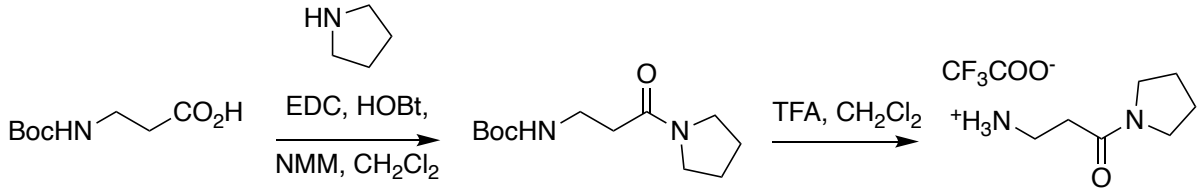

3-((tert-Butoxycarbonyl)amino)propanoic acid (3 mmol), HOBt (4.5 mmol) were dissolved in 30 mL CH_2Cl_2 at 0 ºC. EDC (4.5 mmol) was added and the reaction was stirred for 30 min at 0 ºC. NMM (9 mmol) and pyrrolidine (3.6 mmol) were added subsequently, and the reaction was stirred at ambient temperature overnight. Solution was diluted with CH_2Cl_2 and extracted with 10% citric acid (x 3), Sat. $NaHCO_3$ (x 3) and brine. The organic layer was dried over $MgSO_4$ and reduced in vacuo to obtain the product. This crude material was stirred in 1:1 TFA/CH_2Cl_2 solution (20 mL) for 3 h. After removing excess solvent, product was dried under vacuum and used for the synthesis of peptoid analogue.

yellow oil. ^{1}H NMR (500 MHz, $CDCl_3$) δ c7.78 (s, 3H), 3.50-3.39 (m, 4H), 3.39-3.32 (m, 2H), 2.75 (t, *J* = 5.6 Hz, 2H), 2.00 (quint, *J* = 6.8 Hz, 2H), 1.91 (quint, *J* = 6.8 Hz, 2H). ^{13}C NMR (126 MHz, $CDCl_3$) δ 169.48, 46.76, 45.94, 36.15, 30.13, 25.48, 23.99.

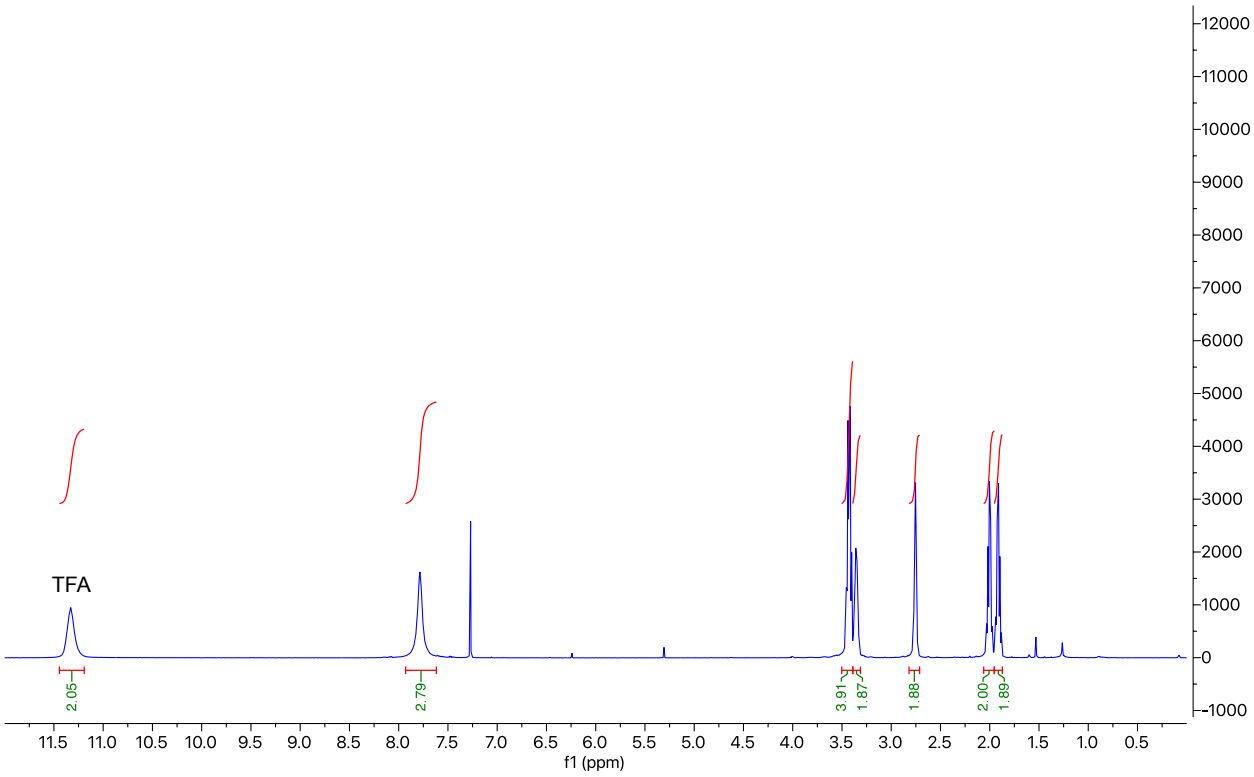

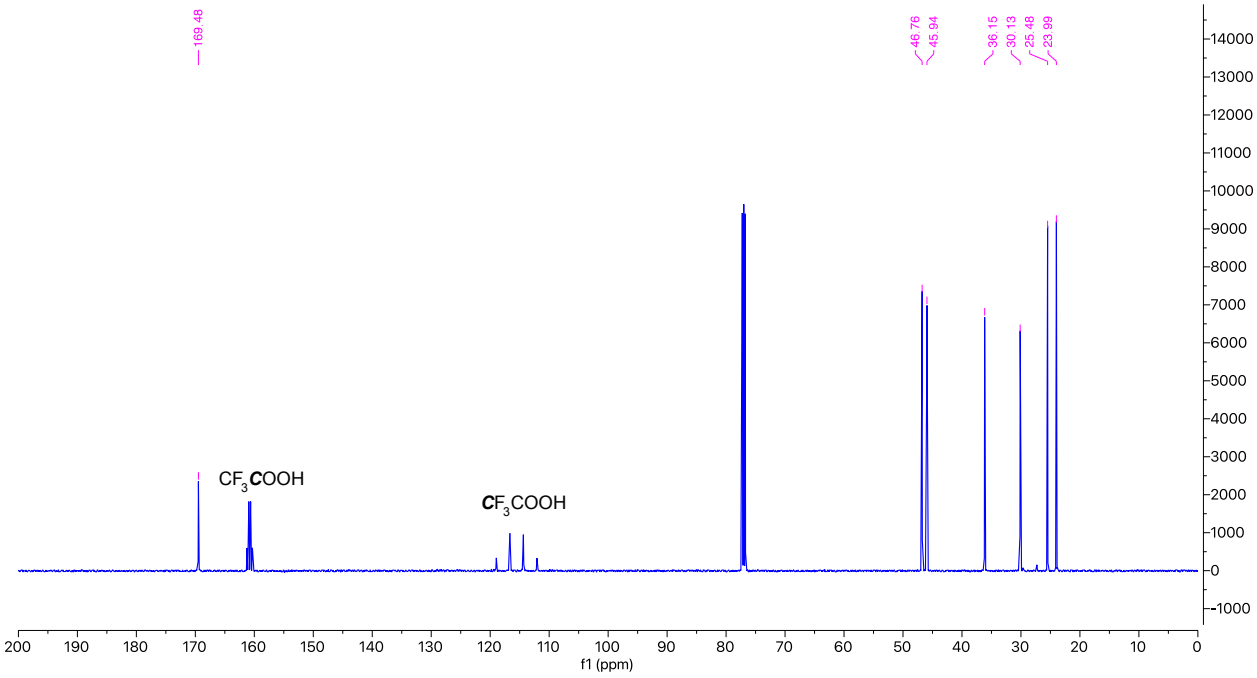

Synthesis Scheme of Cyclic Peptides and Peptoid Monomer

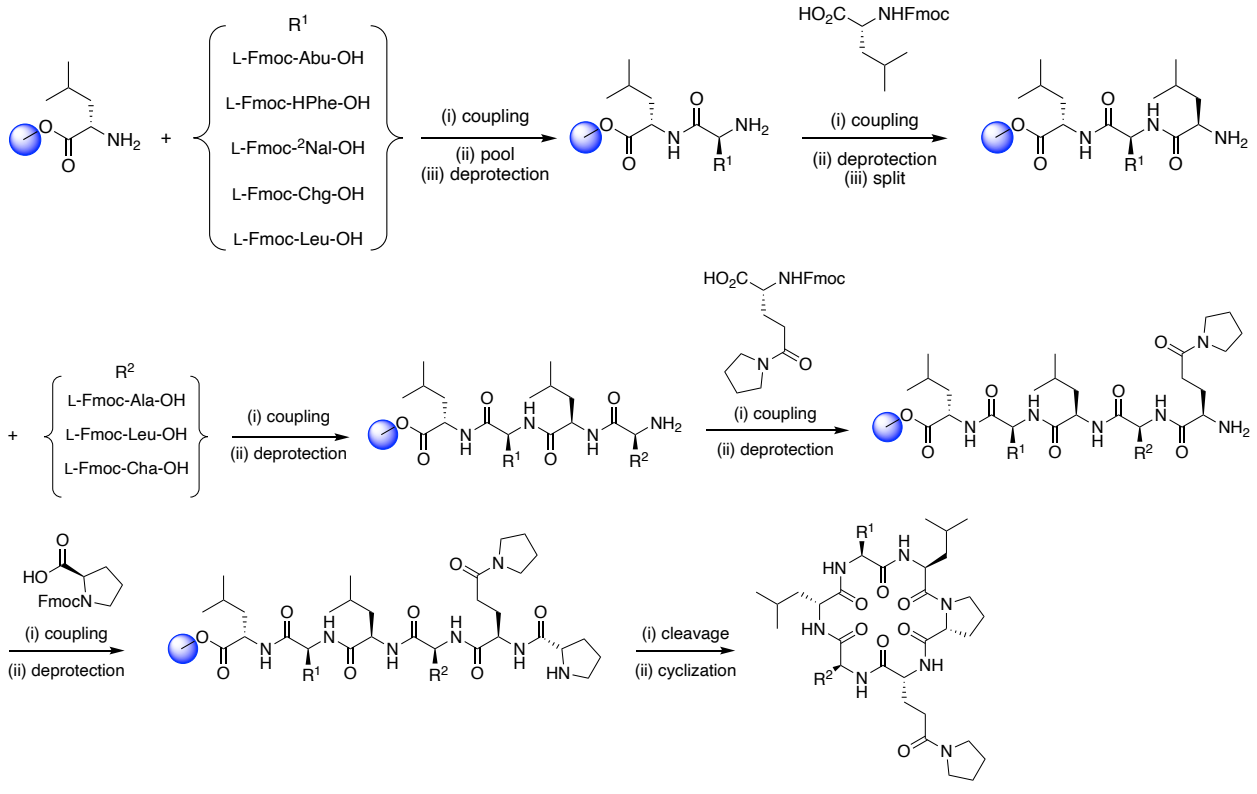

Scheme S3 Synthesis scheme of **3-Pye²** library

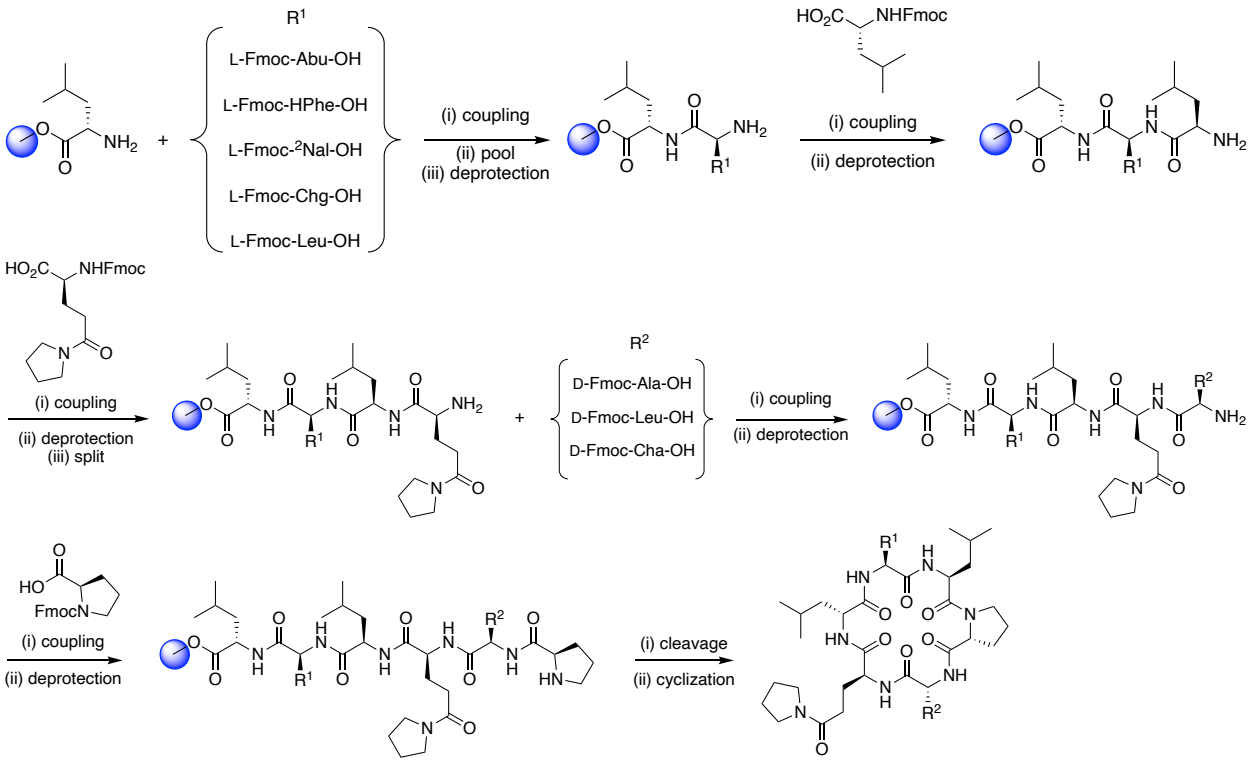

Scheme S4 Synthesis scheme of **3-Pye**[3] library

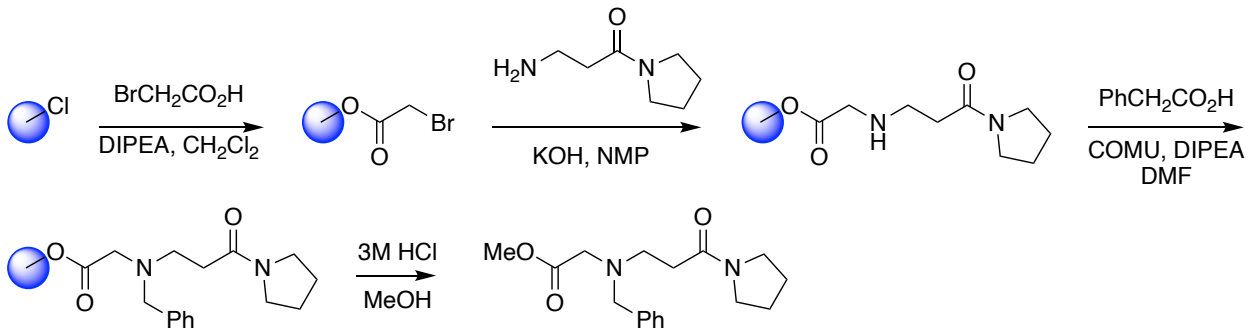

Scheme S5 Synthesis scheme of Pye peptoid monomer.

In Silico Investigation of Side Chain-to-Backbone Hydrogen Bonding of Model Structures

Distance between side chain HBA and the amide HBD of model structures was investigated *in silico* using Discovery Studio as described. SMILE strings of each designed model were obtained from Chemdraw, then 3D structures were generated by Discovery Studio software. A conformer algorithm based on the Merck Molecular Force Field (MMFF) was used to generate the conformations of each model. Initial structures were minimized, then conformation ensembles were generated with SMART minimization method available as the default setting in Discovery Studio. Implicit solvation was incorporated using the Generalized Born model with the dielectric constant set to 4.81 to represent chloroform solvent. Duplicate structures within RMSD < 0.2 Å were discarded. The distance between the *O* acceptor from the side chain and the N*H* acetyl donor was measured and plotted against conformer's energy relative to the lowest energy conformer. Molecules with short HBD-HBA distance at low relative energy conformation have the potential to form intramolecular hydrogen bonding in a low dielectric environment.

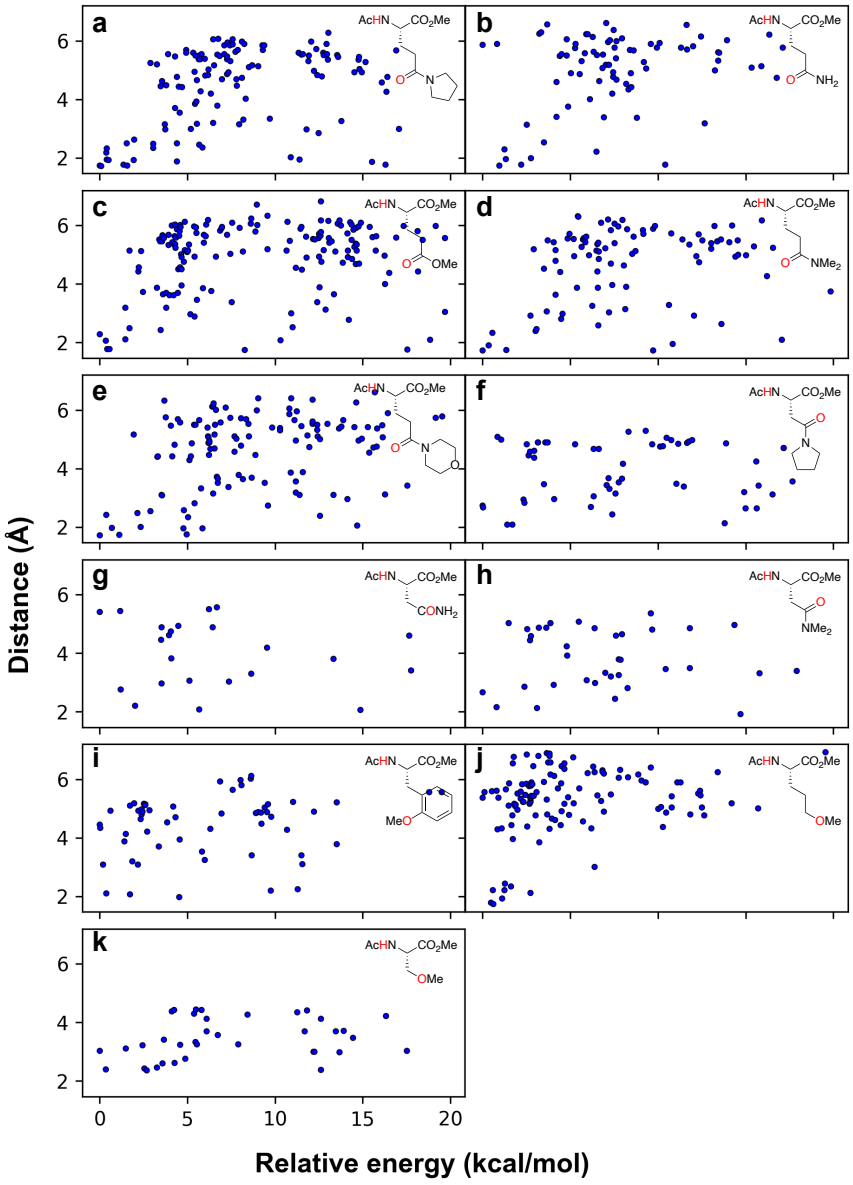

Figure S1. Plots between HBD-HBA distances of each conformer and their relative energy.

Analytical Procedures

General Protocol of UPLC-MS Analysis

UPLC-MS analyses of cyclic peptides were performed via a Thermo Scientific Ultimate 3000 UPLC system, using a Thermo Hypersil GOLD C18 30 mm x 2.1 mm (1.9 µm) column (#25002-032130). Flow rate was set to 1 mL/min and a gradient method was as followed: 0.0-0.5 min, 5% MeCN; 0.5-0.75 min, ramp to 95% MeCN; 0.75-3.0 min, 95% MeCN; 3.0-3.5 min, 5% MeCN. Mass identification and quantification used an inline Thermo Scientific Orbitrap VelosPro (FTMS mode), tuned for maximum ionization of cyclosporin A, background ion locking on octyl phthalate, 200-2000 AMU mass windows, using +/- 0.02 AMU windows for integration.

Shake Flask Partition Experiment

Shake flask partition experiment to measure log $D_{dec/w}$ was performed as described by Naylor, M. R. *et. al*.[1] with minor modification. 1,9-Decadiene and PBS buffer (pH 7.4) were saturated by vortexing with an equal volume for 1-2 min, then centrifuged to allow the emulsion to separate. 8 µL of 400 µM test compounds in DMSO solution were added to 2.0 mL Eppendorf tube followed by 800 µL of saturated 1,9-decadiene and 800 µL saturated PBS buffer to yield a final concentration of 2 µM with 0.5% DMSO. Tubes were sealed carefully and agitated by vortex (30 min) and sonication (30 min). Tubes were then centrifuged for 10 min at 16,000 x g to separate two layers. 150 µL x 4 of each layer was carefully separated to minimize contamination from the pipette tip, especially when collecting the lower aqueous layer: 1) expel an air while passing through organic layer to prevent capillary wicking of organic solvent, 2) gently wipe off organic solvent adhered to tip after collecting and before dispensing. Solutions were collected in 96-well 300 µL conical-bottom plate as quadruplicate for each layer and evaporated overnight in a Genevac centrifugal evaporator (60 °C). Each sample was resuspended with 150 uL of 1:1 MeCN/H_2O, mixed, sealed, and sonicated for 30 min. After a final centrifugation for 10 min at 700 x g, samples were quantified via UPLC-MS in 10uL injections with gradient as described above. The average integrations from quadruplicate data of each layer were used to calculate the partition coefficient (log $D_{dec/w}$) of 1,9-decadiene/water. Carbamazepine was used as a standard in these experiments (log $D_{dec/w}$ = -0.18). LPE was calculated from the equation published previously.[1]

$$\text{LPE} = \log D_{dec/w} - 1.06\text{ALogP} + 5.47$$

Whereas ALogP is a 2D molecular descriptor to represent the octanol/water partition coefficient determined from atoms in a molecule, which was calculated from Discovery Studio software.

Parallel Artificial Membrane Permeability Assay (PAMPA)

A 96-well donor plate with 0.45 µm hydrophobic Immobilon-P membrane supports (Millipore MAIPNTR10) and a 96-well Teflon acceptor plate (Millipore MSSACCEPTOR) were used in the PAMPA permeability test. The acceptor plate was prepared by adding 300 µL of 5% DMSO in PBS buffer (pH 7.4) to each well. Sample solutions were prepared by diluting DMSO stock solutions to a final 2 µM sample concentration in PBS buffer with a final DMSO concentration of 5%.

A 1% (w/v) solution of lecithin (soybean, 90%) in *n*-dodecane was prepared and sonicated before use. 5 µL of the *n*-dodecane / lecithin solution was carefully applied to the underside of membrane supports in the wells of the donor plate, with care taken to not touch the pipet tip to the membrane. After approximately 15 minutes, 150 µL of the 2 µM test compounds were added to the donor wells. The donor plate was then placed on top of the acceptor plate so that the artificial membrane was in contact with the buffer solution below, ensuring that no bubbles form beneath the membrane. A lid was placed on the donor well, and the whole assembly was covered within a sealed chamber and left overnight at room temperature. A wet paper towel was placed inside the chamber to prevent evaporation. After ~15 h (exact time recorded and used for subsequent calculations) the donor and acceptor plates were separated, and 50 µL of each well (donor and acceptor) were mixed with 50 µL MeOH in another 96-well 300 µL conical-bottom plate and sealed. These solutions were analyzed as quadruplicate via UPLC-MS as described above. Permeability (%T) was quantified as the ratio of

analyte area in the acceptor well divided by a theoretical equilibrium ratio based on amounts of combined analyte found in the donor and acceptor wells as follows:

$$\boldsymbol{AnalyteEquil} = \frac{(Ia * Va) + (Id * Vd)}{Va + Vd}$$

$$\%\boldsymbol{T} = \left(\frac{Ia}{[\boldsymbol{AnalyteEquil}]}\right) * 100$$

Recovery (%R) was quantified as the ratio of total compound identified in the donor and acceptor wells relative to the total compound identified in the original dilution sample.

$$\%\boldsymbol{R} = \frac{(Ia * Va) + (Id * Vd)}{Ir * Vd} * 100$$

Permeation rates (P_{app}) were calculated from %T by the following equations:

$$\boldsymbol{C} = \frac{Vd * Va}{(Vd + Va) * Msa * Ts}$$

$$\boldsymbol{P_{app}}\ (cm/s) = -\boldsymbol{C} * \ln\left(1 - \left(\frac{\%\boldsymbol{T}}{100}\right)\right)$$

Where:

- Active surface area of membrane (mm^2): **Msa** = 240
- Volume of acceptor well (µL): **Va** = 300
- Volume of donor well (µL): **Vd** = 150
- Assay run time (s): **Ts**
- Donor intensity: **Id**
- Acceptor intensity: **Ia**
- Recovery intensity: **Ir**

In addition, propranolol was used as a standard reference to confirm the assay was performed correctly, which had log P_{app} ~ -5.

Thermodynamic Solubility Assay

20 µL of 10 mM stock solutions were dispensed into a 96-well conical plate and evaporated overnight in a Genevac centrifugal evaporator (60 °C). 100 uL of PBS (pH 7.4) was reintroduced to the plate to yield a maximum 2mM concentration, then the plate was sealed and sonicated for 1 h. The plate was then gently agitated at 37 °C for ~24 h. The mixtures were filtered through a 0.7 µm glass fiber filter plate (Agilent 200965-100) into a 96-well conical plate. The filtrate can be further diluted with MeCN in a new 96-well plate (dilution factor can be up to 40) and sealed for quantification via UPLC-MS. Standard curves of each compound were acquired from serial dilution of stock solution with DMSO (50 µM to 0.1 µM) and used to calculate concentrations of analytes. All standards and analytes were performed in triplicate and averaged.

Table S1. Experimental Data of Pye-scanning Cyclic Hexapeptides

ID	log $D_{dec/w}$	LPE	PAMPA P_{app} x 10^{-6} (cm/s)	PAMPA log P_{app}	Solubility (μM)	Caco-2 log P_{app} (cm/s)
1	2.03	3.54	8.11 ± 0.28	-5.09 ± 0.02	16 ± 3	
1-Pye^2	1.26	4.12	1.72 ± 0.08	-5.77 ± 0.02	640 ± 4	
1-Pye^3	-0.41	2.45	0.66 ± 0.07	-6.19 ± 0.05	545 ± 97	
1-Pye^4	0.02	2.89	0.30 ± 0.01	-6.53 ± 0.01	580 ± 54	
1-Pye^5	-0.42	2.45	0.32 ± 0.03	-6.50 ± 0.05	505 ± 21	
1-Pye^6	-0.30	2.56	0.66 ± 0.19	-6.20 ± 0.14	720 ± 27	
2	1.96	3.47	5.26 ± 1.85	-5.30 ± 0.14	241 ± 20	
2-Pye^2	-0.29	2.58	0.56 ± 0.11	-6.26 ± 0.08	607 ± 22	
2-Pye^3	-0.29	2.58	1.09 ± 0.46	-5.99 ± 0.17	446 ± 16	
2-Pye^4	0.04	2.91	1.29 ± 0.89	-5.96 ± 0.27	456 ± 91	
2-Pye^5	-0.82	2.04	0.13 ± 0.03	-6.89 ± 0.09	553 ± 44	
2-Pye^6	-0.29	2.58	1.50 ± 0.86	-5.89 ± 0.28	562 ± 92	
3	2.04	3.55	7.98 ± 0.41	-5.10 ± 0.02	63 ± 6	-5.58
3-Pye^2	1.06	3.93	1.46 ± 0.09	-5.84 ± 0.03	734 ± 29	-6.41
3-Pye^3	-0.22	2.65	0.23 ± 0.02	-6.64 ± 0.03	144 ± 20	-7.15
3-Pye^4	0.21	3.07	0.14 ± 0.01	-6.86 ± 0.04	578 ± 125	-6.77
3-Pye^5	0.14	3.00	0.28 ± 0.02	-6.55 ± 0.03	554 ± 17	-6.70
3-Pye^6	0.16	3.02	0.18 ± 0.02	-6.74 ± 0.06	598 ± 11	

Table S2. Experimental Data of 3-Pye^2 Library

ID	MW	R^1	R^2	RT (sec)	ALogP	log $D_{dec/w}$	P_{app} x 10^{-6} cm/s	log P_{app}	% recovery	solubility (μM)
3-Pye^2(Ala^{3}Abu^5)	661.42	Abu	Ala	97.3	0.516	-1.4	0.030 ± 0.002	-7.53 ± 0.02	96.3 ± 3.6	
3-Pye^2(Ala^3)	689.45	Leu	Ala	100.1	1.224	-0.010	0.21 ± 0.02	-6.68 ± 0.05	89.5 ± 3.1	
3-Pye^2(Abu^5)	703.46	Abu	Leu	100.5	1.748	0.060	0.20 ± 0.01	-6.71 ± 0.02	94.6 ± 2.0	
3-Pye^2(Ala^{3}Chg^5)	715.46	Chg	Ala	101.9	1.832	0.46	0.78 ± 0.05	-6.11 ± 0.03	84.7 ± 0.6	
3-Pye^2(Ala^{3}HPhe^5)	737.45	HPhe	Ala	101.9	2.004	0.48	1.25 ± 0.10	-5.90 ± 0.03	87.9 ± 0.4	
3-Pye^2	731.50	Leu	Leu	103.6	2.456	1.2	1.28 ± 0.04	-5.89 ± 0.01	63.1 ± 2.5	
3-Pye^2(Ala^{3}Nal^5)	773.45	^{2}Nal	Ala	103.0	2.457	0.90	3.04 ± 0.33	-5.52 ± 0.05	52.5 ± 2.6	
3-Pye^2(Cha^{3}Abu^5)	743.50	Abu	Cha	103.5	2.745	1.1	2.05 ± 0.10	-5.69 ± 0.02	87.3 ± 6.9	
3-Pye^2(Chg^5)	757.51	Chg	Leu	105.7	3.064	1.6	5.94 ± 0.62	-5.23 ± 0.05	88.1 ± 4.4	
3-Pye^2(HPhe^5)	779.50	HPhe	Leu	105.3	3.236	1.5	5.65 ± 0.54	-5.25 ± 0.04	104.1 ± 4.9	82 ± 6
3-Pye^2(Cha^3)	771.53	Leu	Cha	106.6	3.453	2.1	8.93 ± 0.68	-5.05 ± 0.03	70.6 ± 5.5	111 ± 29
3-Pye^2(Nal^5)	815.50	^{2}Nal	Leu	106.4	3.688	2.1	8.21 ± 1.73	-5.09 ± 0.10	58.3 ± 6.7	67 ± 44
3-Pye^2(Cha^{3}Chg^5)	797.54	Chg	Cha	109.5	4.061	2.6	14.11 ± 1.20	-4.85 ± 0.04	59.2 ± 3.9	74 ± 10
3-Pye^2(Cha^{3}HPhe^5)	819.53	HPhe	Cha	108.4	4.233	2.5	13.57 ± 1.09	-4.87 ± 0.03	69.9 ± 3.9	4.0 ± 0.4
3-Pye^2(Cha^{3}Nal^5)	855.53	^{2}Nal	Cha	109.9	4.685	3.0	5.36 ± 1.08	-5.28 ± 0.09	24.2 ± 1.3	N.D.

N.D. = not detectable

Table S3. Experimental Data of 3-Pye^3 Library

ID	MW	R^1	R^2	RT (sec)	ALogP	log $D_{dec/w}$	P_{app} x 10^{-6} cm/s	log P_{app}	% recovery
3-Pye^3(Ala^{2}Abu^5)	661.42	Abu	Ala	98.0	0.516	-1.9	0.004 ± 0.001	-8.39 ± 0.12	98.9 ± 2.9
3-Pye^3(Ala^2)	689.45	Leu	Ala	100.8	1.224	-1.2	0.030 ± 0.003	-7.50 ± 0.05	81.0 ± 3.5

3-Pye^3(Abu^5)	703.46	Abu	Leu	100.7	1.748	-0.25	0.03 ± 0.01	-7.46 ± 0.08	71.9 ± 3.5
3-Pye^3(Ala^{2}Chg^5)	715.46	Chg	Ala	102.9	1.832	-0.73	0.15 ± 0.03	-6.83 ± 0.09	86.5 ± 2.8
3-Pye^3(Ala^{2}HPhe^5)	737.45	HPhe	Ala	102.2	2.004	-0.57	0.25 ± 0.06	-6.61 ± 0.10	89.6 ± 2.8
3-Pye^3	731.50	Leu	Leu	103.2	2.456	0.18	0.20 ± 0.02	-6.70 ± 0.03	50.0 ± 0.6
3-Pye^3(Ala^{2}Nal^5)	773.45	^{2}Nal	Ala	102.9	2.457	-0.090	0.52 ± 0.11	-6.29 ± 0.09	70.5 ± 2.9
3-Pye^3(Cha^{2}Abu^5)	743.50	Abu	Cha	104.3	2.745	0.34	0.41 ± 0.03	-6.39 ± 0.03	60.2 ± 4.4
3-Pye^3(Chg^5)	757.51	Chg	Leu	105.3	3.064	0.63	0.64 ± 0.10	-6.20 ± 0.07	79.0 ± 3.6
3-Pye^3(HPhe^5)	779.50	HPhe	Leu	104.8	3.236	0.55	1.06 ± 0.17	-5.98 ± 0.07	79.3 ± 2.9
3-Pye^3(Cha^2)	771.53	Leu	Cha	107.6	3.453	1.2	2.22 ± 0.31	-5.66 ± 0.06	46.5 ± 1.2
3-Pye^3(Nal^5)	815.50	^{2}Nal	Leu	104.9	3.688	1.2	1.89 ± 0.39	-5.73 ± 0.09	56.8 ± 3.0
3-Pye^3(Cha^{2}Chg^5)	797.54	Chg	Cha	109.2	4.061	1.7	3.35 ± 0.86	-5.49 ± 0.12	56.4 ± 3.7
3-Pye^3(Cha^{2}HPhe^5)	819.53	HPhe	Cha	108.5	4.233	1.6	4.15 ± 1.19	-5.40 ± 0.14	56.7 ± 5.1
3-Pye^3(Cha^{2}Nal^5)	855.53	^{2}Nal	Cha	108.5	4.685	2.2	4.04 ± 1.67	-5.43 ± 0.22	26.3 ± 3.0

Table S4. Experimental Data of Cyclic Hexapeptides with Different HBAs

ID	ALogP	log $D_{dec/w}$	LPE	PAMPA P_{app} x 10^{-6} (cm/s)	PAMPA log P_{app}	Solubility (μM)
3-Glu(OMe)^2	2.46	0.69	3.6	1.97 ± 0.56	-5.72 ± 0.13	714 ± 28
3-Gln(NMe$_2$)^2	2.00	0.43	3.8	0.70 ± 0.29	-6.18 ± 0.19	1657 ± 29
3-Asn(Pyr)^2	2.13	0.53	3.7	0.56 ± 0.01	-6.25 ± 0.01	669 ± 67
3-Asn(NMe$_2$)^2	1.67	0.24	3.9	0.28 ± 0.02	-6.56 ± 0.03	1118 ± 69

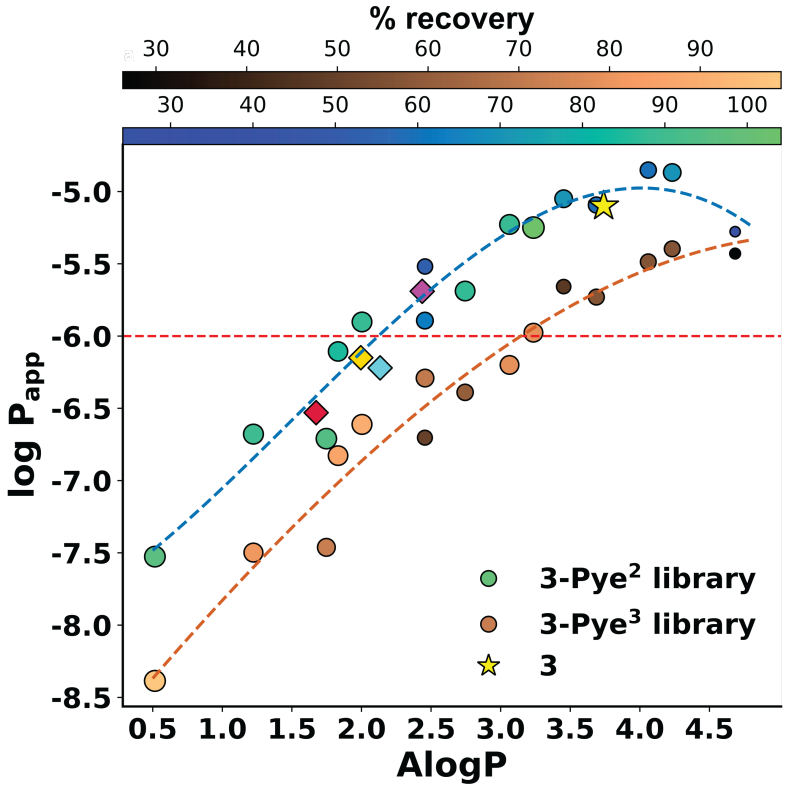

Figure S2. Comparison of PAMPA permeability data of **3-Glu(OMe)^2** (magenta diamond), **3-Asn(Pyr)^2** (blue diamond), **3-Gln(NMe$_2$)^2** (yellow diamond) and **3-Asn(NMe$_2$)^2** (red diamond) to the **3-Pye^2** and **3-Pye^3** libraries.

NMR Spectra of Amide Proton Temperature Coefficient Experiment

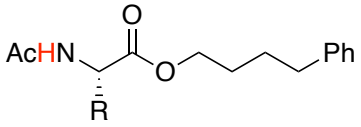

4

ID	R	δ_{NH} (300 K)	$\delta_{NH}/\Delta T$ (ppb/K)
4-Ala	-CH_3	6.08	-3.54
4-Val		5.97	-3.31
4-Leu		5.86	-3.02
4-Ile		5.96	-2.95
4-Gln	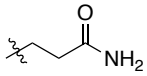	6.59	-5.37
4-Glu(OMe)	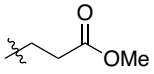	6.18	-3.51
4-Gln(NMe_2)	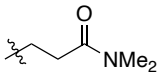	6.88	-6.48
4-Gln(Pyr)	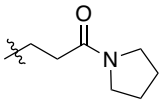	7.11	-7.84
4-Asn(Pyr)	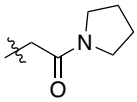	6.81	-1.66
4-Asn(NMe_2)	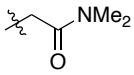	6.89	-1.52

4-Ala

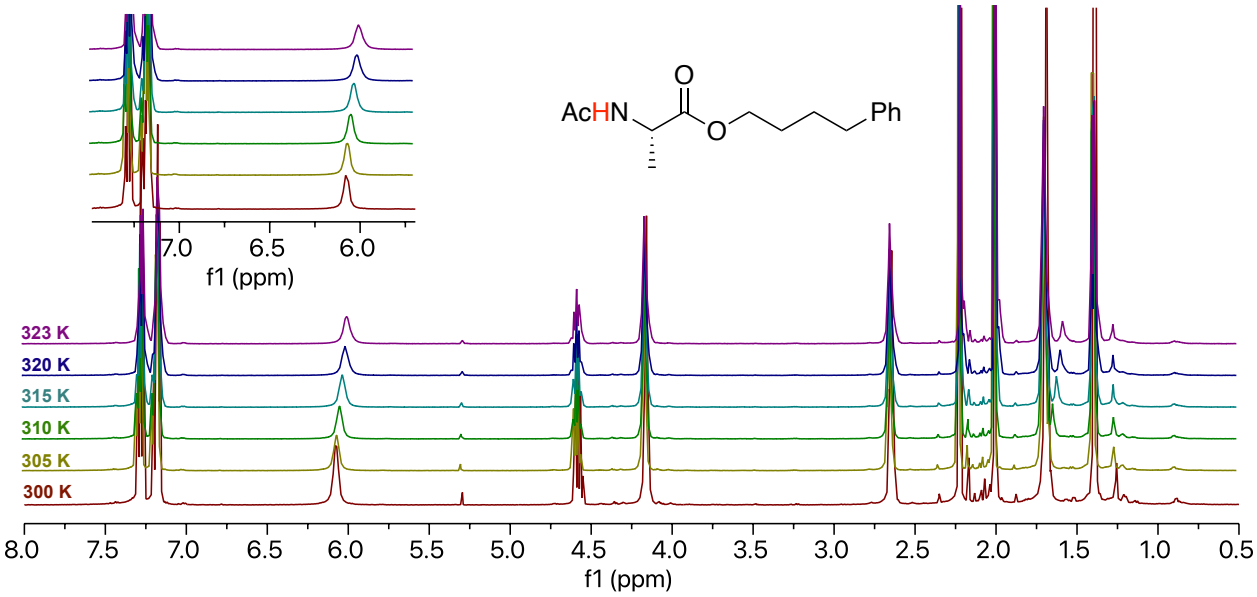
AcHN
O
O
Ph
323 K
320 K
315 K
310 K
305 K
300 K
7.0
6.5
6.0
f1 (ppm)
8.0
7.5
7.0
6.5
6.0
5.5
5.0
4.5
4.0
3.5
3.0
2.5
2.0
1.5
1.0
0.5
f1 (ppm)

4-Val

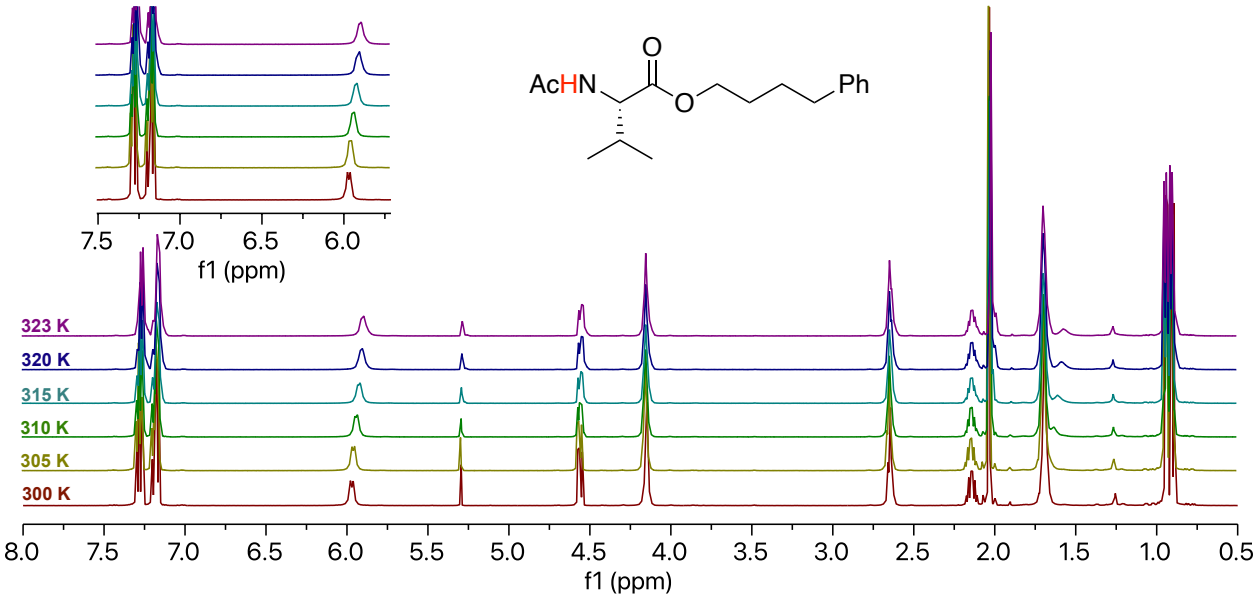
AcHN
O
O
Ph
323 K
320 K
315 K
310 K
305 K
300 K
7.5
7.0
6.5
6.0
f1 (ppm)
8.0
7.5
7.0
6.5
6.0
5.5
5.0
4.5
4.0
3.5
3.0
2.5
2.0
1.5
1.0
0.5
f1 (ppm)

4-Leu

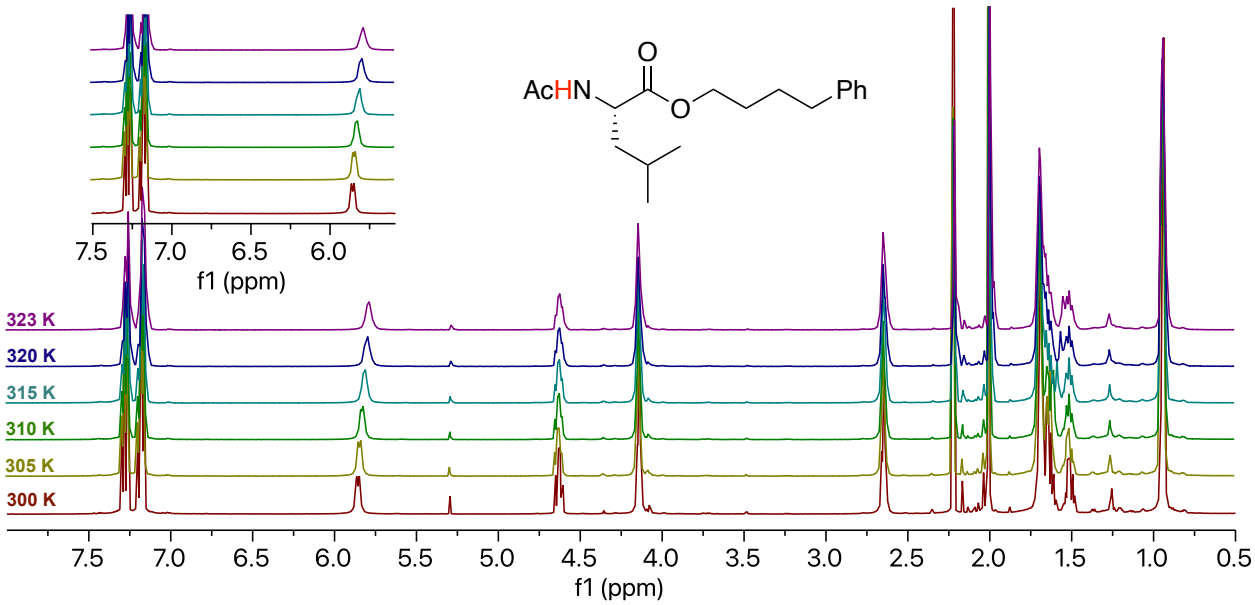
AcHN
O
O
Ph
323 K
320 K
315 K
310 K
305 K
300 K
7.5 7.0 6.5 6.0
f1 (ppm)
7.5 7.0 6.5 6.0 5.5 5.0 4.5 4.0 3.5 3.0 2.5 2.0 1.5 1.0 0.5
f1 (ppm)

4-Ile

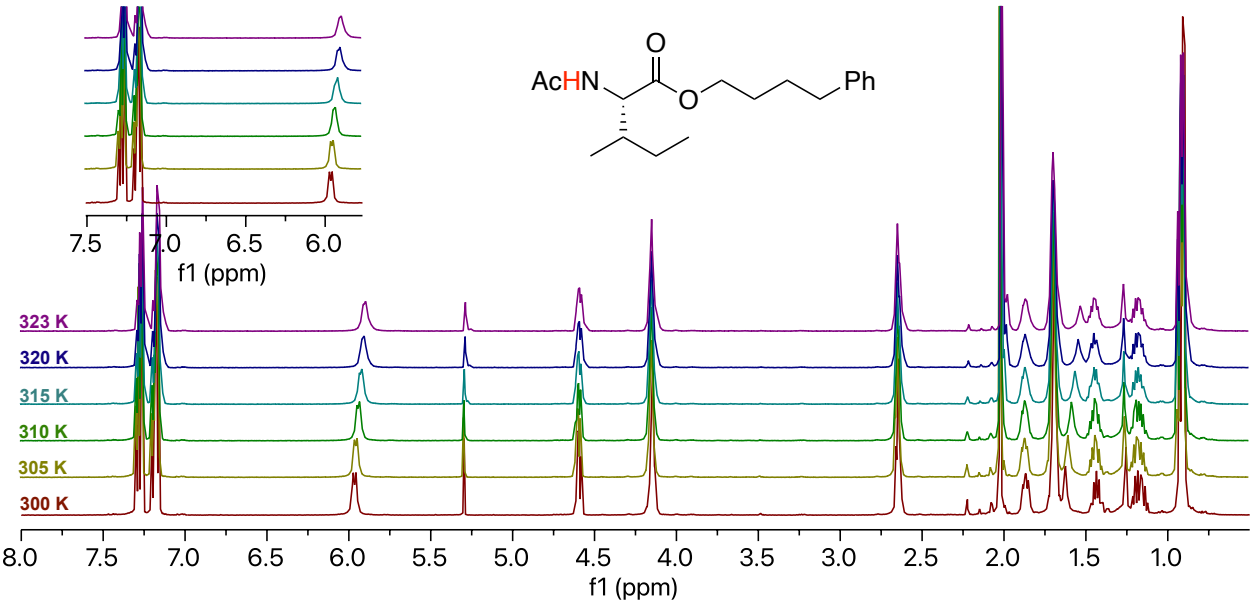
AcHN
O
O
Ph
323 K
320 K
315 K
310 K
305 K
300 K
7.5 7.0 6.5 6.0
f1 (ppm)
8.0 7.5 7.0 6.5 6.0 5.5 5.0 4.5 4.0 3.5 3.0 2.5 2.0 1.5 1.0
f1 (ppm)

4-Gln

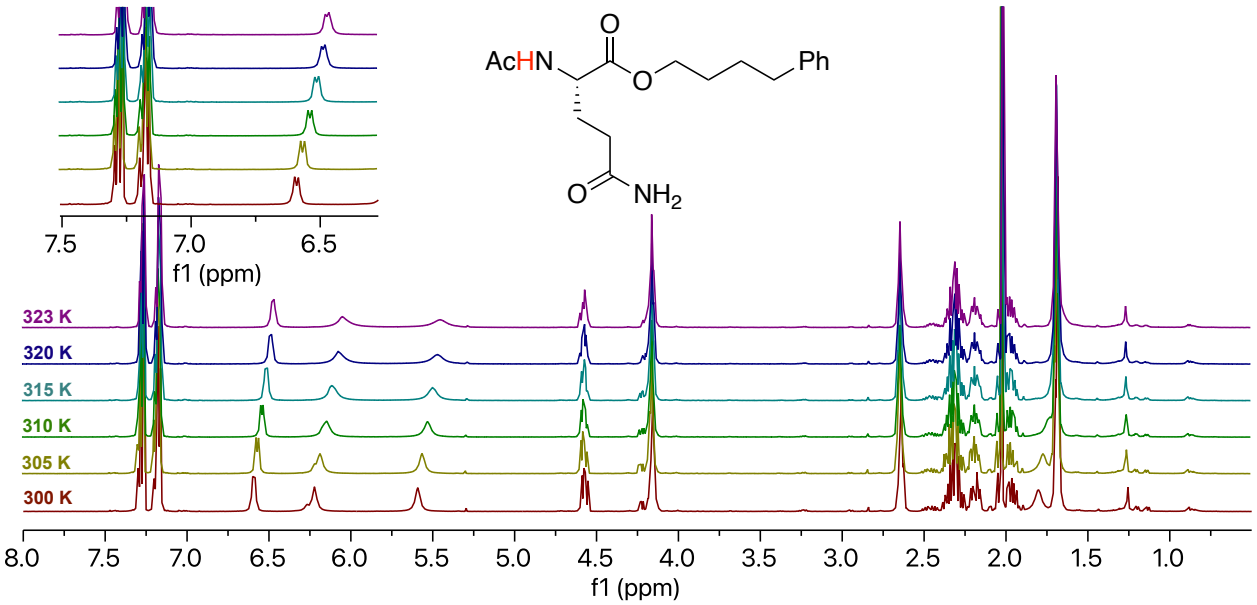

4-Glu(OMe)

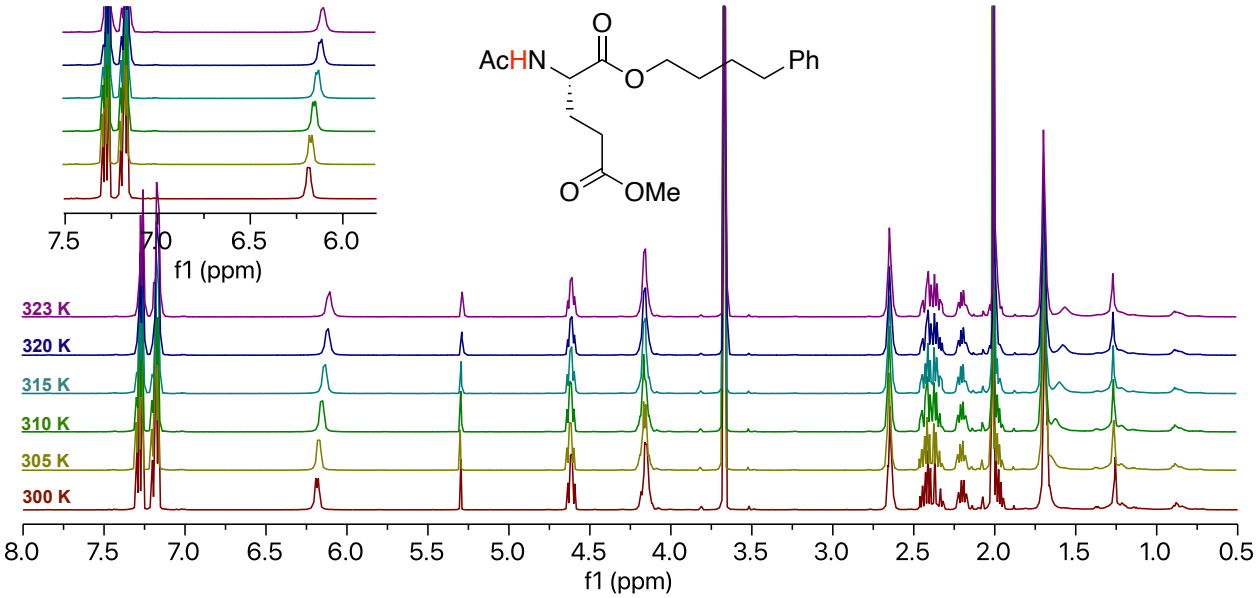

4-Gln(NMe$_2$)

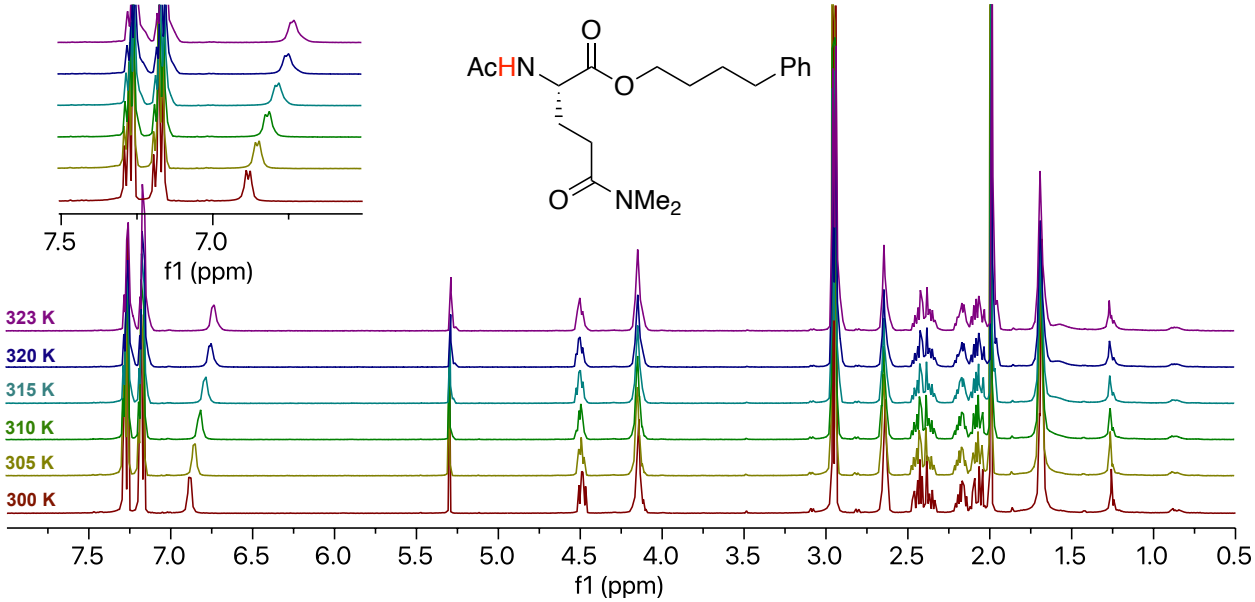

4-Gln(Pyr)

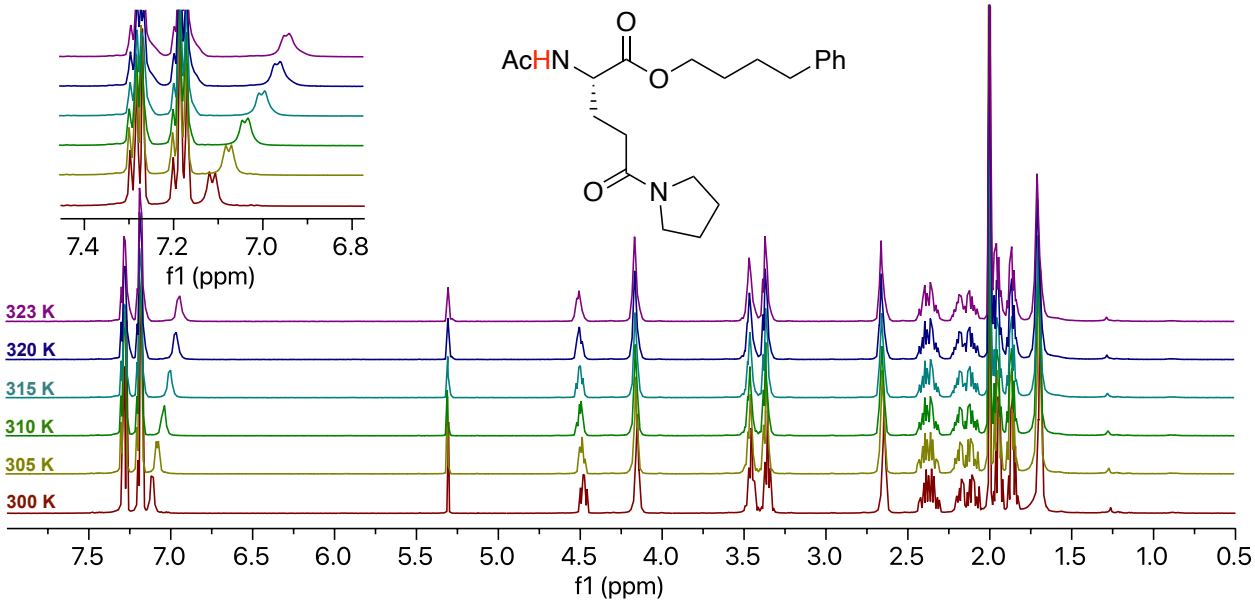

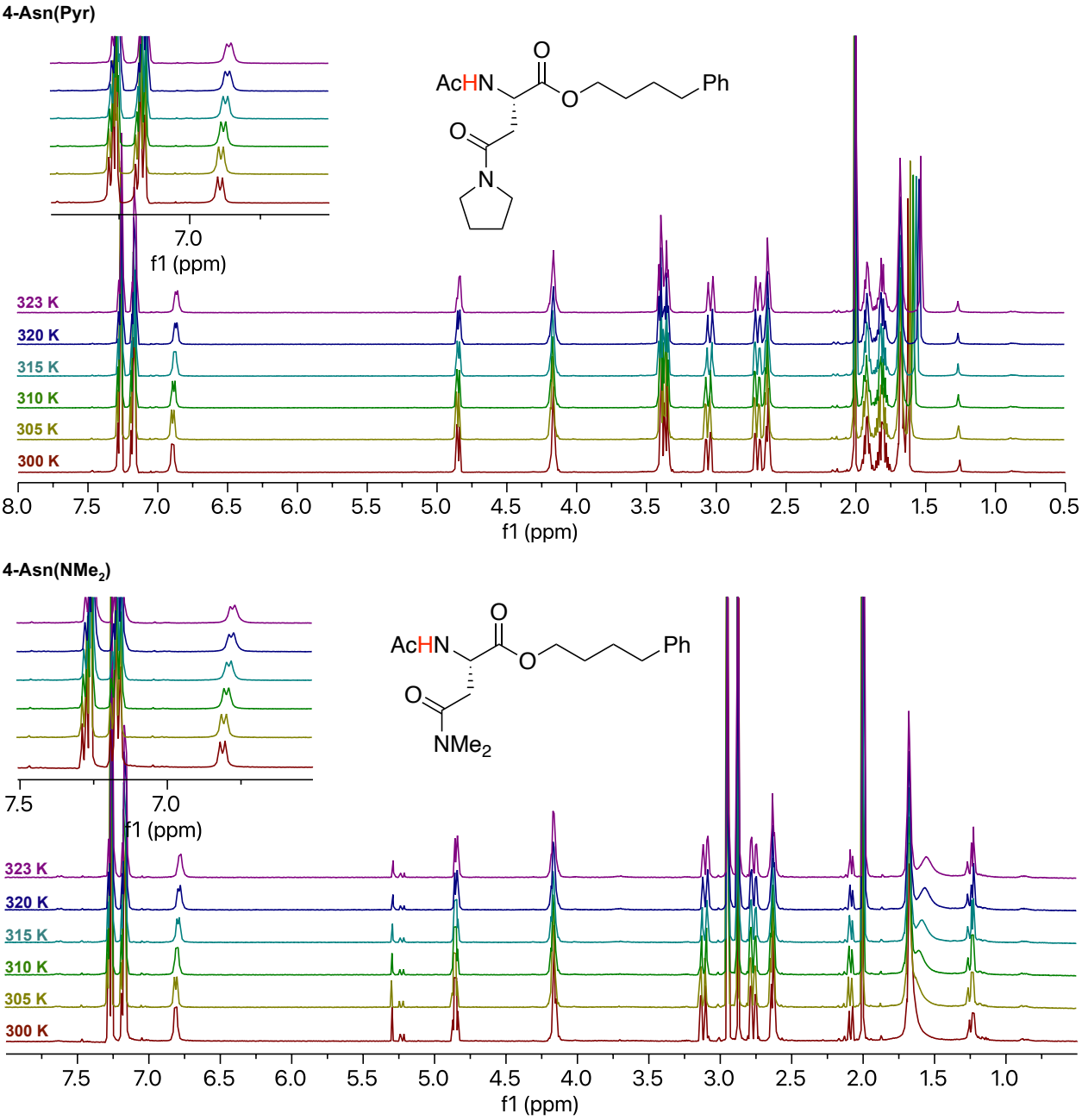

Figure S3. ^{1}H NMR of model structures **4** at different temperatures.

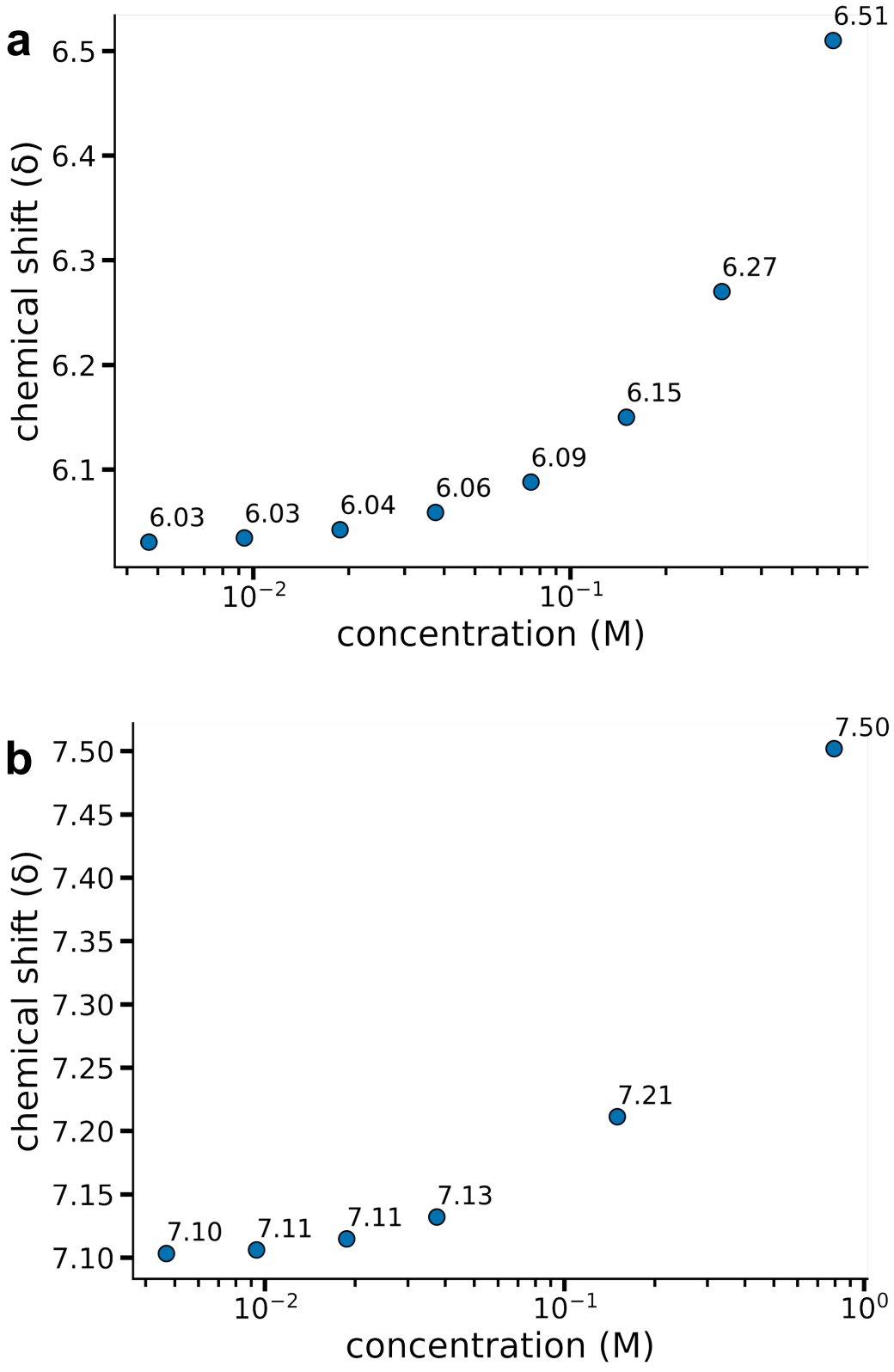

Figure S4. Amide NH chemical shift of (**a**) **4-Ala** and (**b**) **4-Gln(Pyr)** at various concentrations.

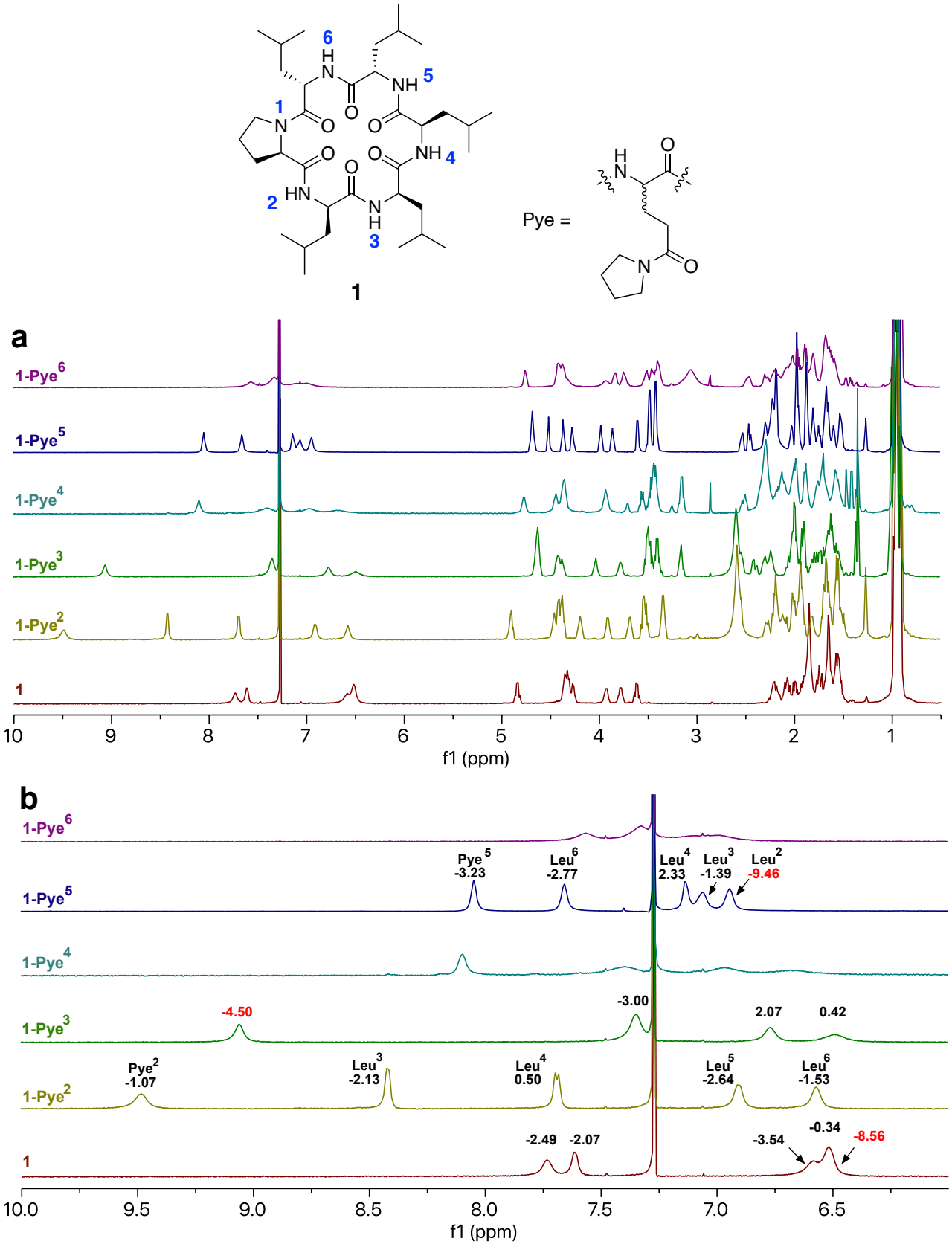
1
Pye =
a
1-Pye6
1-Pye5
1-Pye4
1-Pye3
1-Pye2
1
10
9
8
7
6
5
4
3
2
1
f1 (ppm)
b
1-Pye6
1-Pye5
1-Pye4
1-Pye3
1-Pye2
1
Pye5 -3.23
Leu6 -2.77
Leu4 2.33
Leu3 -1.39
Leu2 -9.46
-4.50
-3.00
2.07
0.42
Pye2 -1.07
Leu3 -2.13
Leu4 0.50
Leu5 -2.64
Leu6 -1.53
-2.49
-2.07
-3.54
-0.34
-8.56
10.0
9.5
9.0
8.5
8.0
7.5
7.0
6.5
f1 (ppm)

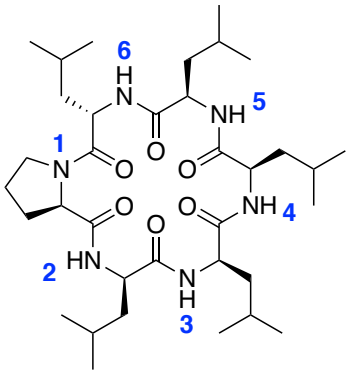
6
H
N
5
NH
1
N
O
O
O
O
O
NH
4
2
HN
O
N
H
3

2

Pye =

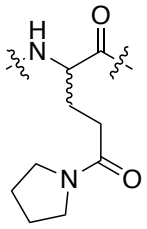
H
N
O
N
O

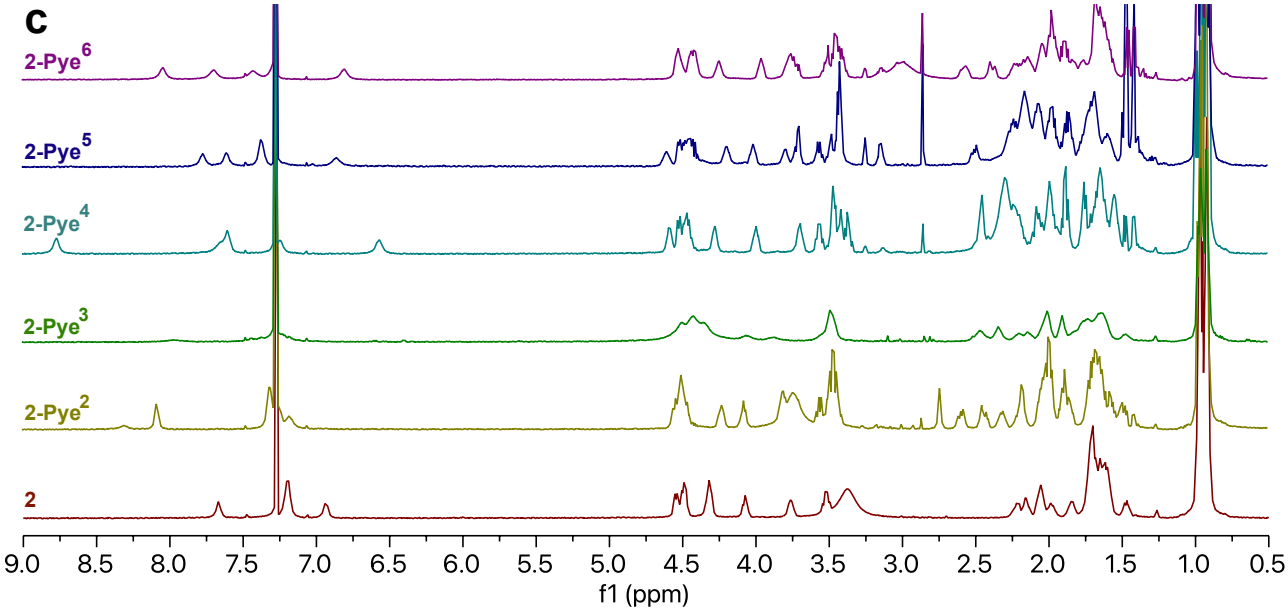
c
2-Pye6
2-Pye5
2-Pye4
2-Pye3
2-Pye2
2
9.0
8.5
8.0
7.5
7.0
6.5
6.0
5.5
5.0
4.5
4.0
3.5
3.0
2.5
2.0
1.5
1.0
0.5
f1 (ppm)

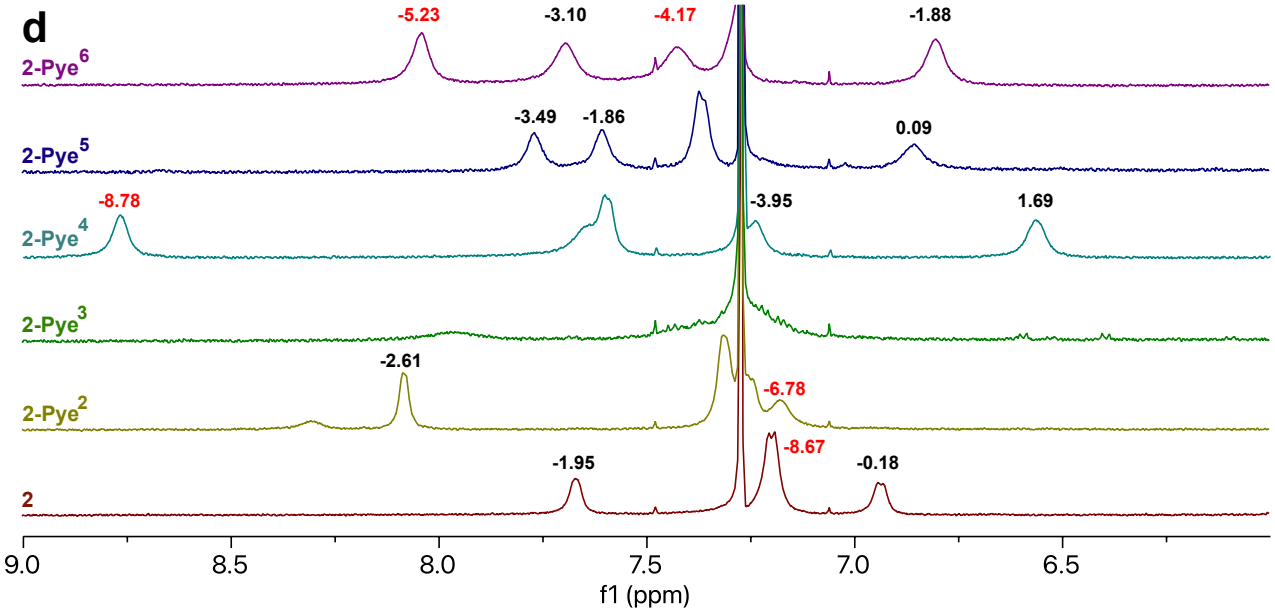
d
-5.23
-3.10
-4.17
-1.88
2-Pye6
-3.49
-1.86
0.09
2-Pye5
-8.78
-3.95
1.69
2-Pye4
2-Pye3
-2.61
-6.78
2-Pye2
-8.67
-1.95
-0.18
2
9.0
8.5
8.0
7.5
7.0
6.5
f1 (ppm)

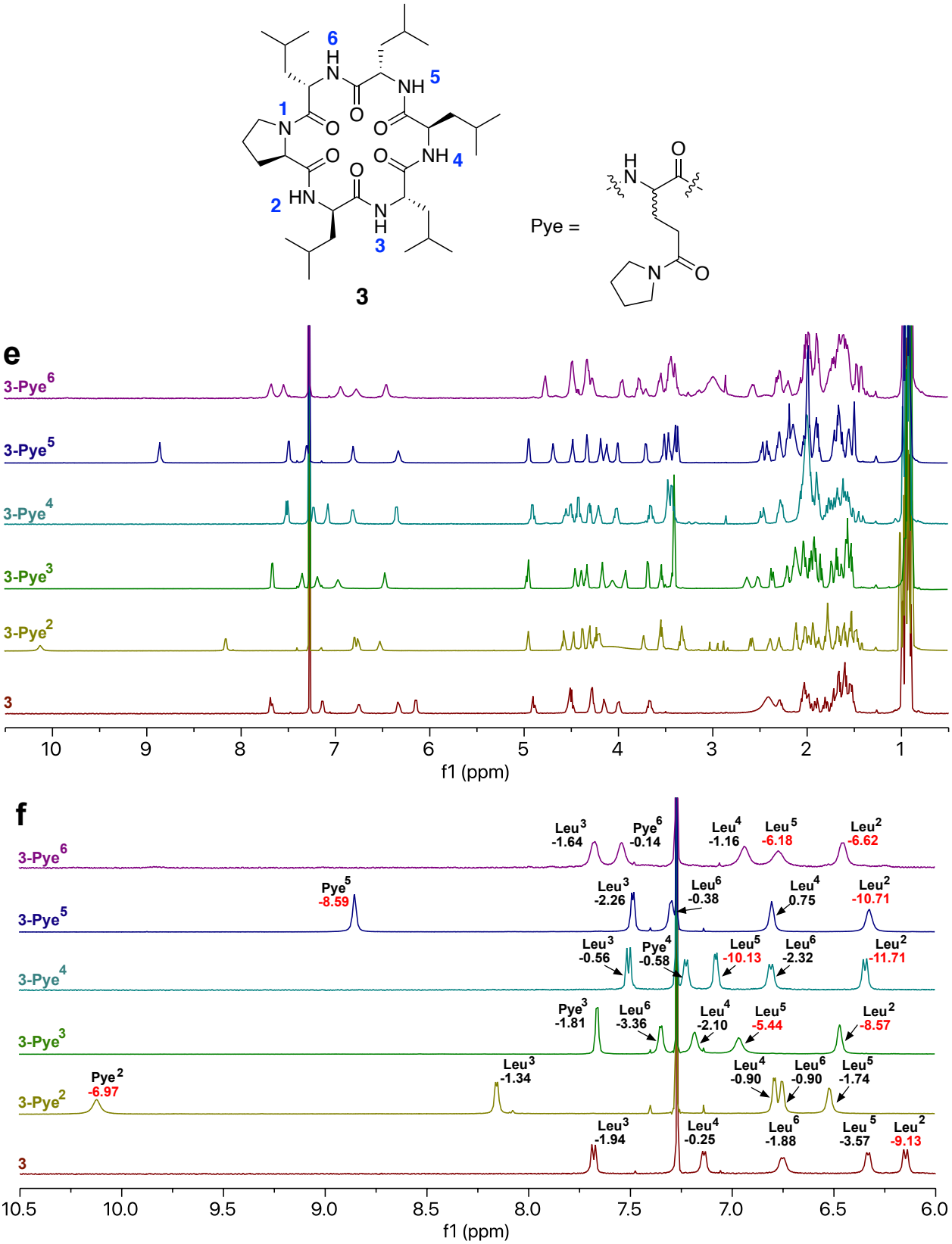

Figure S5 ^{1}H NMR of cyclic hexapeptides **1**, **2**, **3** and their derivatives at ~10 mM. Values indicate the amide temperature coefficients in ppb/K.

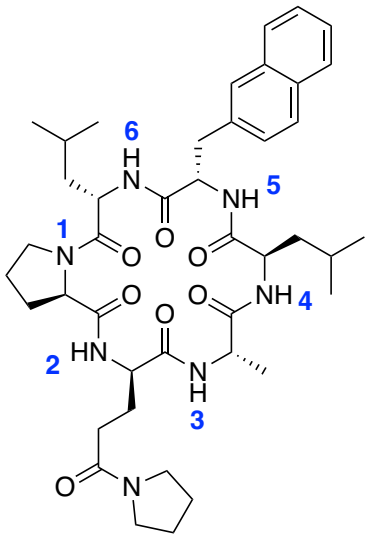

3-Pye^{2}(Ala^{3}Nal^{5})

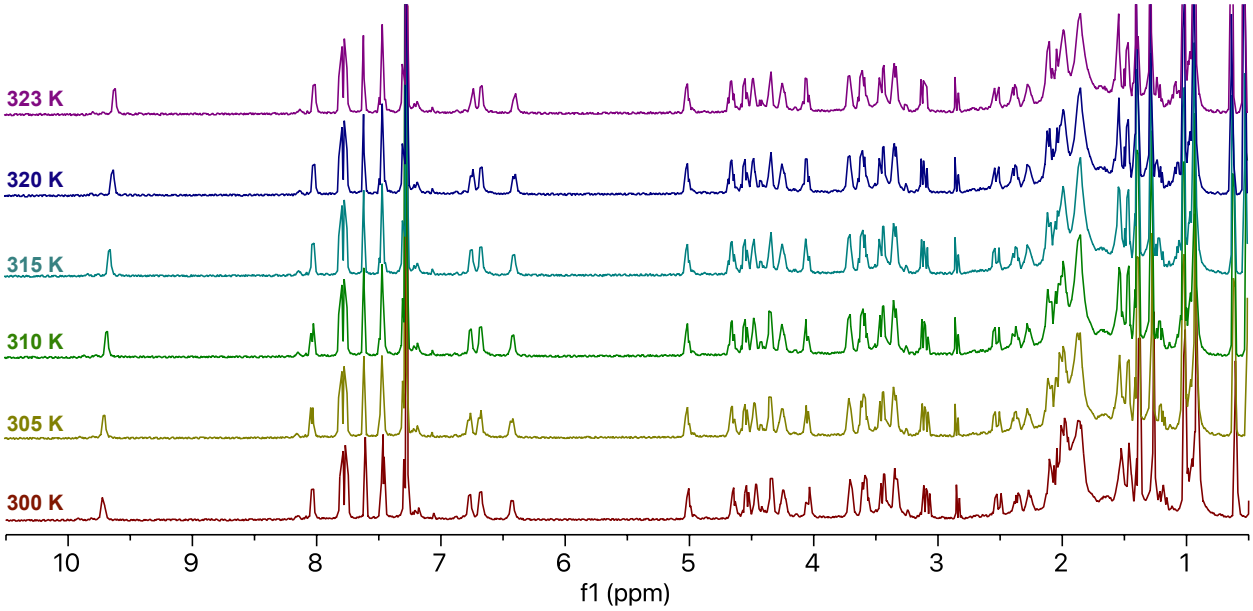

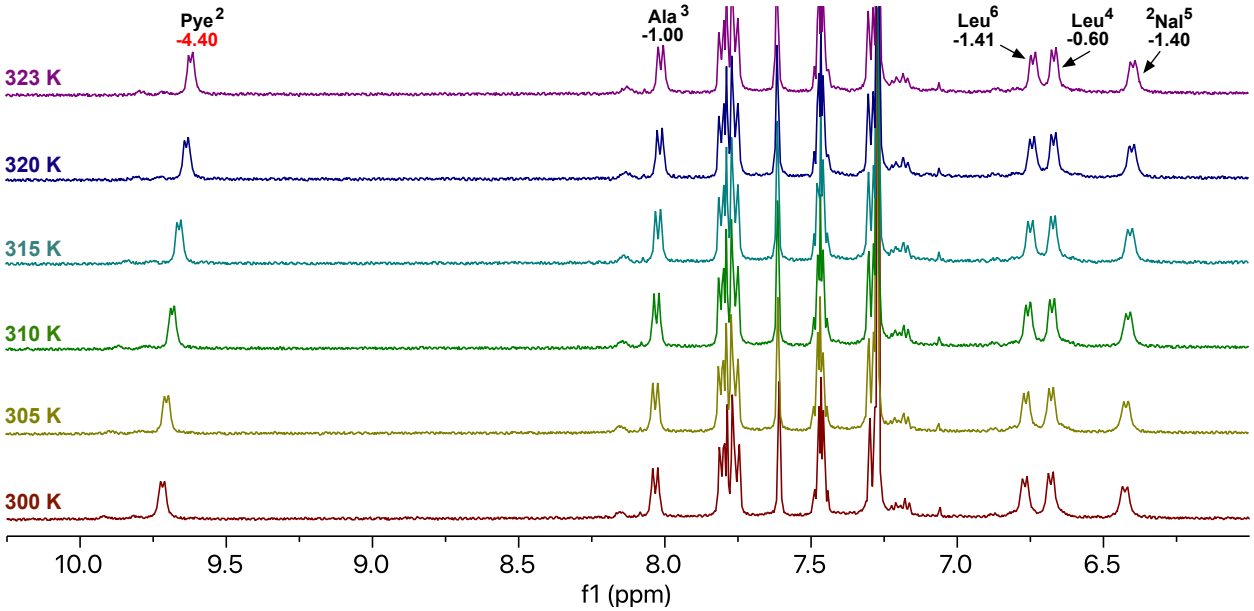

Figure S6. ^{1}H NMR of **3-Pye^{2}(Ala^{3}Nal^{5})**.

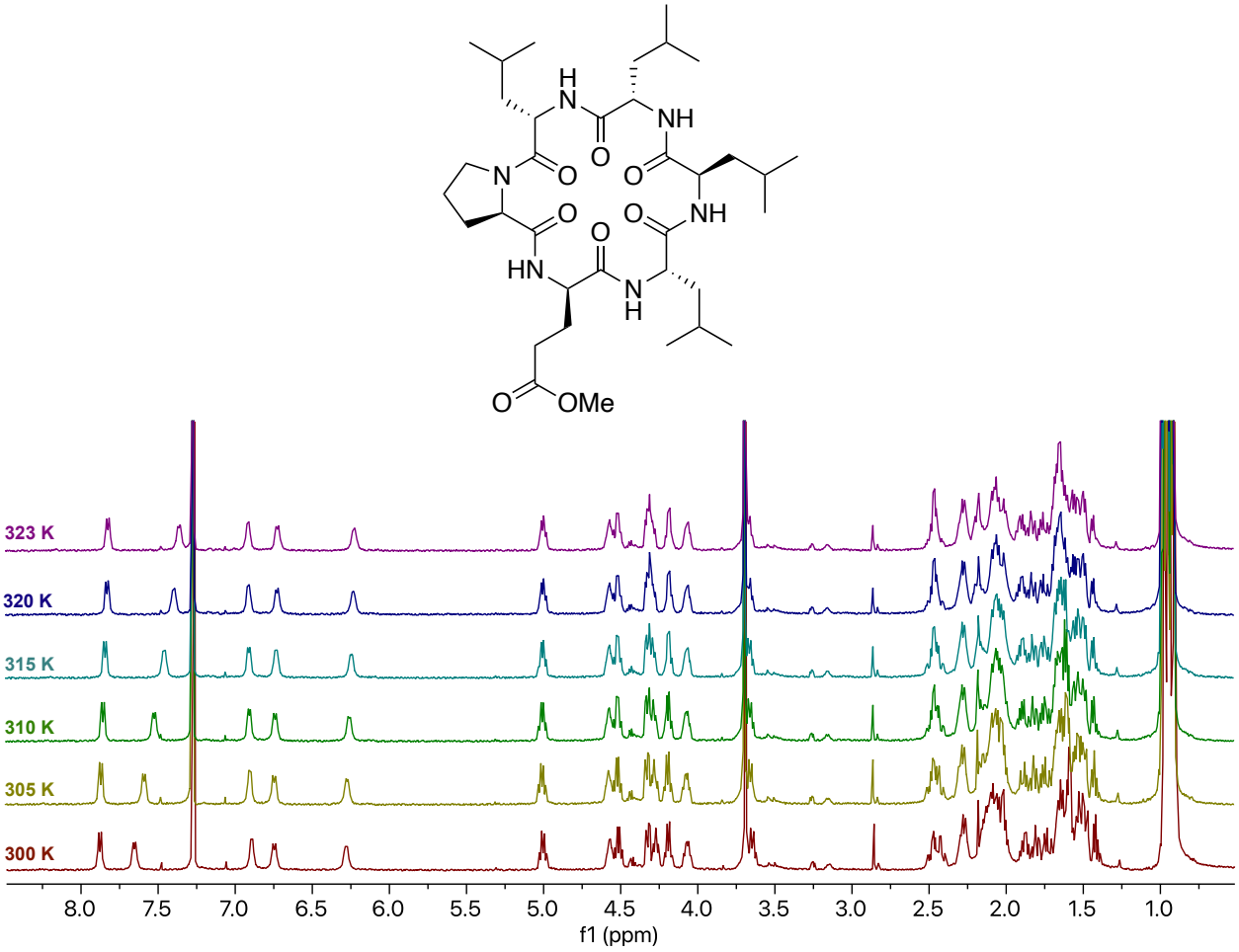

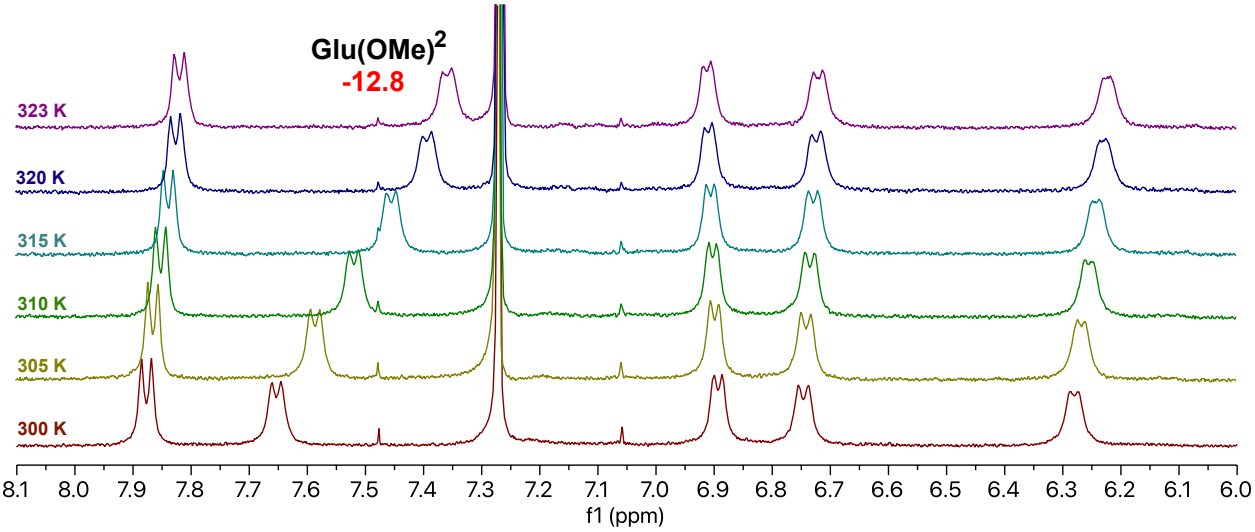

Figure S7. ^{1}H NMR of **3-Glu(OMe)^{2}**.

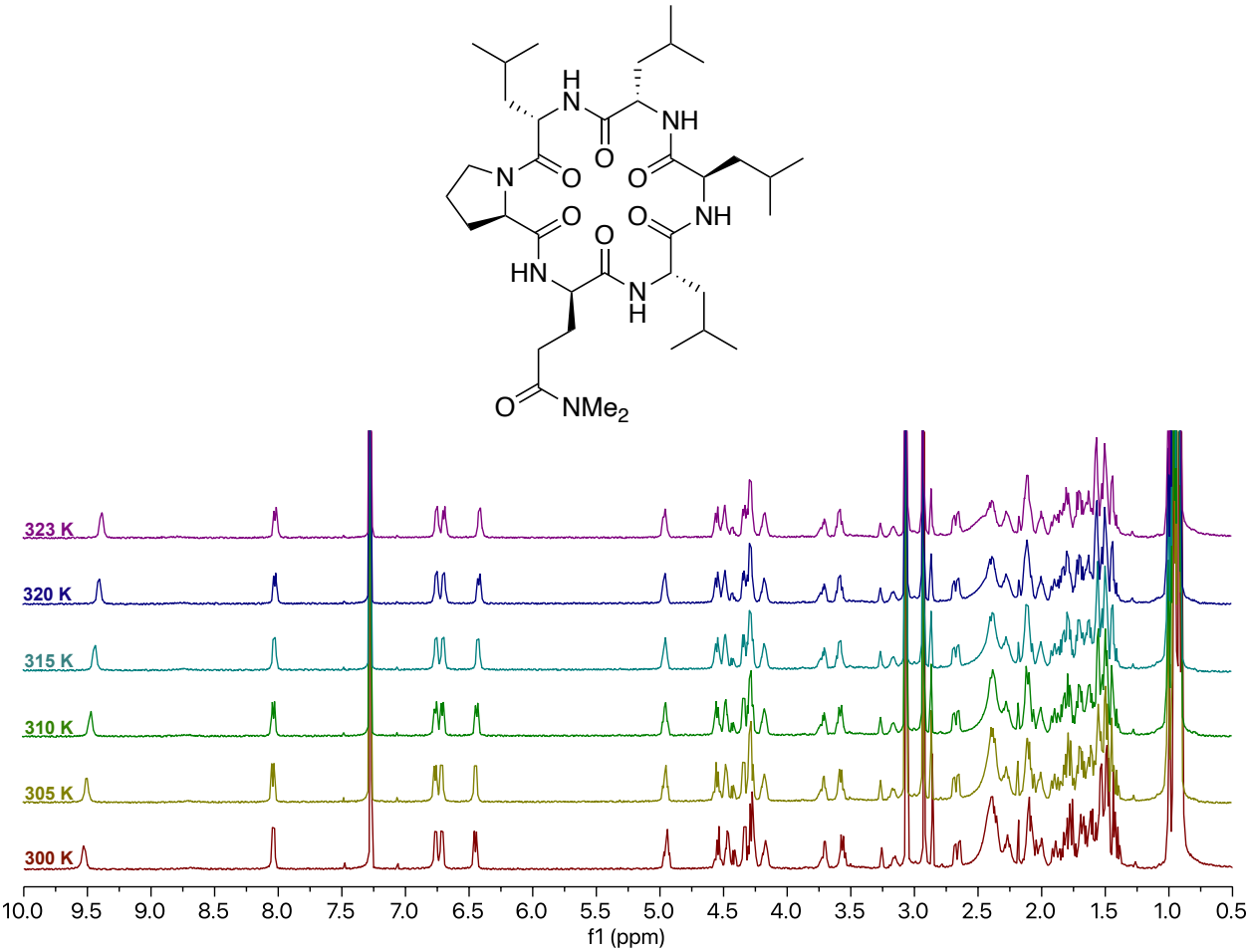

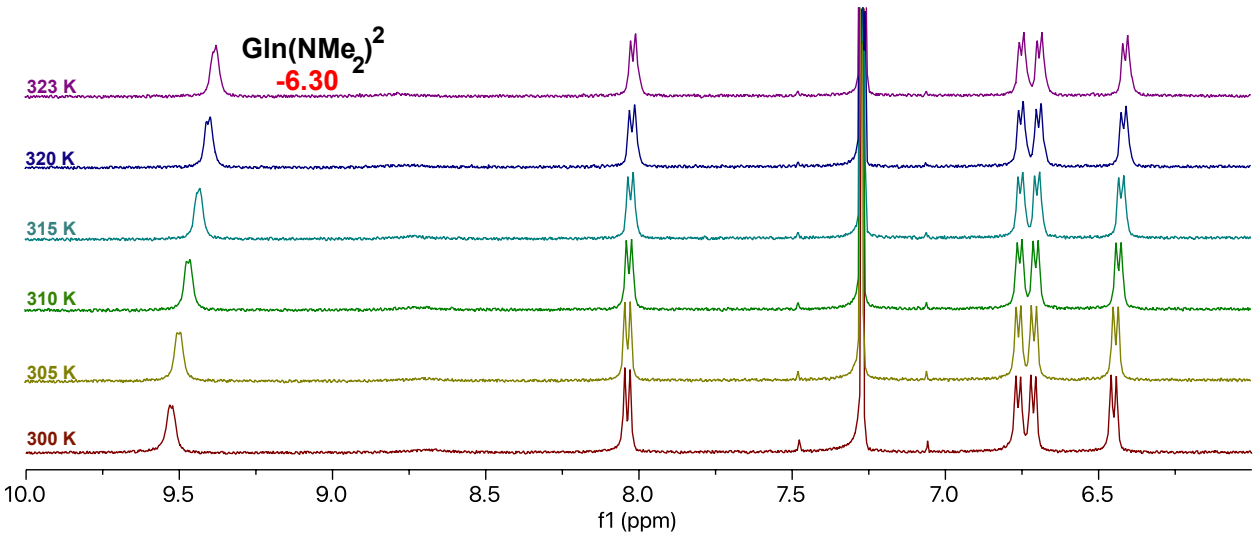

Figure S8. ^{1}H NMR of **3-Glu(NMe$_2$)^2**.

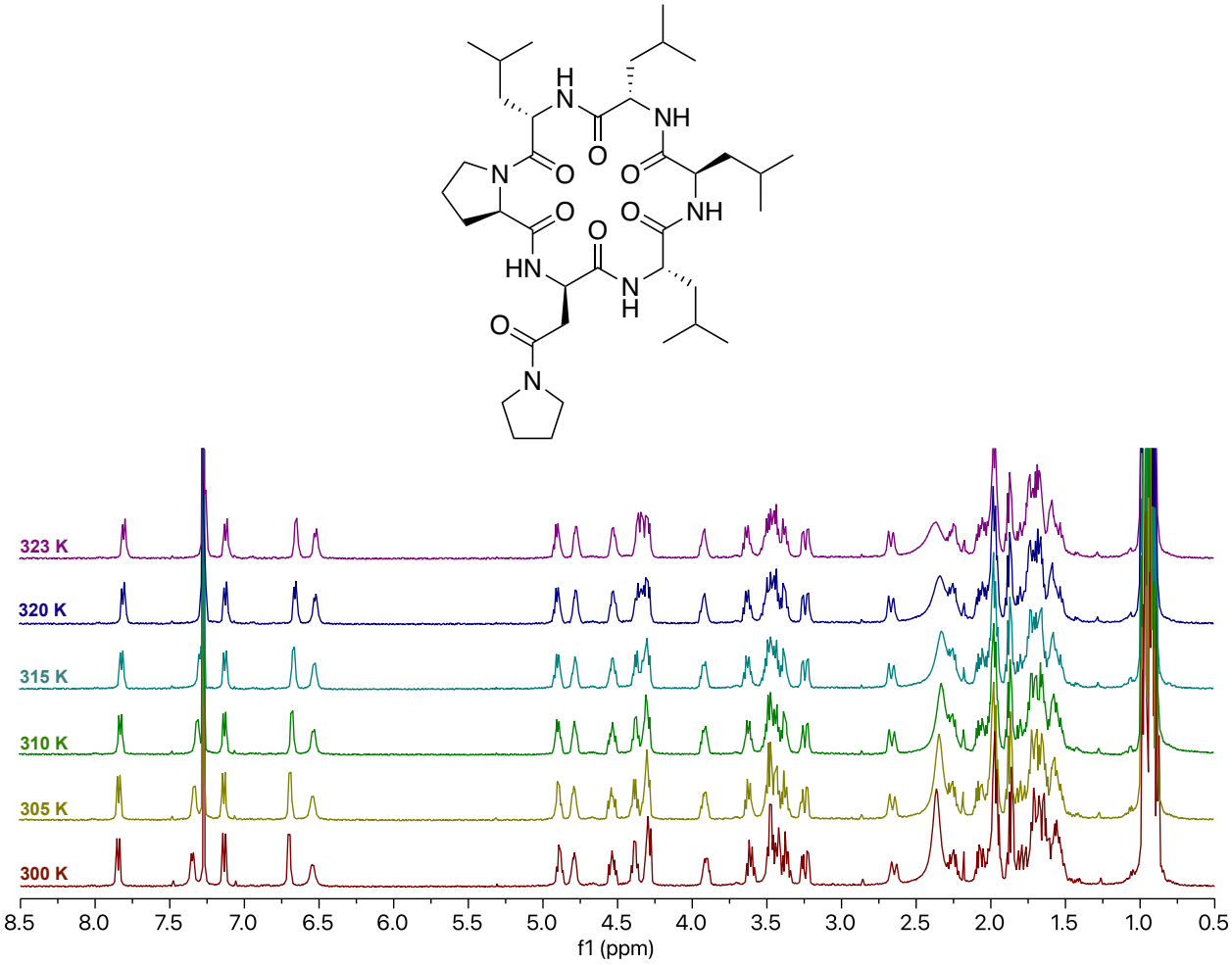

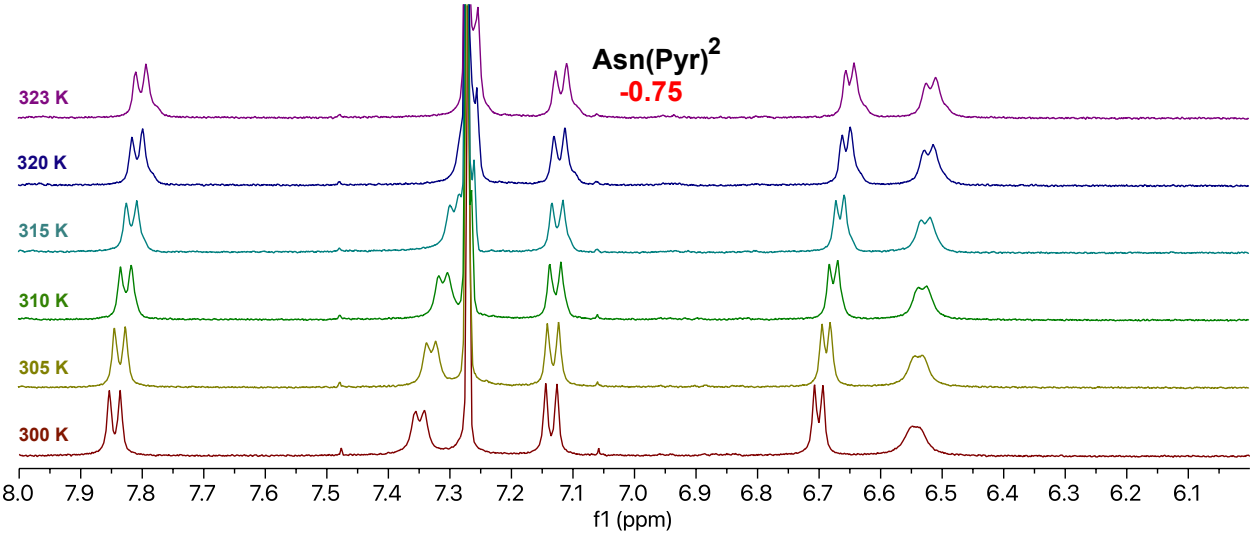

Figure S9. ^{1}H NMR of **3-Asn(Pyr)^{2}**.

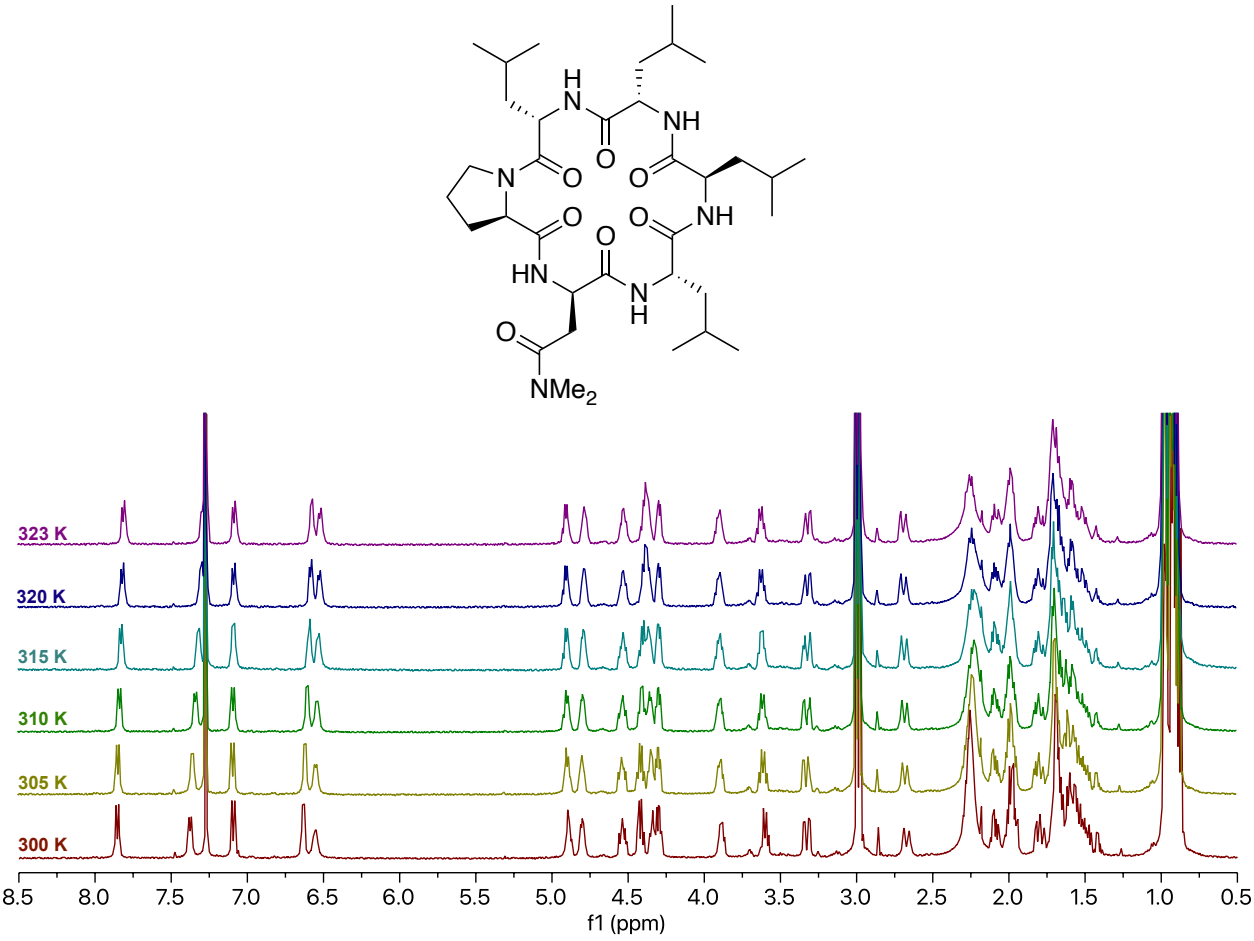

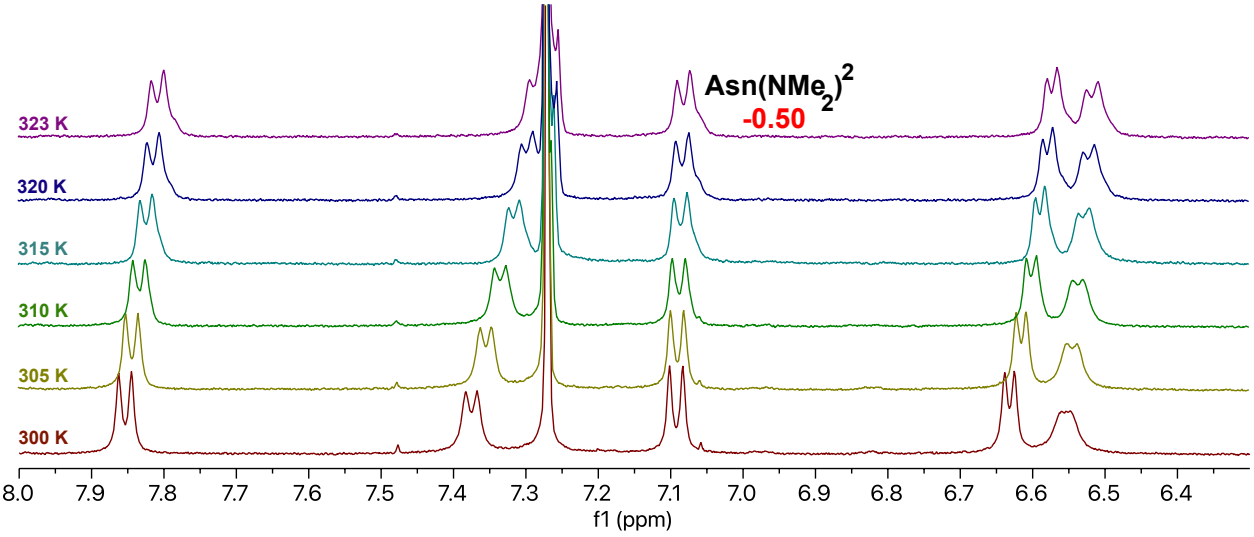

Figure S10. ^{1}H NMR of **3-Asn(NMe$_2$)^2**.

NOE Buildups and Interproton Distances

Interproton distance measurement was done by initial rate approximation.[2-5] ^{1}H-^{1}H NOESY spectra were recorded without solvent suppression with alternated mixing times of 200, 300, 400, 500, 600, 700 and 800 ms. The relaxation delay was set to 2 s. 16 scans were recorded with 2048 points in the direct dimension (F2) and 512 points in the indirect dimension (F1). NOE intensities were calculated by normalization of the integrals of both cross peaks and diagonal peaks of protons *a* and *b*.

$$\mathrm{NOE} = \left[\frac{(\text{cross peak } a * \text{cross peak } b)}{(\text{diagonal peak } a * \text{diagonal peak } b)}\right]^{1/2}$$

Seven normalized NOE intensities were obtained from the different mixing times. Slope from four consecutive mixing time of normalized NOE intensities giving a linear regression ($R^2 \geq 0.95$) was designated as the buildup rates (σ_{ab}).

$$r_{ab} = r_{ref}\left(\frac{\sigma_{ref}}{\sigma_{ab}}\right)^{1/6}$$

The distance between protons *a* and *b* (in Ångström) is indicated by r_{ab} while r_{ref} is the reference distance derived from δ-proline geminal protons (1.78 Å). The buildup rate of the reference protons is indicated by σ_{ref} and σ_{ab} is the buildup rate of protons *a* and *b*. The 10% deviation of calculated distances was applied to account for any errors from NOESY records and calculations. The summary of distance ranges comparing to the distance from crystal structure was summarized in Table S4.

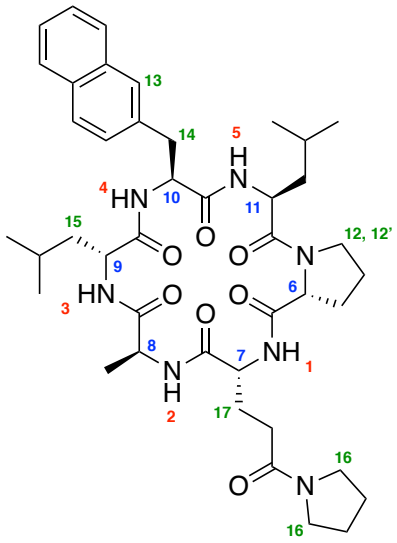

Table S5. Interproton Distances of 3-Pye^2(Ala^{3}Nal^5) Derived from NOE Buildup Rate in $CDCl_3$ and from Crystal Structure

No.	Proton *a*	Proton *b*	$\delta^{1}H_a$	$\delta^{1}H_b$	σ (x 10^{-5})	R^2	r_{ab} [Å]	r_{ab} range (± 10%)	Crys. r_{ab}	Cluster 4 466 conformers		T = 300K ensemble 5000 conformers	
										Avg. r_{ab}	Avg. violation	Avg. r_{ab}	Avg. violation
1	1	2	9.81	8.06	1.47	0.98	2.39	2.15 – 2.63	2.66	2.48	-0.15	2.78	0.15
2	1	12	9.81	4.24	0.65	1.00	2.74	2.46 – 3.01	2.95	3.52	0.51	3.47	0.46
3	1	7	9.81	4.48	0.48	0.99	2.88	2.60 – 3.17	2.65	2.91	-0.26	2.82	-0.35
4	2	5	8.06	6.77	0.21	0.97	3.30	2.97 – 3.63	3.23	3.42	-0.21	3.83	0.20
5	2	8	8.06	4.56	0.50	0.97	2.86	2.58 – 3.15	2.78	2.92	-0.23	2.92	-0.23
6	13	10	7.62	4.66	0.62	0.99	2.76	2.48 – 3.03	2.88	3.44	0.41	3.09	0.06
7	13	14	7.62	3.46	0.98	1.00	2.56	2.30 – 2.81	2.62	2.98	0.17	2.96	0.15
8	5	4	6.76	6.42	1.72	1.00	2.33	2.09 – 2.56	2.54	2.07	-0.49	2.60	0.04
9	5	11	6.76	5.02	0.68	0.98	2.72	2.45 – 2.99	2.79	2.94	-0.05	2.87	-0.12
10	3	15	6.66	1.19	1.48	0.99	2.38	2.15 – 2.62	2.63	2.54	-0.08	2.76	0.14
11	3	8	6.66	4.56	2.00	1.00	2.27	2.04 – 2.50	2.14	2.50	0.00	2.86	0.36
12	4	14	6.42	3.10	1.23	0.98	2.46	2.21 – 2.71	2.42	3.27	0.56	2.94	0.23
13	4	9	6.42	4.06	4.01	0.98	2.02	1.82 – 2.22	2.10	2.45	0.23	2.24	0.02
14	4	10	6.42	4.66	1.00	0.99	2.55	2.29 – 2.80	2.73	2.85	0.05	2.84	0.04
15	11	12	5.02	4.26	2.88	0.97	2.13	1.92 – 2.35	2.14	2.33	-0.02	2.28	-0.07
16	11	12'	5.02	3.61	1.65	1.00	2.34	2.11 – 2.58	2.95	2.35	-0.23	2.55	-0.03
17	10	16	4.66	3.60	0.47	0.95	2.89	2.60 – 3.18	2.95	4.03	0.85	4.21	1.03
18	7	17	4.48	2.38	2.15	1.00	2.24	2.02 – 2.47	2.30	2.27	-0.20	2.27	-0.20
19	9	15	4.05	1.02	1.83	0.97	2.30	2.07 – 2.53	2.33	2.63	0.10	2.62	0.09
Ref.	12	12'	4.26	3.61	8.58	1.00	1.78						
										stdev	0.33		0.31

^{1}H NMR

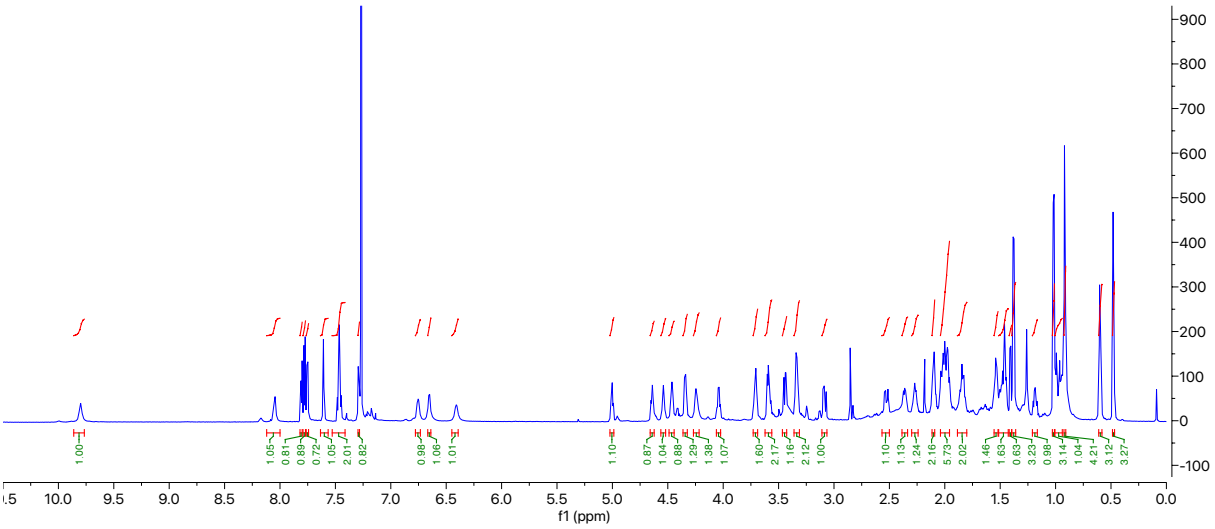

^{1}H NMR (800 MHz, $CDCl_3$) δ 9.80 (br, 1H), 8.05 (d, *J* = 8.7 Hz, 1H), 7.80 (d, *J* = 7.6 Hz, 1H), 7.78 (d, *J* = 8.4 Hz, 1H), 7.75 (d, *J* = 7.0 Hz, 1H), 7.61 (s, 1H), 7.49 – 7.44 (m, 2H), 7.29 (d, *J* = 9.4 Hz, 1H), 6.75 (br, 1H), 6.65 (d, *J* = 7.9 Hz, 1H), 6.41 (br, 1H), 5.00 (td, *J* = 8.1, 4.8 Hz, 1H), 4.64 (td, *J* = 9.2, 4.5 Hz, 1H), 4.54 (p, *J* = 7.0 Hz, 1H), 4.49 – 4.44 (m, 1H), 4.34 (dd, *J* = 9.0, 3.8 Hz, 1H), 4.27 – 4.22 (m, 1H), 4.04 (q, *J* = 8.0 Hz, 1H), 3.74 – 3.68 (m, 1H), 3.62 – 3.56 (m, 2H), 3.45 (dd, *J* = 14.2, 4.5 Hz, 1H), 3.36 – 3.31 (m, 2H), 3.09 (dd, *J* = 14.2, 9.6 Hz, 1H), 2.53 (dd, *J* = 17.1, 8.2 Hz, 1H), 2.39 – 2.34 (m, 1H), 2.30 – 2.24 (m, 1H), 2.13 – 2.07 (m, 2H), 2.06 – 1.94 (m, 5H), 1.85 (m, 2H), 1.54 – 1.51 (m, 1H), 1.51 – 1.43 (m, 2H), 1.41 (d, *J* = 6.7 Hz, 1H), 1.38 (d, *J* = 6.9 Hz, 3H), 1.21 – 1.16 (m, 1H), 1.02 (d, *J* = 6.0 Hz, 3H), 1.01 – 0.94 (m, 1H), 0.92 (d, *J* = 6.3 Hz, 3H), 0.60 (d, *J* = 6.6 Hz, 3H), 0.48 (d, *J* = 6.6 Hz, 3H).

^{13}C NMR

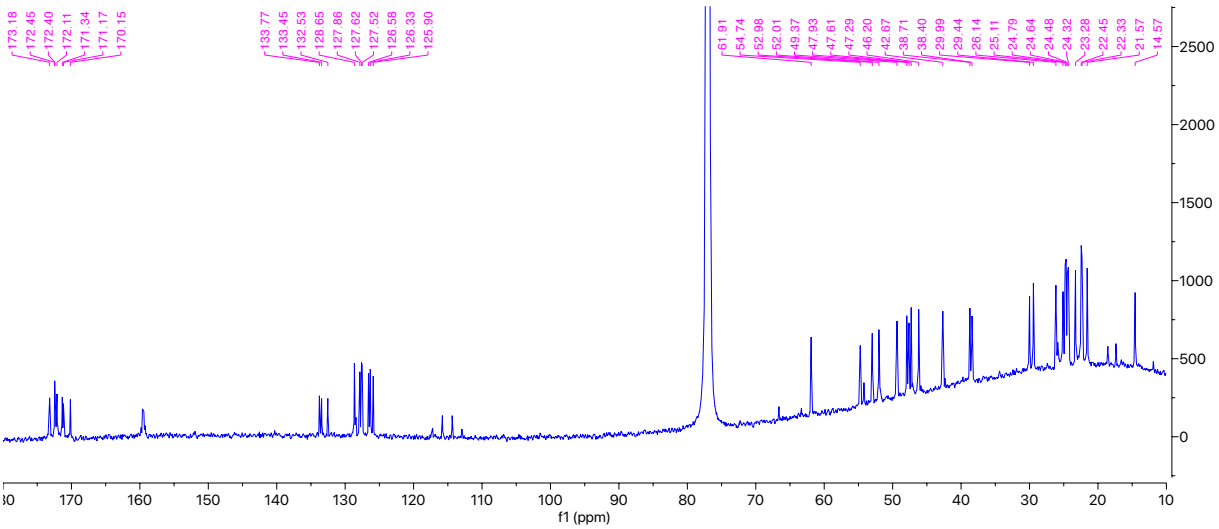

^{13}C NMR (201 MHz, $CDCl_3$) δ 173.18, 172.45, 172.40, 172.11, 171.34, 171.17, 170.15, 133.77, 133.45, 132.53, 128.65, 127.86, 127.62, 127.52, 126.58, 126.33, 125.90, 61.91, 54.74, 52.98, 52.01, 49.37, 47.93, 47.61, 47.29, 46.20, 42.67, 38.71, 38.40, 29.99, 29.44, 26.14, 25.11, 24.79, 24.64, 24.48, 24.32, 23.28, 22.45, 22.33, 21.57, 14.57.

^{1}H-^{1}H COSY

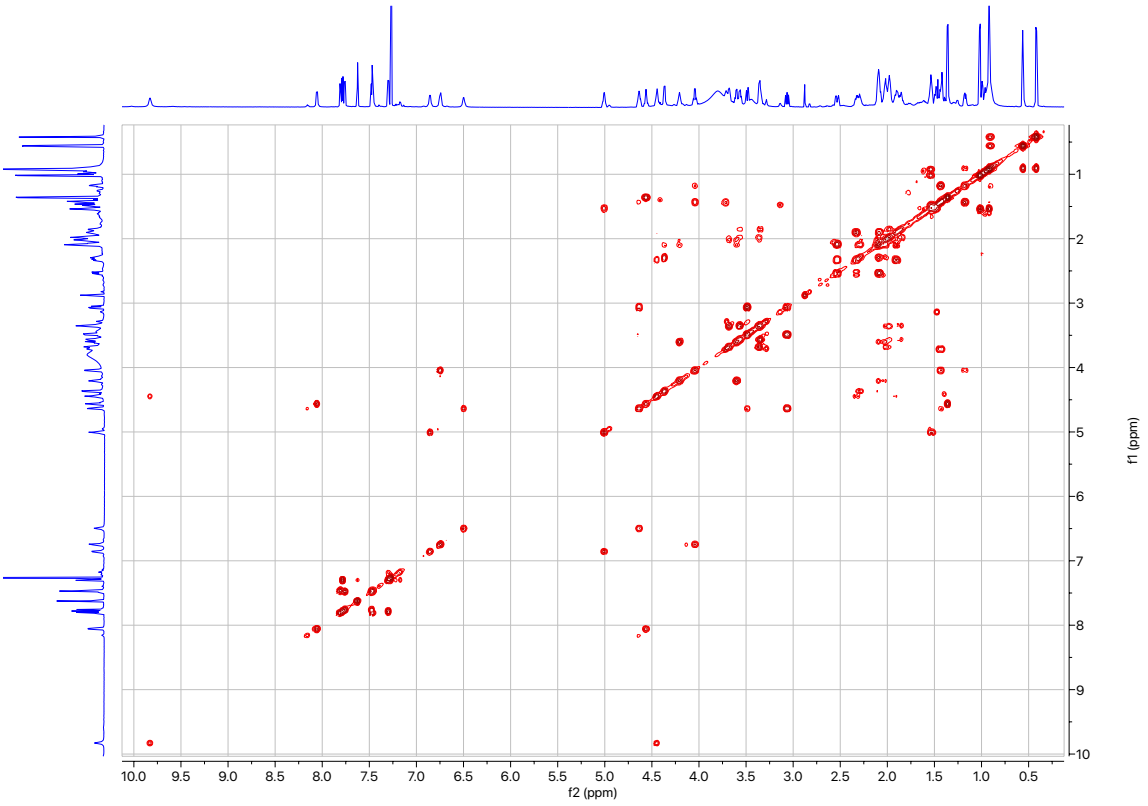

^{1}H-^{13}C HSQC

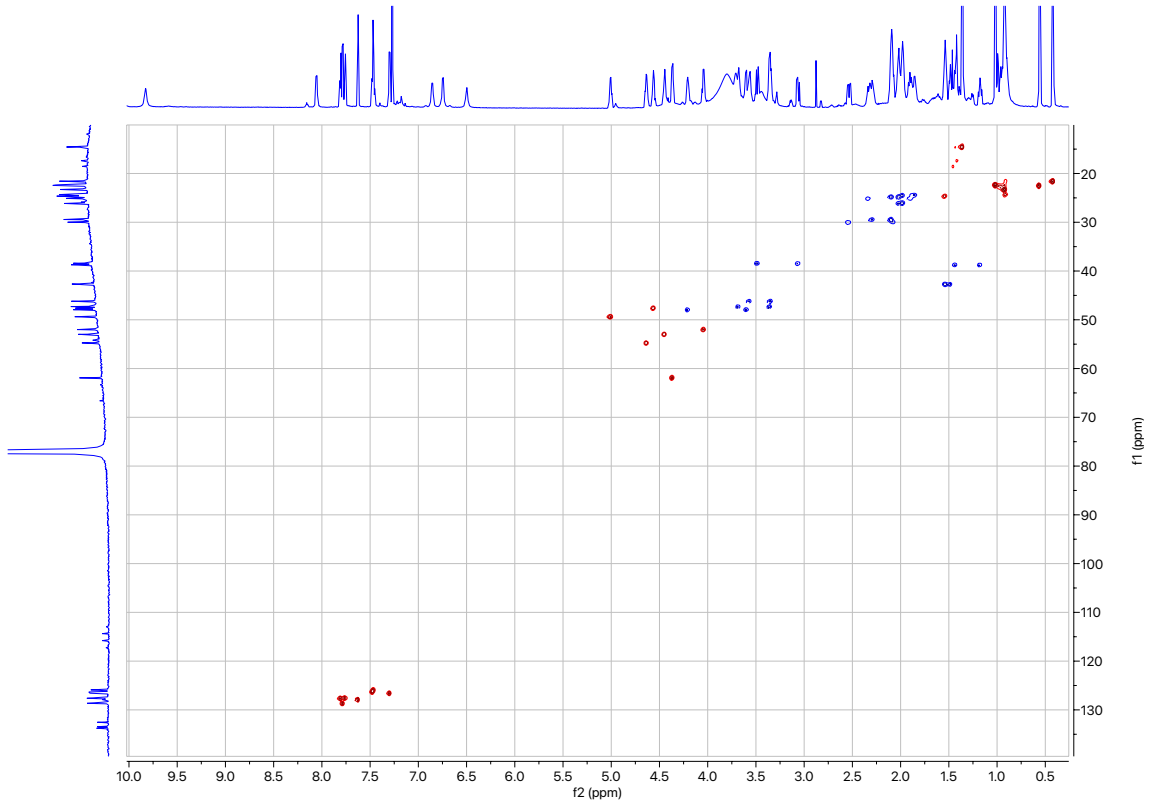

^{1}H-^{1}H TOCSY

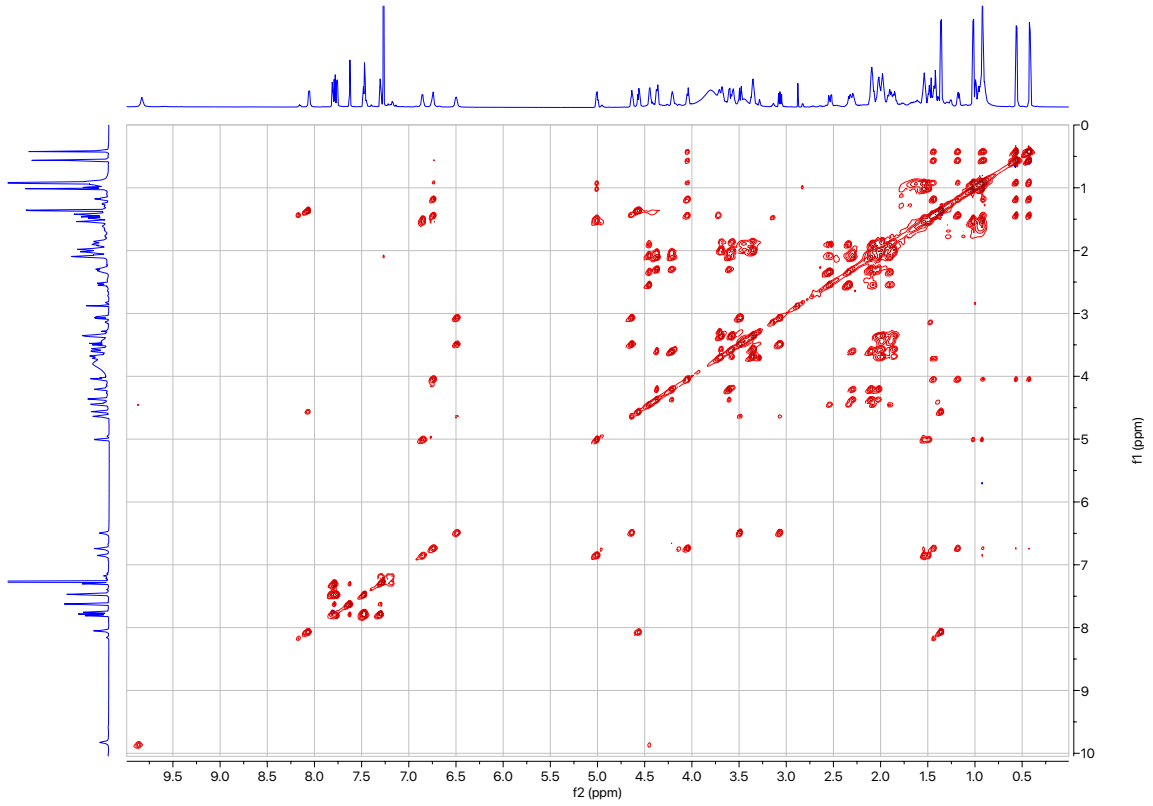

^{1}H-^{13}C HSQC-TOCSY

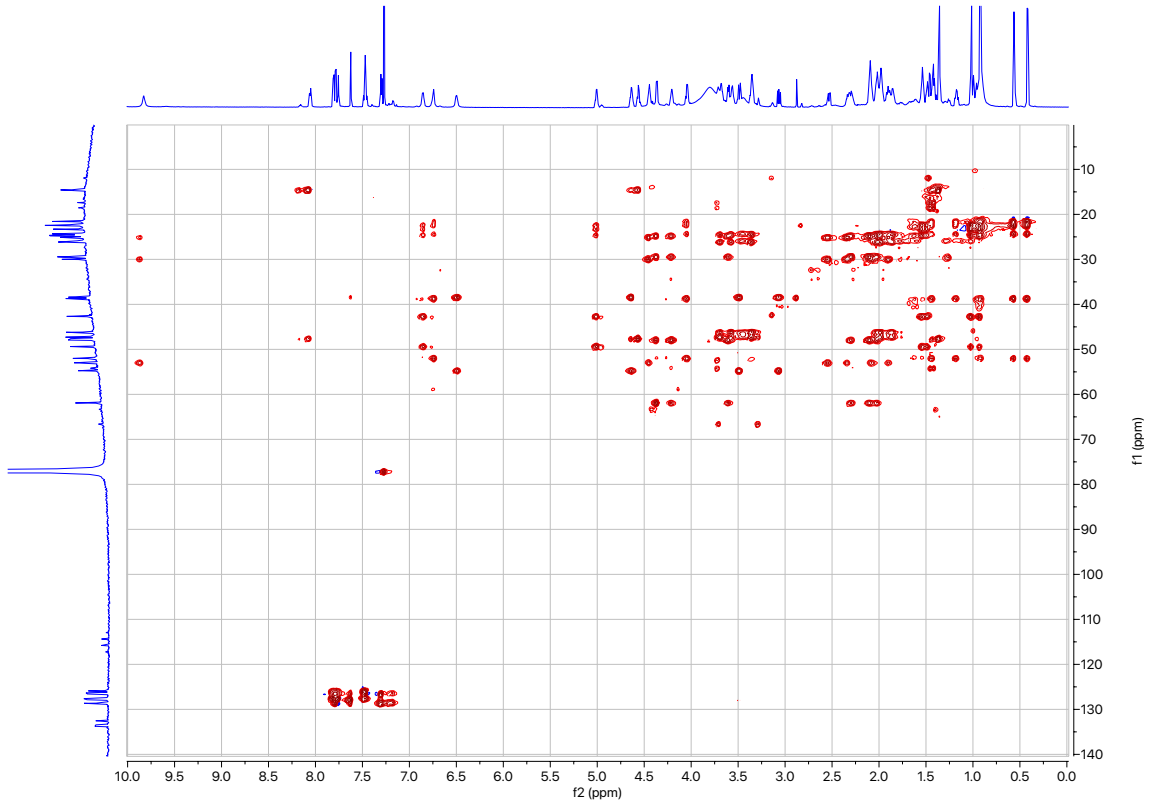

^{1}H-^{1}H NOESY

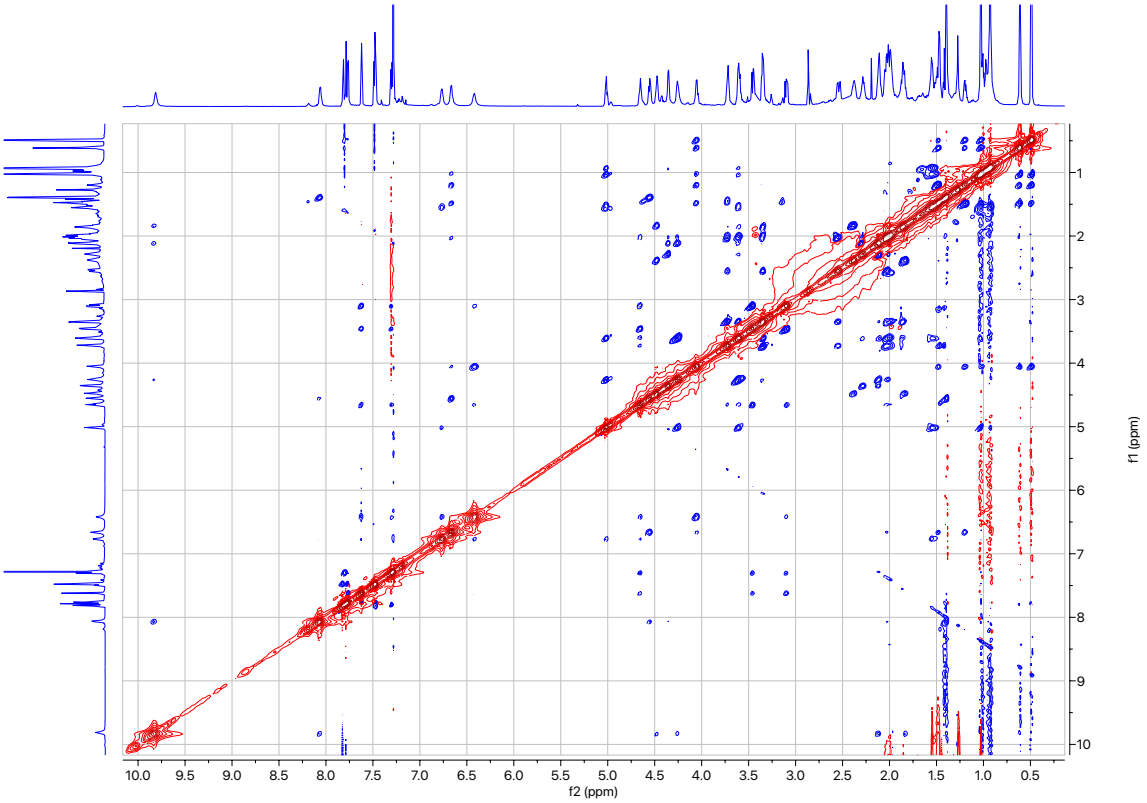
10.0
9.5
9.0
8.5
8.0
7.5
7.0
6.5
6.0
5.5
5.0
4.5
4.0
3.5
3.0
2.5
2.0
1.5
1.0
0.5
f2 (ppm)
1
2
3
4
5
6
7
8
9
10
f1 (ppm)

Intramolecular Hydrogen Bonding (IMHB) Patterns

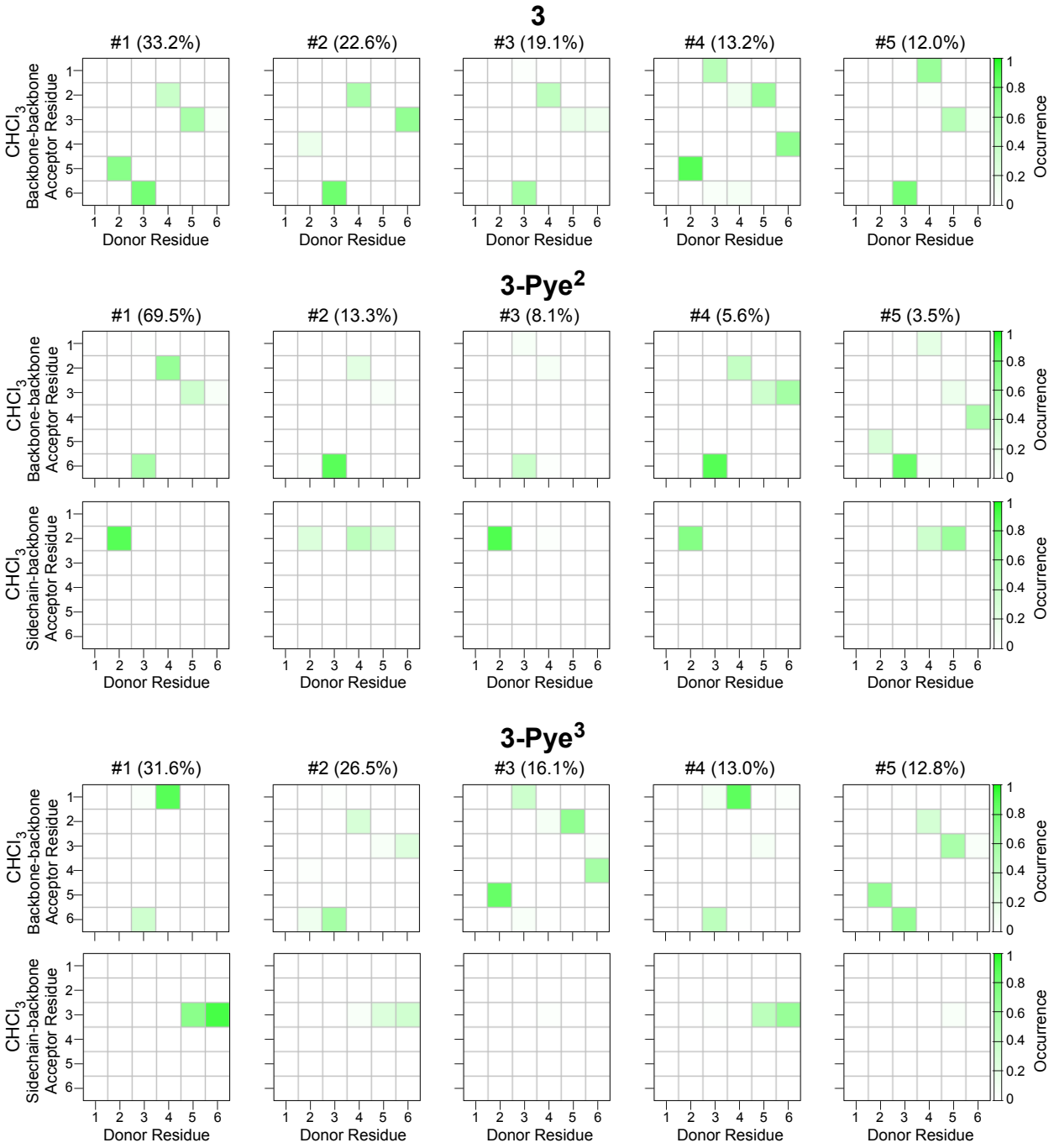

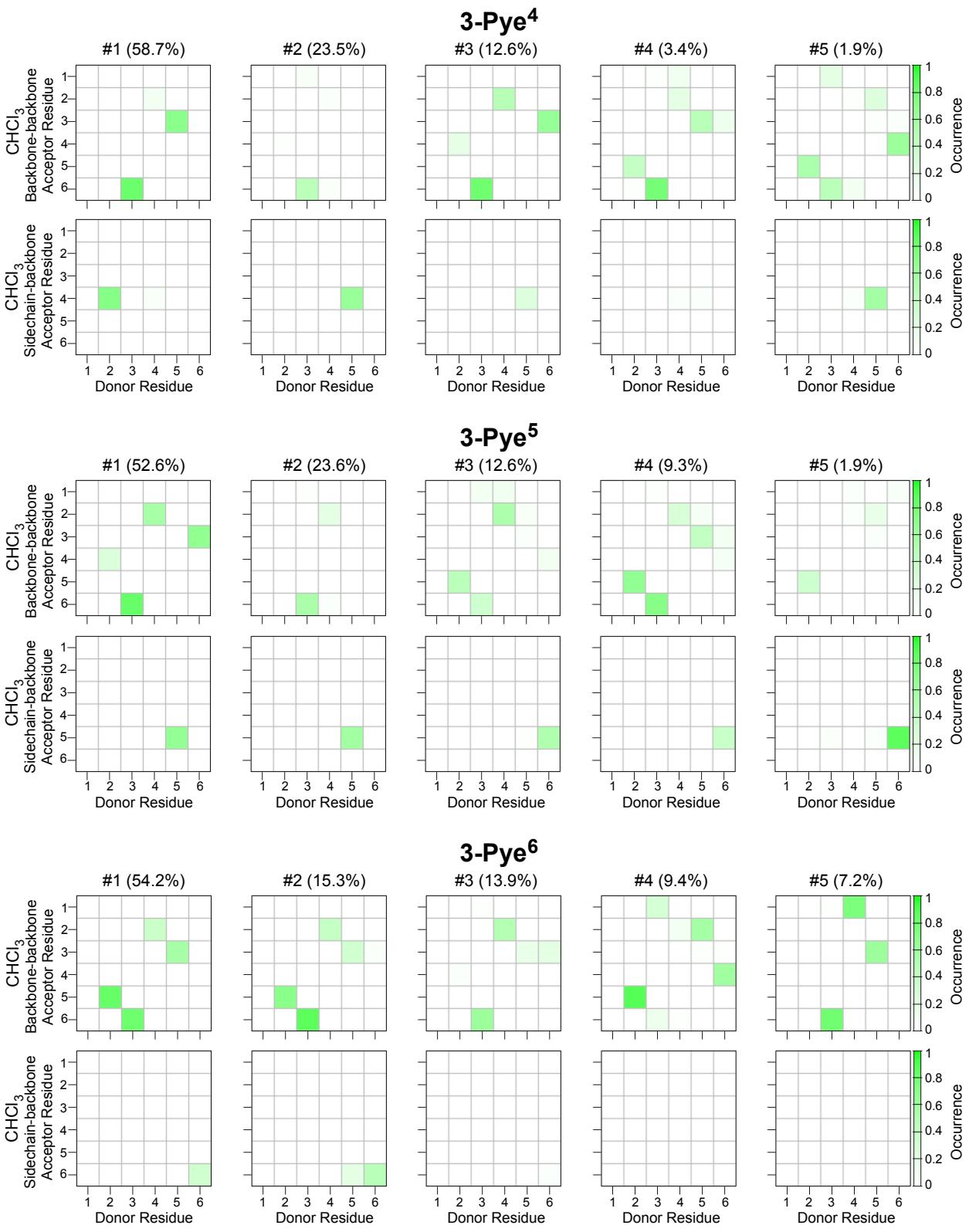
3-Pye4
#1 (58.7%)
#2 (23.5%)
#3 (12.6%)
#4 (3.4%)
#5 (1.9%)
3-Pye5
#1 (52.6%)
#2 (23.6%)
#3 (12.6%)
#4 (9.3%)
#5 (1.9%)
3-Pye6
#1 (54.2%)
#2 (15.3%)
#3 (13.9%)
#4 (9.4%)
#5 (7.2%)
CHCl3 Backbone-backbone Acceptor Residue
CHCl3 Sidechain-backbone Acceptor Residue
Donor Residue
Occurrence

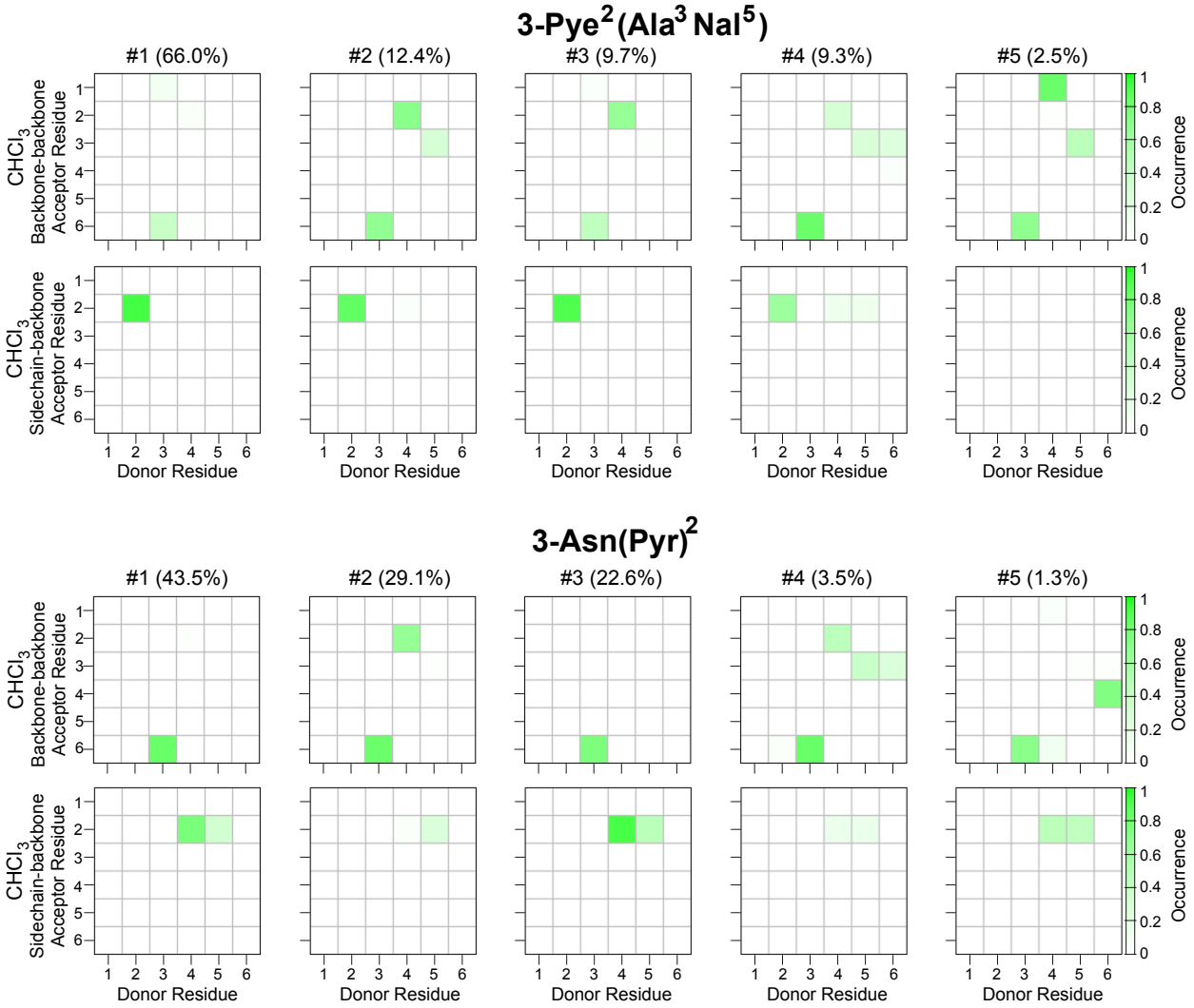

Figure S11 IMHB patterns of compound **3** series.

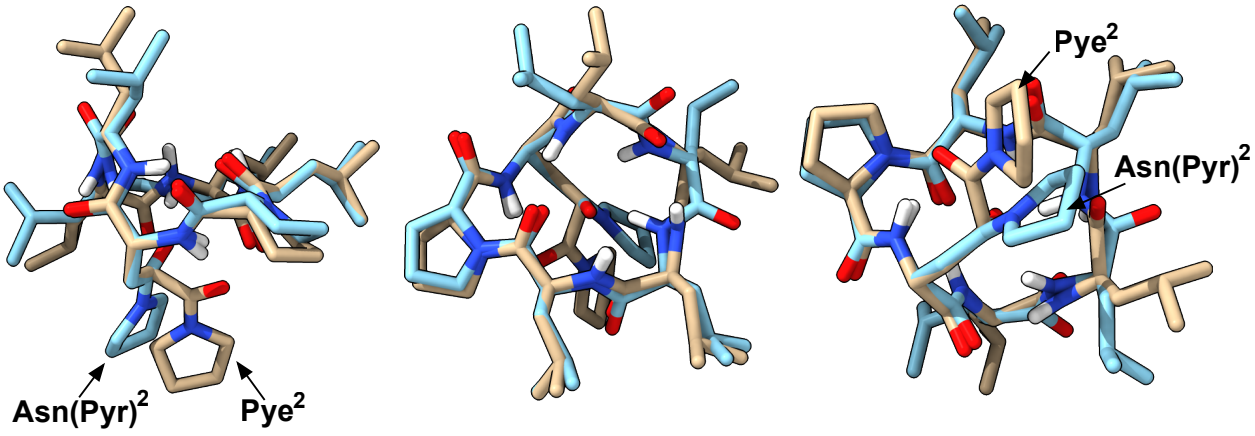

Figure S12 Overlay between **3-Pye²** (gold) and **3-Asn(Pyr)²** (blue). Backbone rmsd = 0.72 Å

General Procedure of X-ray Structure Determination

Crystals of **3-Pye^2(Ala^{3}Nal^5)** and **3-Pye^2(HPhe^5)** were obtained by pentane-THF vapor diffusion. In each case, a prism was microscopically selected under crossed polarizers, mounted on a MiTeGen polyimide loop, and cooled to 100 K on a Rigaku Synergy-S X-ray diffractometer. Diffraction of Cu Kα radiation from a PhotonJet-S microfocus source was detected using a HyPix-6000HE hybrid photon counting detector. Bijvoet pairs were collected for absolute structure determination. Screening, indexing, data collection, and data processing were performed with CrysAlis^{Pro}.[6] The structure was solved using SHELXT and refined using SHELXL following established strategies.[7-9] All non-H atoms were refined anisotropically. H atoms were placed at calculated positions and refined with a riding model and coupled isotropic displacement parameters (1.5 × U_{eq} for methyl groups and 1.2 × U_{eq} for all others). Anomalous dispersion was used to refine the absolute structure (Flack) parameter.

Crystal Data and Structure Refinement for 3-Pye^2(HPhe^5)

Empirical formula	C42 H65 N7 O7
Formula weight	780.01
Temperature	100.1(1) K
Wavelength	1.54184 Å
Crystal system	Trigonal
Space group	$P3_221$
Unit cell dimensions	a = 18.9888(2) Å
	b = 18.9888(2) Å
	c = 22.4565(2) Å
Volume	7012.41(16) Å^3
Z	6
Density (calculated)	1.108 Mg/m^3
Absorption coefficient	0.614 mm^{-1}
F(000)	2532
Crystal size	0.32 x 0.07 x 0.06 mm^3
Theta range for data collection	2.687 to 70.071°.
Index ranges	-17<=h<=23, -22<=k<=23, -27<=l<=27
Reflections collected	60958
Independent reflections	8894 [R(int) = 0.0306]
Completeness to theta = 67.684°	100.0 %
Absorption correction	Gaussian
Max. and min. transmission	1.000 and 0.763
Refinement method	Full-matrix least-squares on F^2
Data / restraints / parameters	8894 / 1611 / 711
Goodness-of-fit on F^2	1.040

Final R indices [I>2σ(I)]	R1 = 0.0606, wR2 = 0.1734
R indices (all data)	R1 = 0.0637, wR2 = 0.1773
Absolute structure parameter	0.1(3)
Extinction coefficient	n/a
Largest diff. peak and hole	0.400 and -0.252 e.Å^{-3}

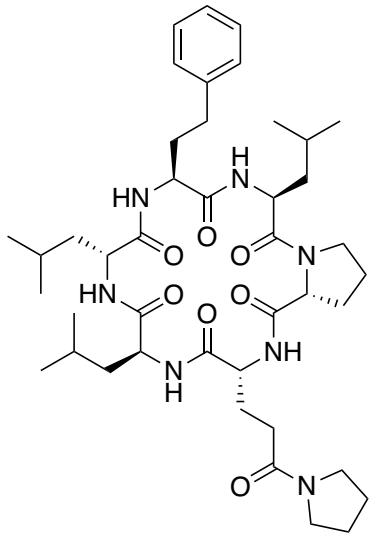

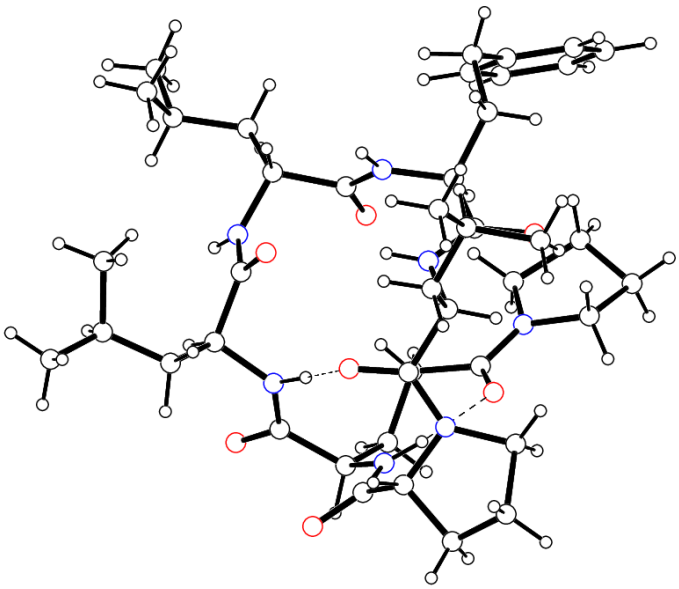

Crystal Data and Structure Refinement for 3-Pye^2(Ala^{3}Nal^5)

Empirical formula	C42 H59 N7 O7
Formula weight	773.96
Temperature	100.0(1) K
Wavelength	1.54184 Å
Crystal system	Trigonal
Space group	$P3_221$
Unit cell dimensions	a = 18.8195(2) Å
	b = 18.8195(2) Å
	c = 22.4826(3) Å
Volume	6895.94(17) Å^3
Z	6
Density (calculated)	1.118 Mg/m^3
Absorption coefficient	0.622 mm^{-1}
F(000)	2496
Crystal size	0.13 x 0.07 x 0.05 mm^3
Theta range for data collection	2.711 to 70.067°.
Index ranges	-22<=h<=20, -22<=k<=22, -27<=l<=26
Reflections collected	90045
Independent reflections	8733 [R(int) = 0.0369]
Completeness to theta = 67.684°	100.0 %
Absorption correction	Gaussian
Max. and min. transmission	1.000 and 0.858
Refinement method	Full-matrix least-squares on F^2
Data / restraints / parameters	8733 / 1957 / 806
Goodness-of-fit on F^2	1.044
Final R indices [I>2σ(I)]	R1 = 0.0714, wR2 = 0.2074
R indices (all data)	R1 = 0.0781, wR2 = 0.2172
Absolute structure parameter	0.1(4)
Extinction coefficient	n/a
Largest diff. peak and hole	0.473 and -0.291 e.Å^{-3}

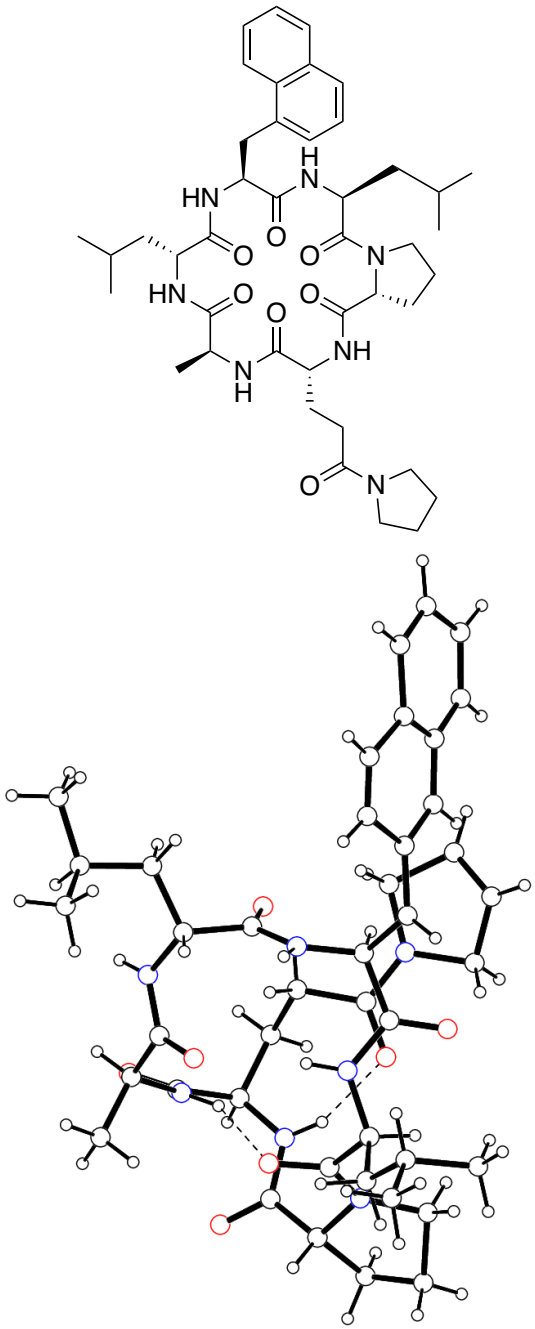
HN
H
N
O
O
O
N
HN
O
O
O
O
NH
N
H
O
N

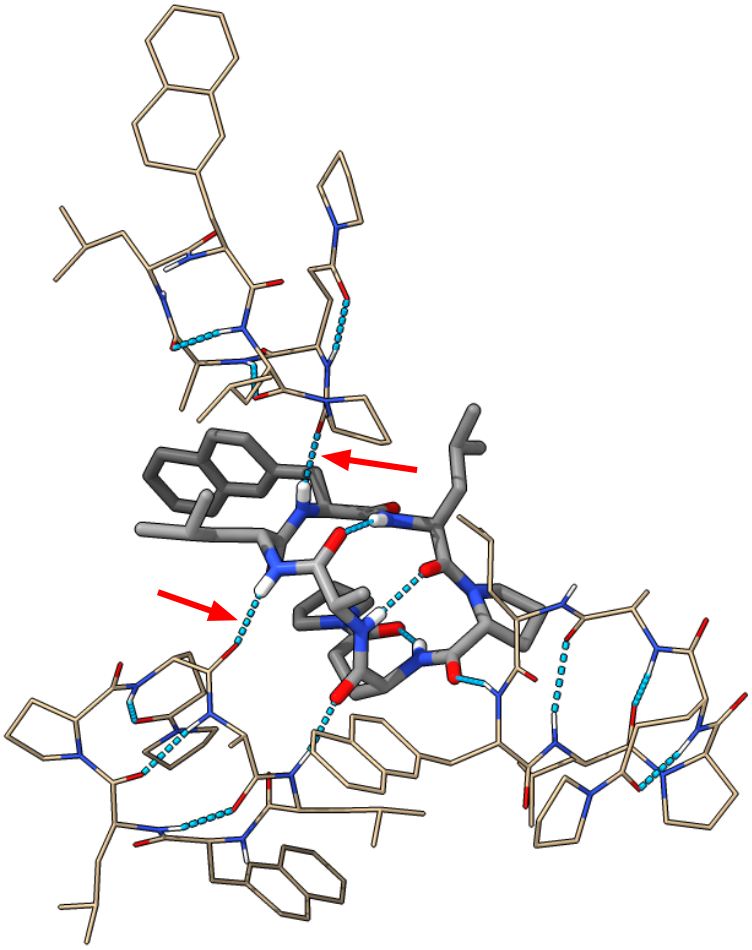

Figure S13. Crystal lattice of **3-Pye^{2}-Ala^{3}-^{2}Nal^{5}** shows intermolecular hydrogen bonds (red arrows).

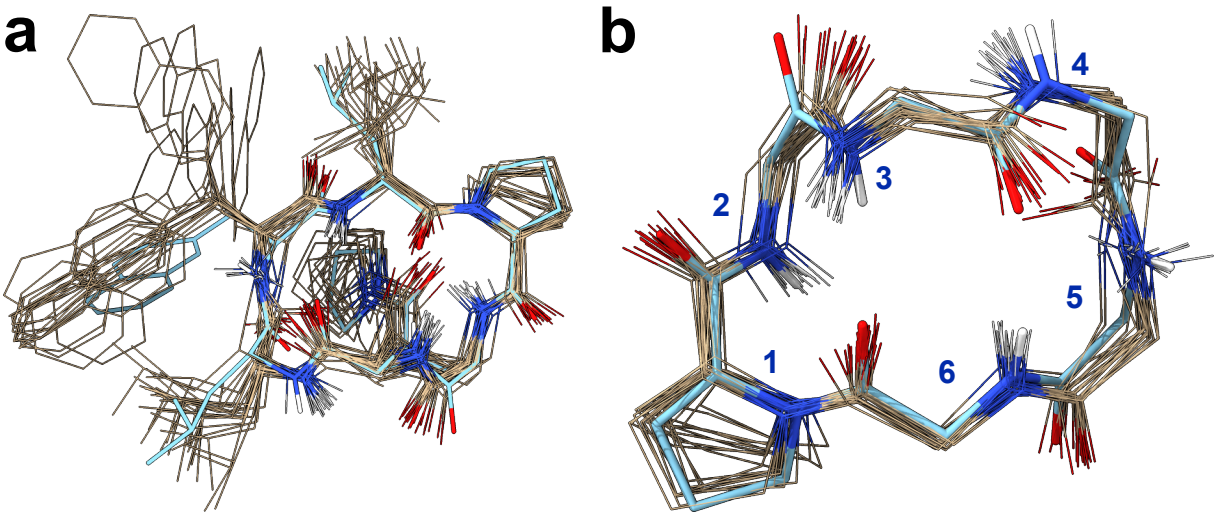

Figure S14. (**a**) Overlays of **3-Pye^{2}(Ala^{3}Nal^{5})** crystal structure (blue) and 20 simulated McMD structures (gold). (**b**) Crystal structure and simulated structures show similar backbone geometry. Amide protons of simulated 3rd and 6th residues are consistent to the crystal structure, while amide 4th and 5th NH distort from crystal structure which allow to form IMHB.

LC-MS Spectra

Column: Kinetex® C18 (30 x 2.1 mm, 2.6 µm 100 Å)

Wavelength: 200 or 254 nm

Temperature: 50 ºC

Flow rate: 0.4 mL/min

Injection: 10 µL

Mobile phase: A phase: 0.1% formic acid in Milli-Q water

B phase: 0.1% formic acid in CH_3CN

Gradient elution: 0-6 min (20-100% B), 6-7 min (100% B)

LCMS of compound **1**

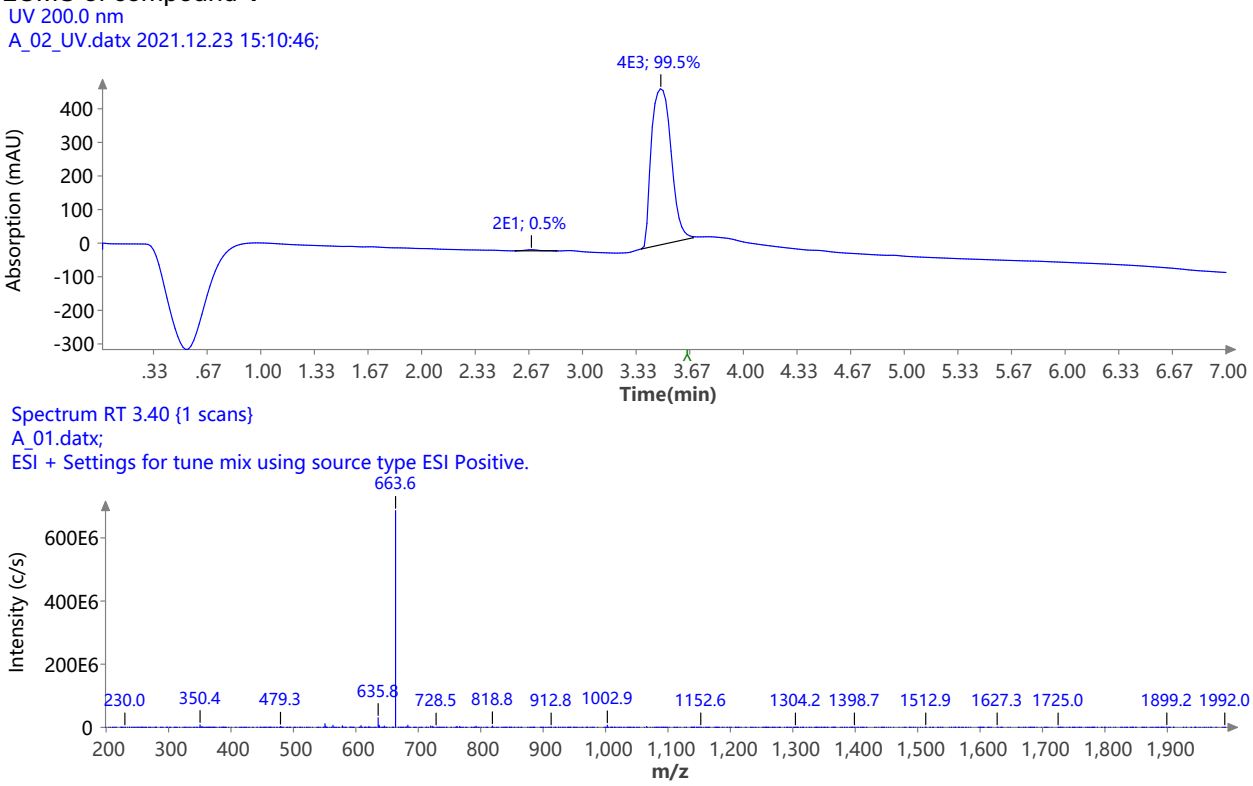

LCMS of compound **1-Pye^2**

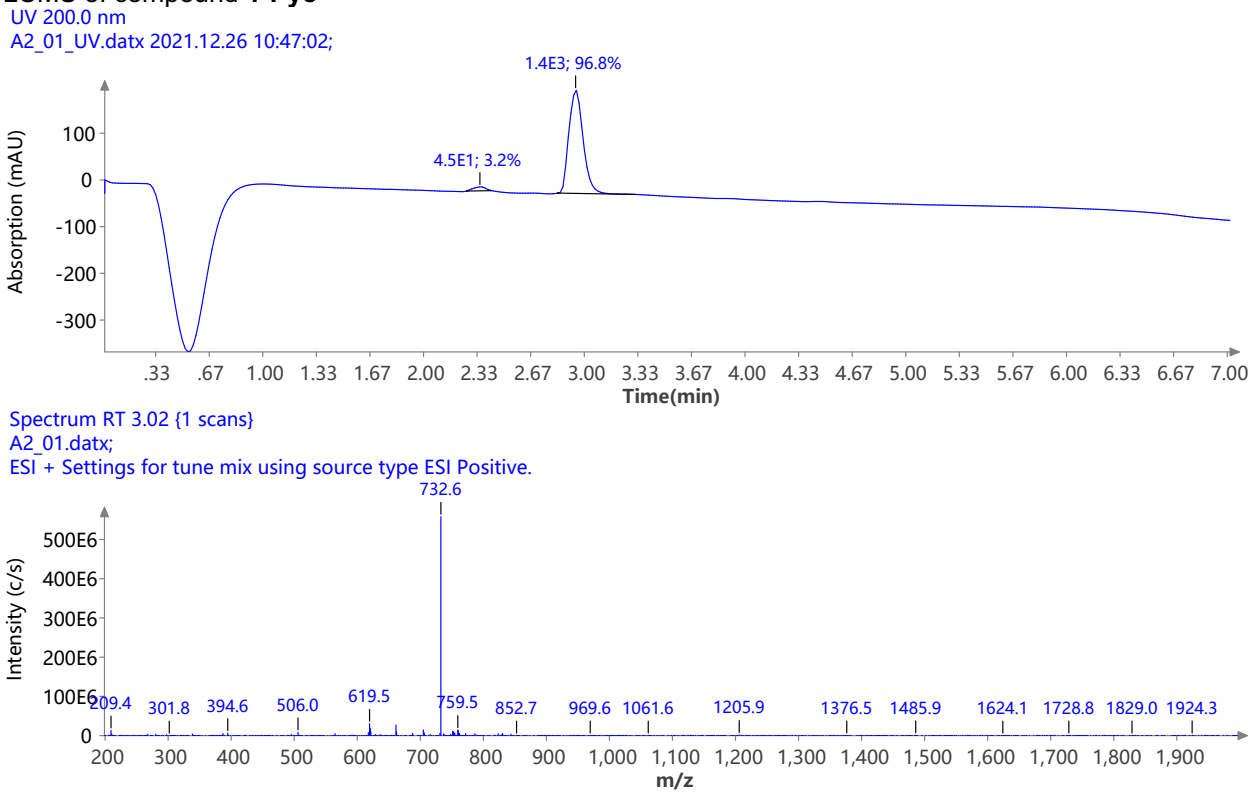

LCMS of compound **1-Pye^3**

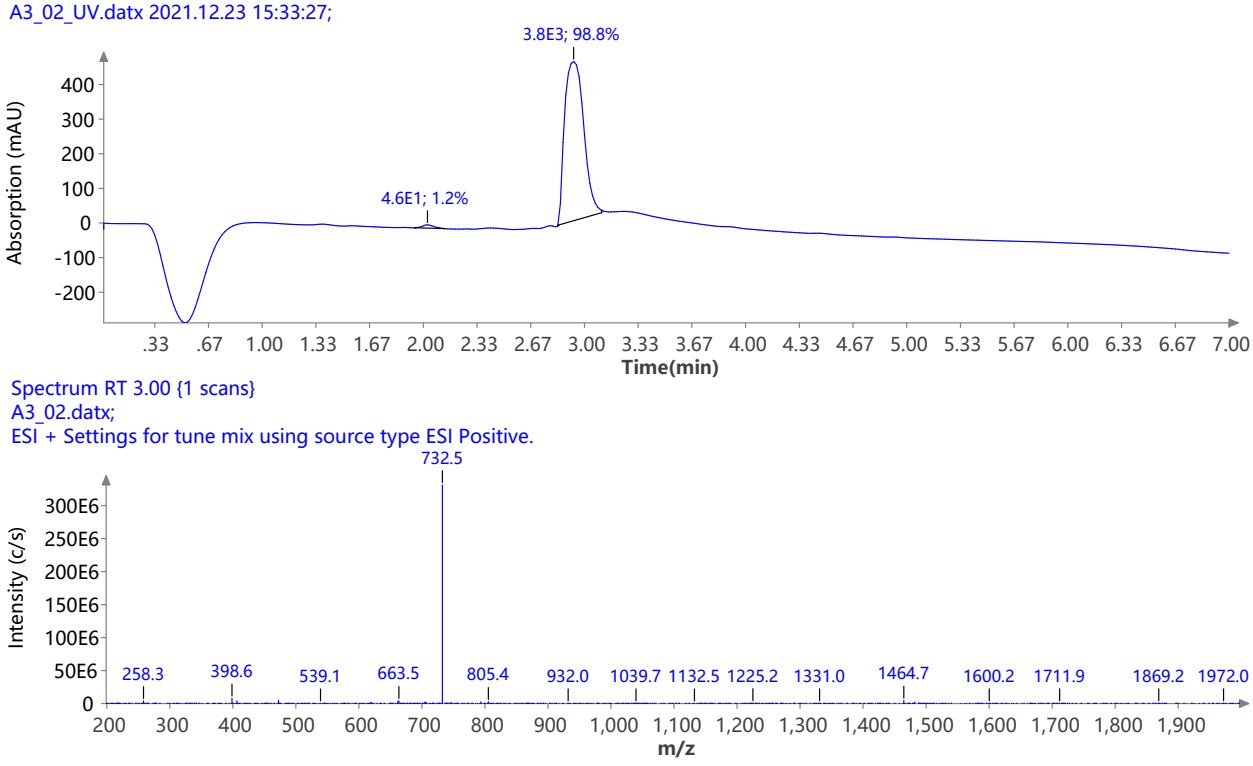

LCMS of compound **1-Pye[4]**

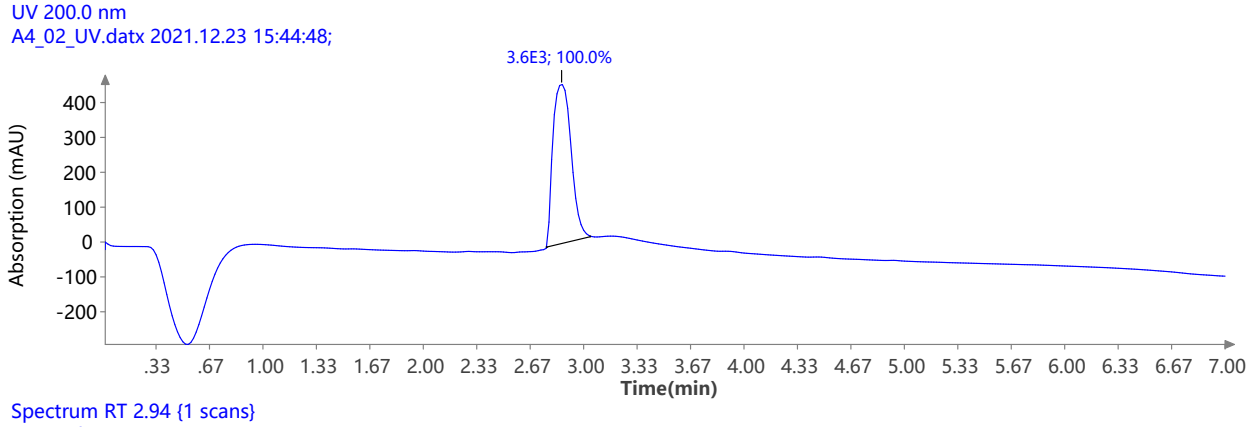

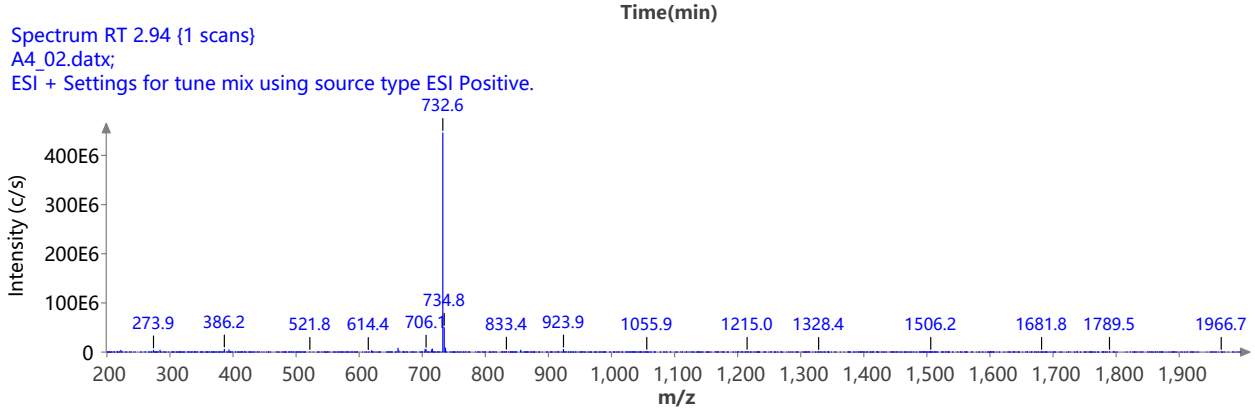

LCMS of compound **1-Pye[5]**

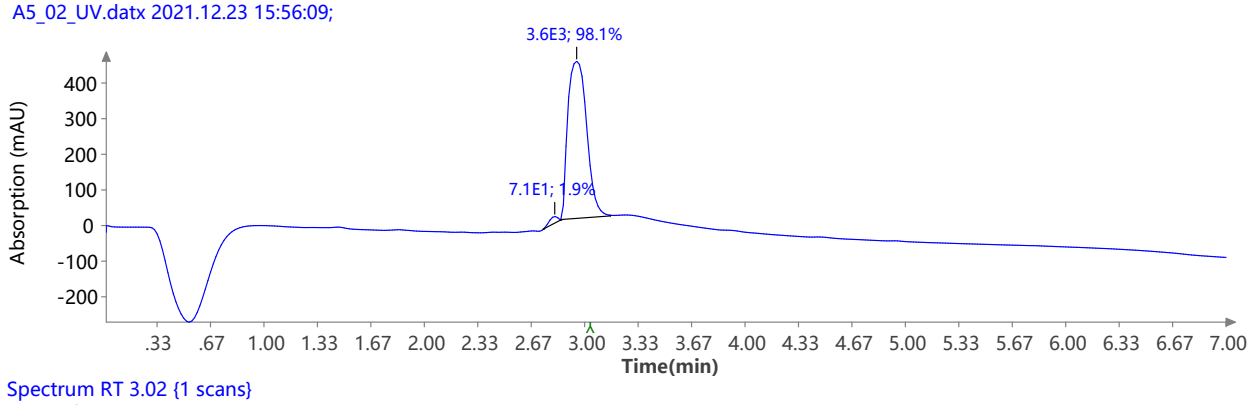

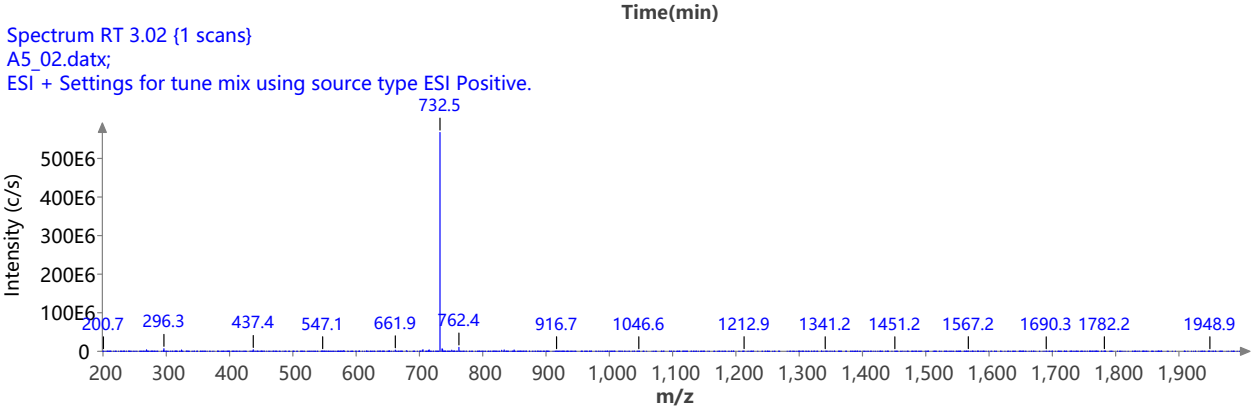

LCMS of compound **1-Pye**[6]

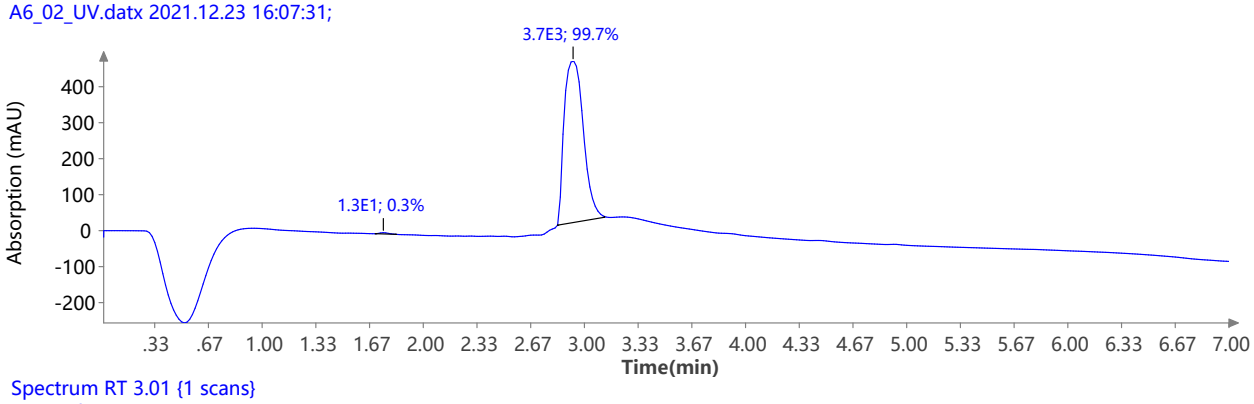

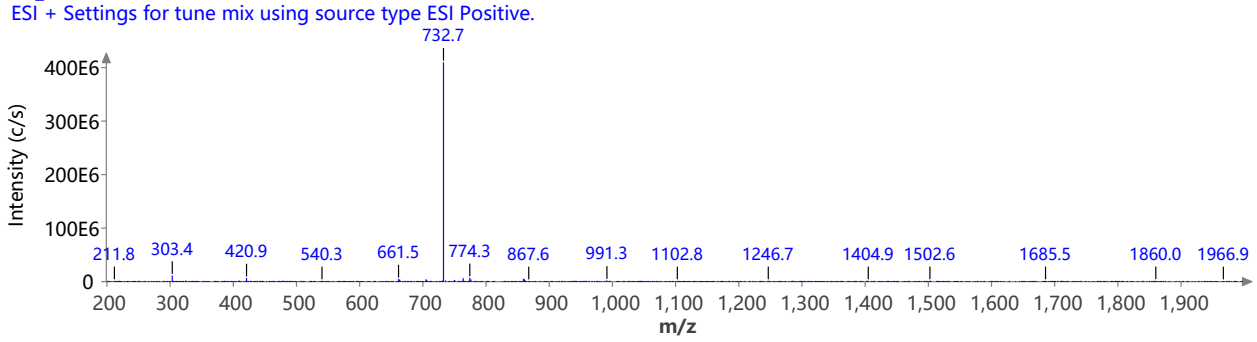

LCMS of compound **2**

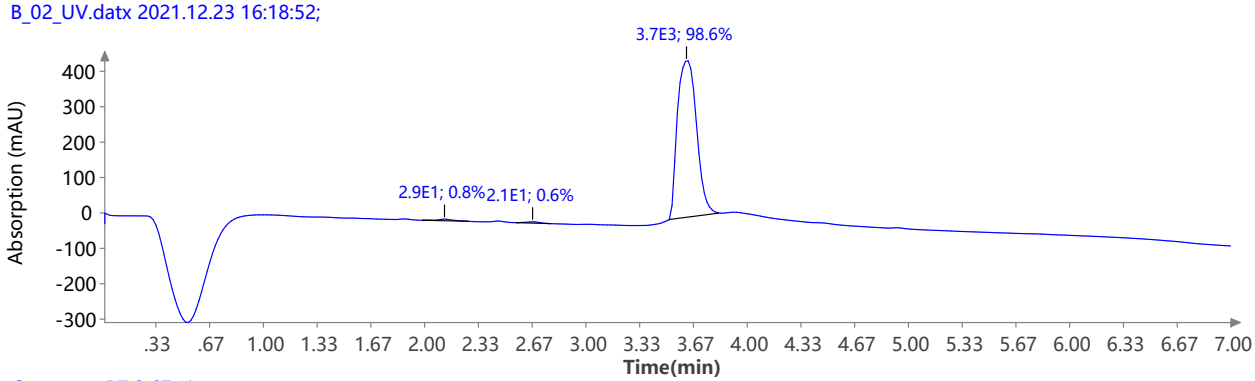

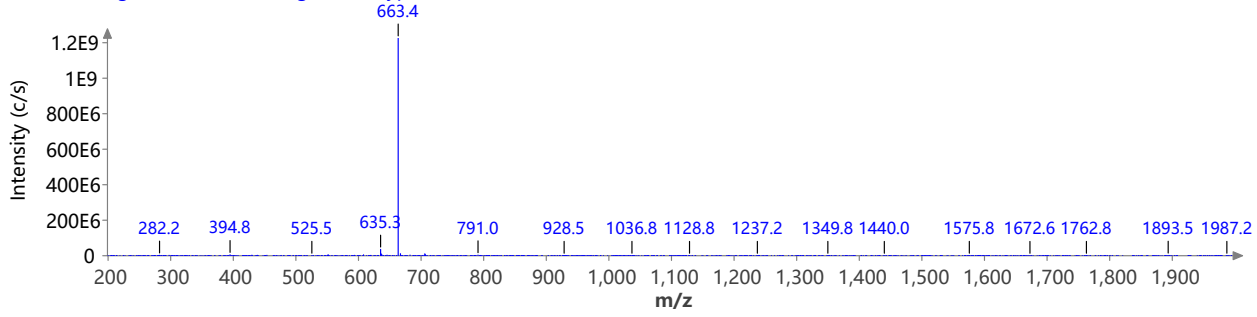

LCMS of compound **2-Pye^2**

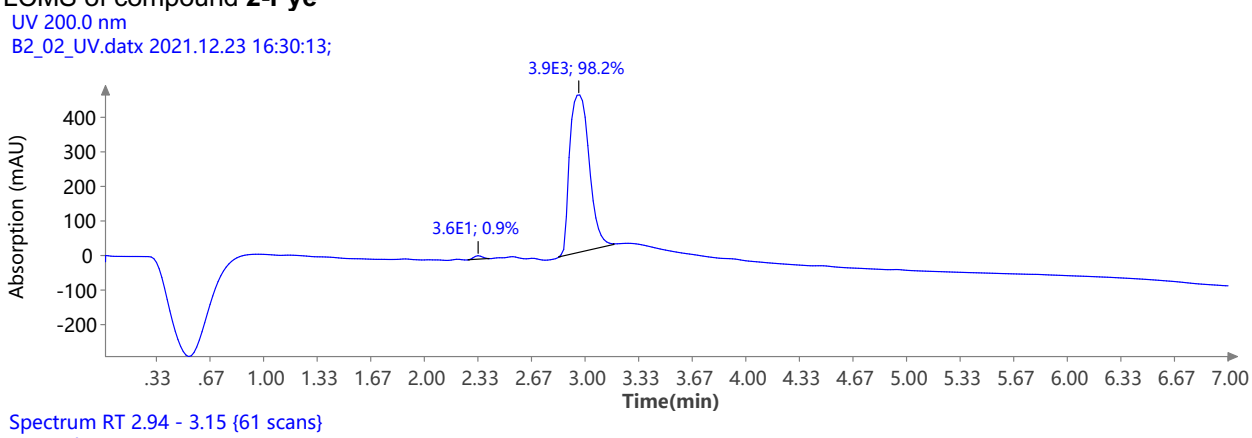

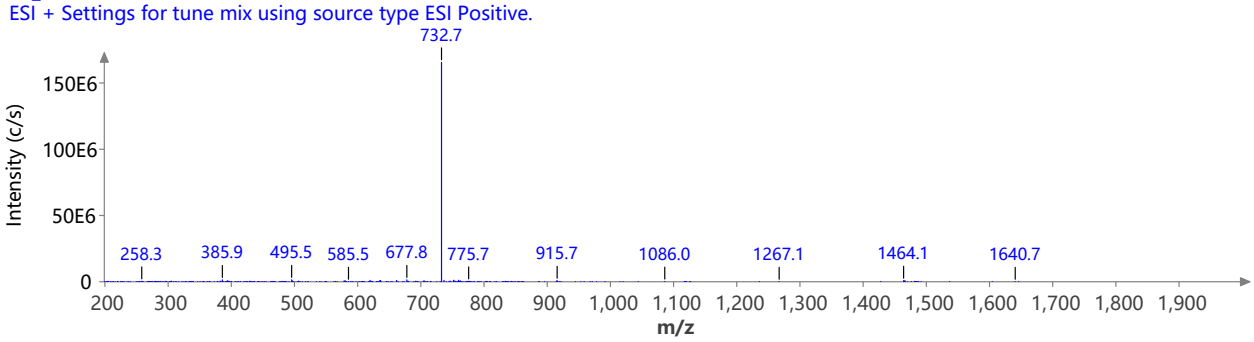

LCMS of compound **2-Pye^3**

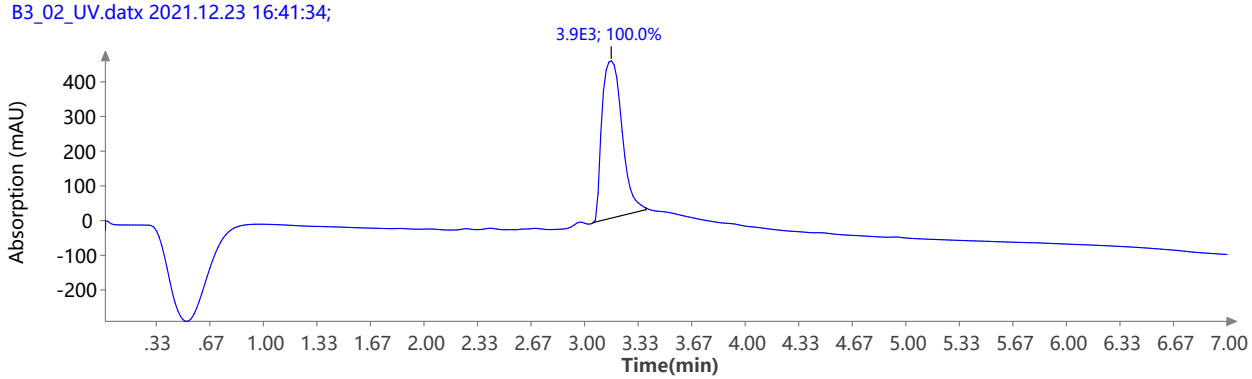

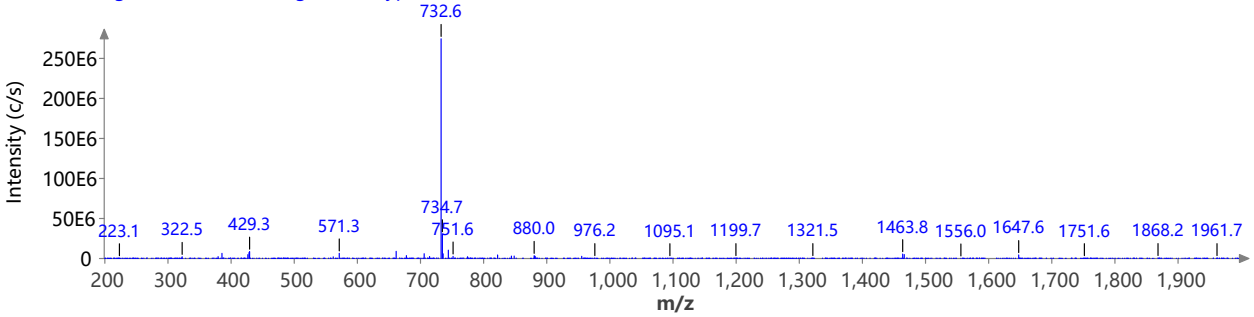

LCMS of compound **2-Pye**[4]

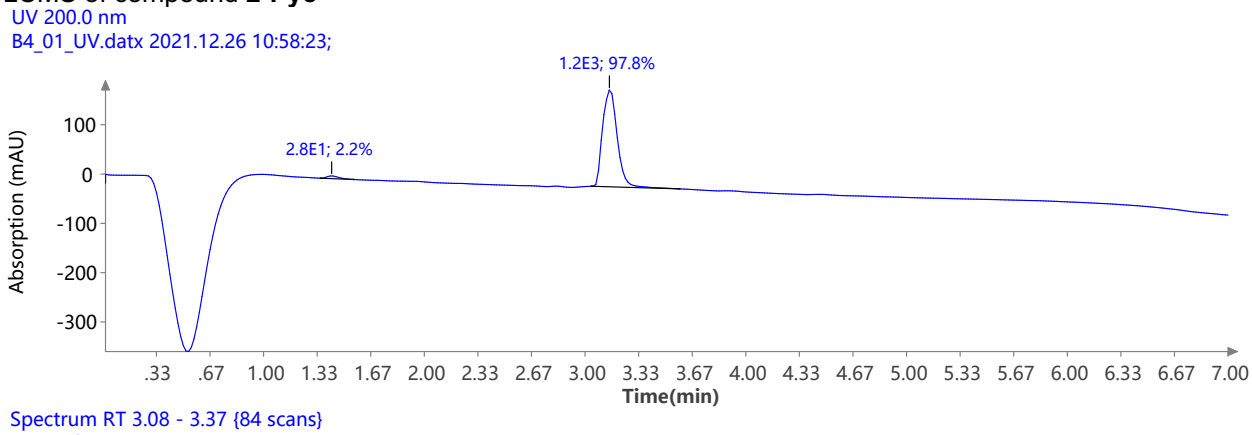

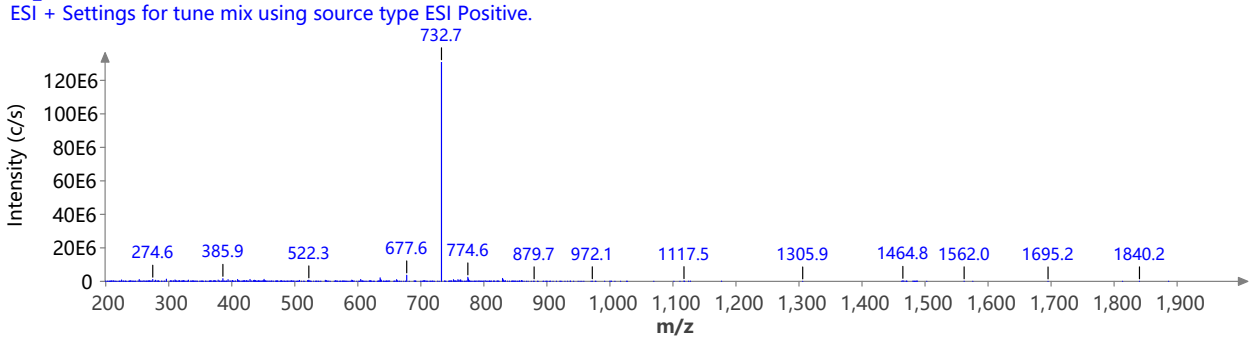

LCMS of compound **2-Pye**[5]

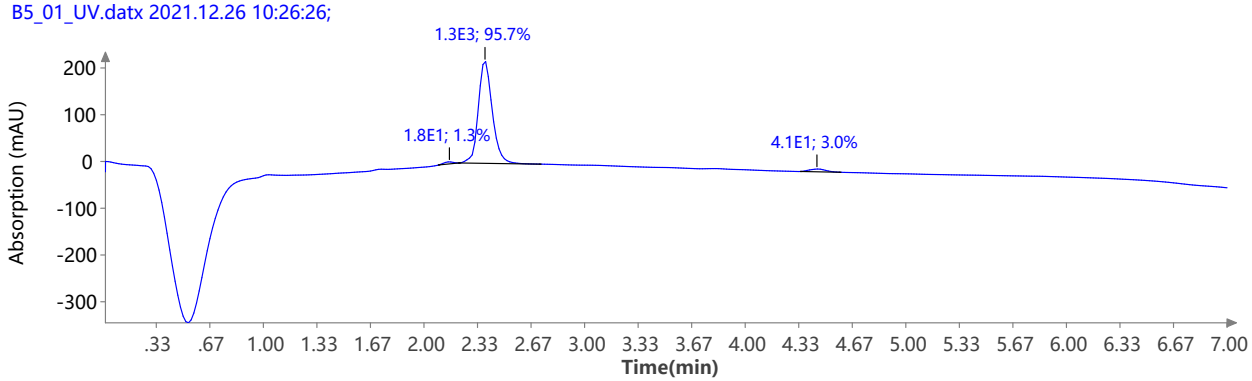

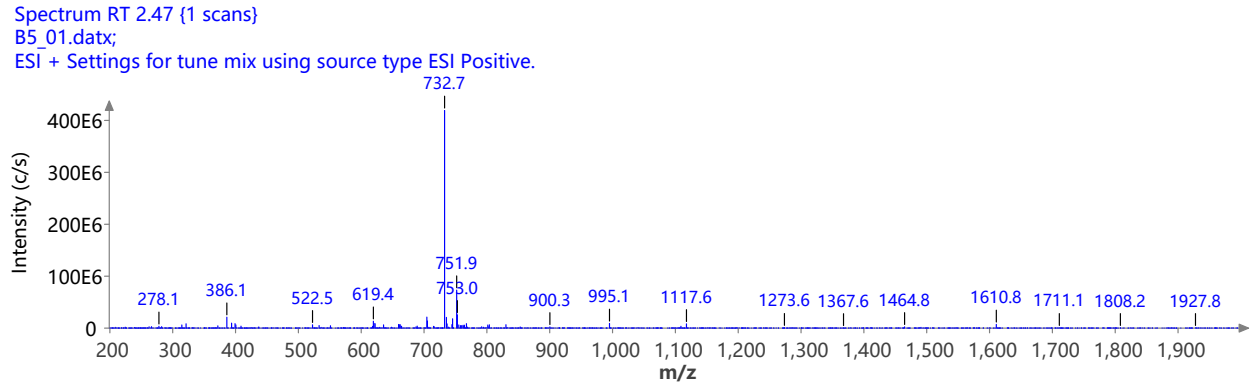

LCMS of compound **2-Pye**[6]

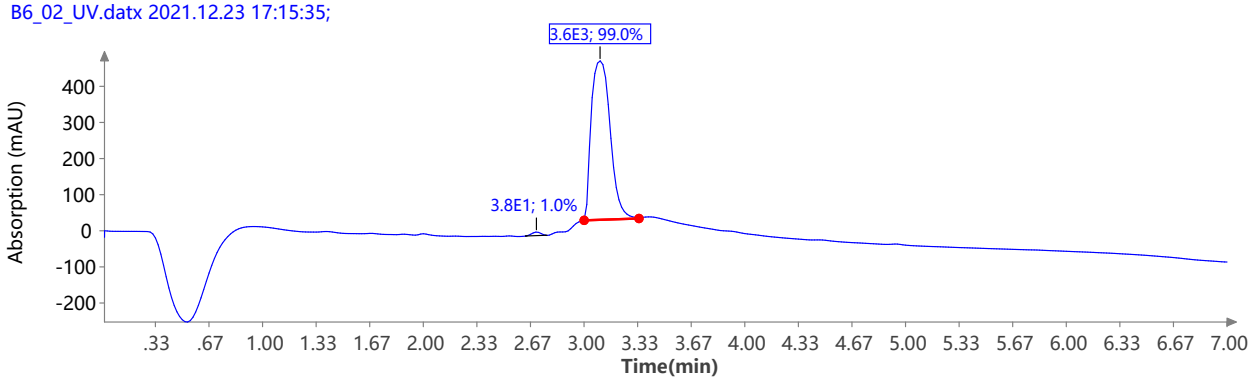

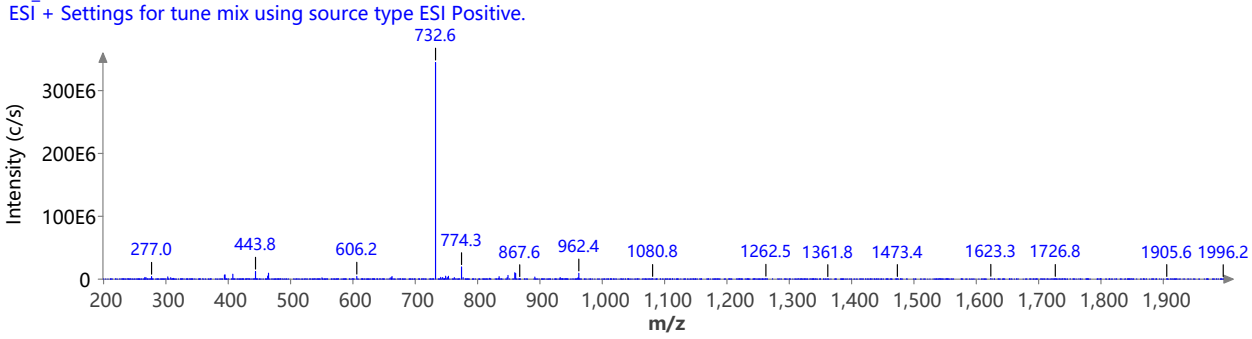

LCMS of compound **3**

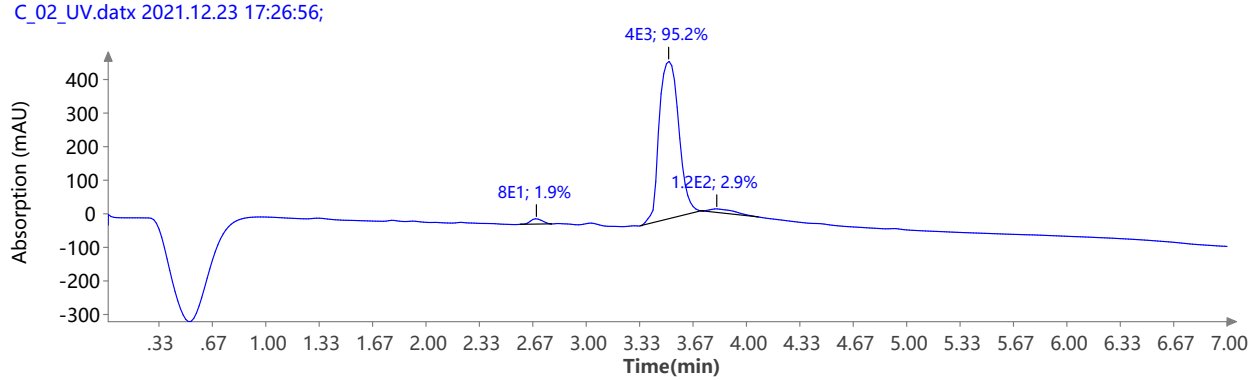

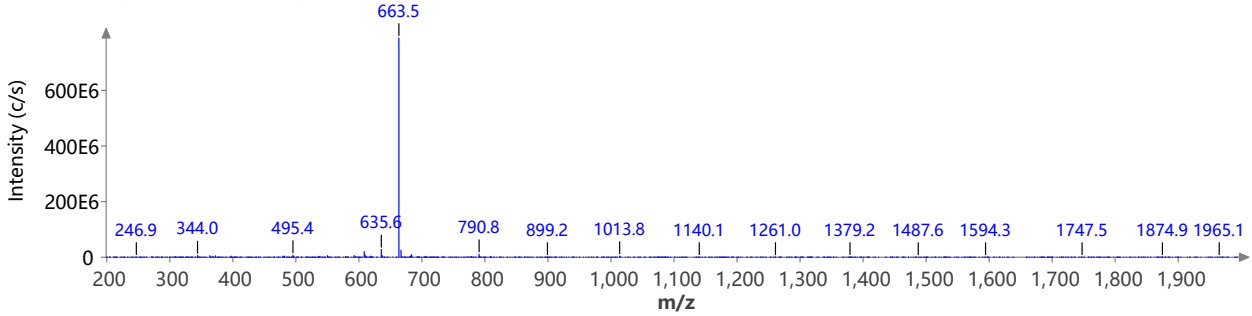

LCMS of compound **3-Pye^2**

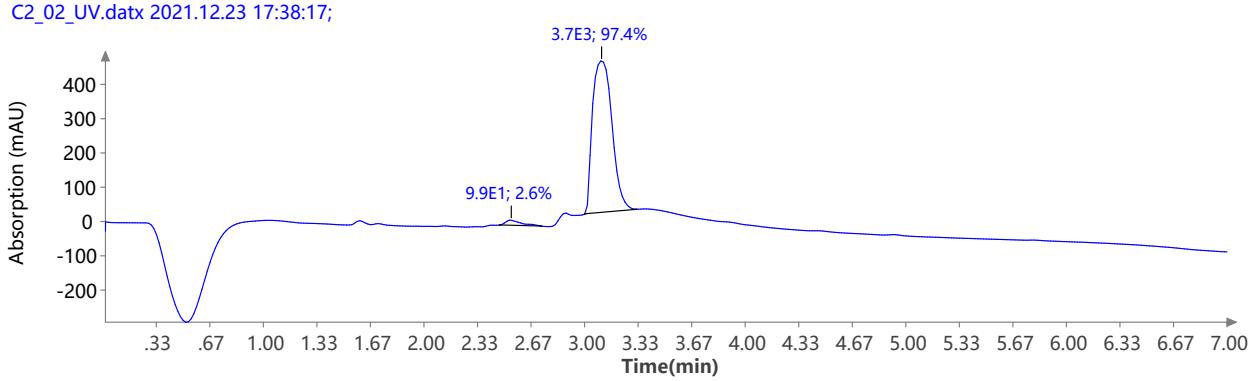

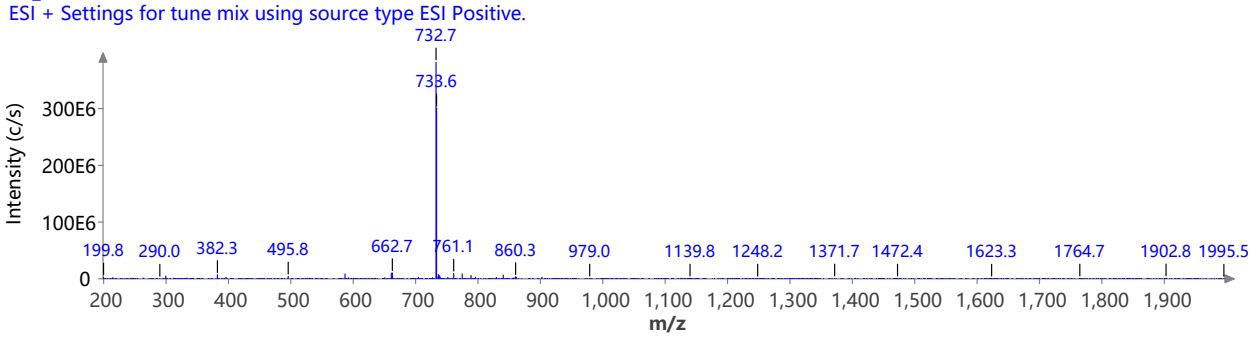

LCMS of compound **3-Pye^3**

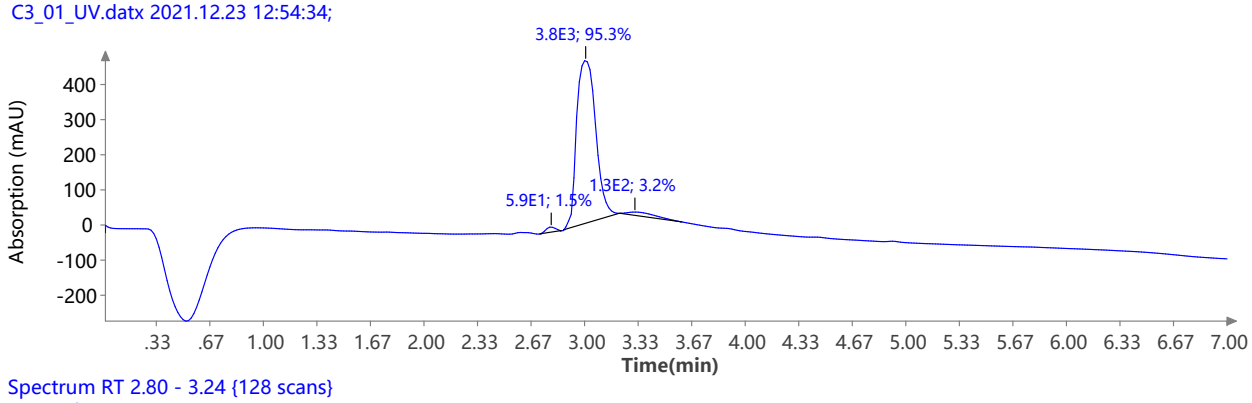

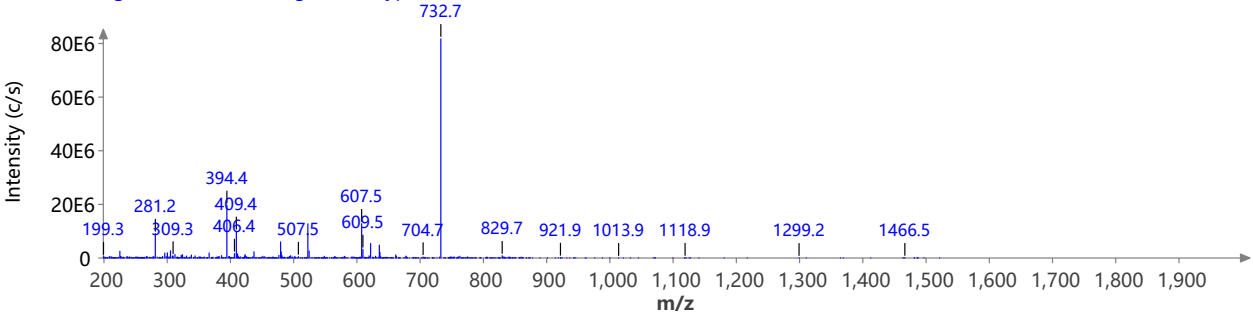

LCMS of compound **3-Pye^4**

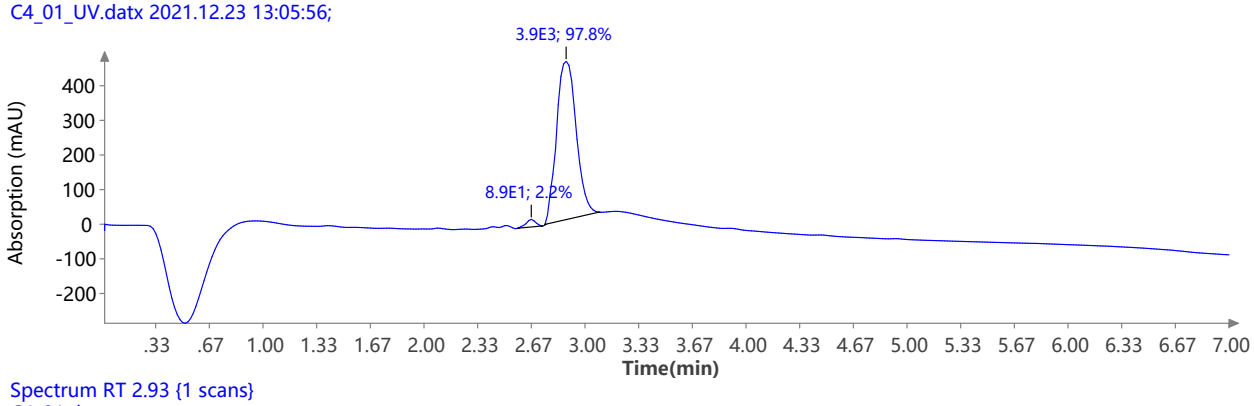

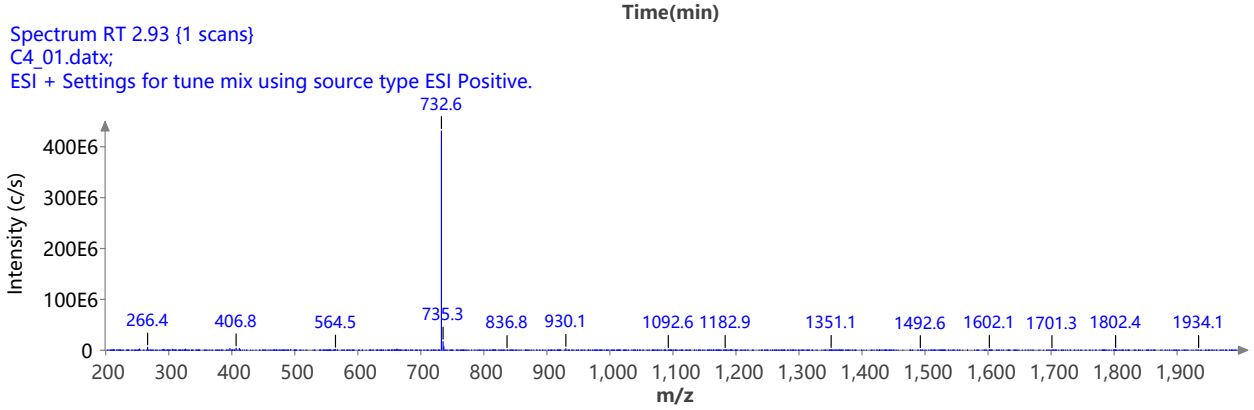

LCMS of compound **3-Pye^5**

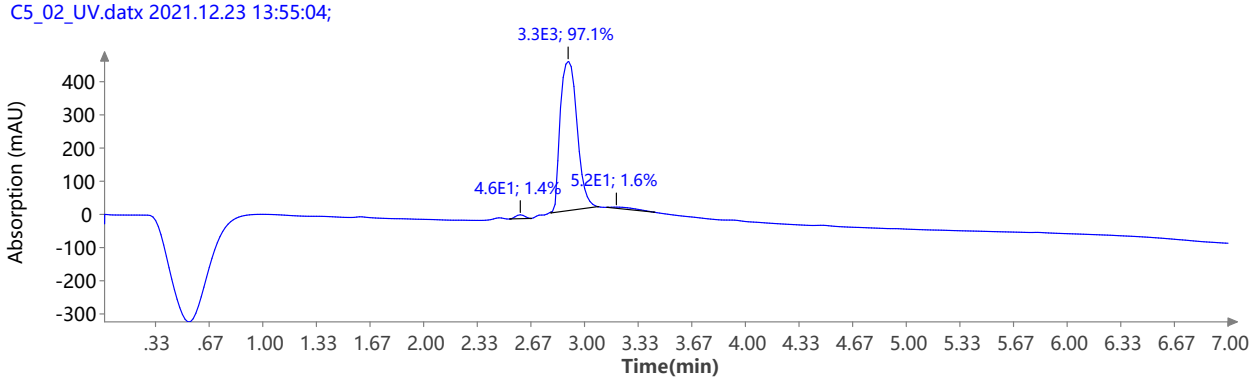

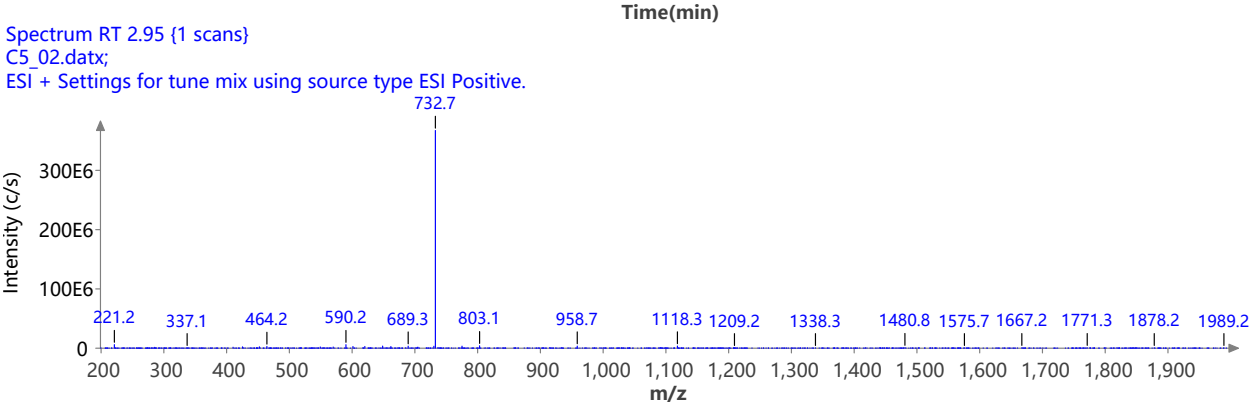

LCMS of compound **3-Pye**[6]

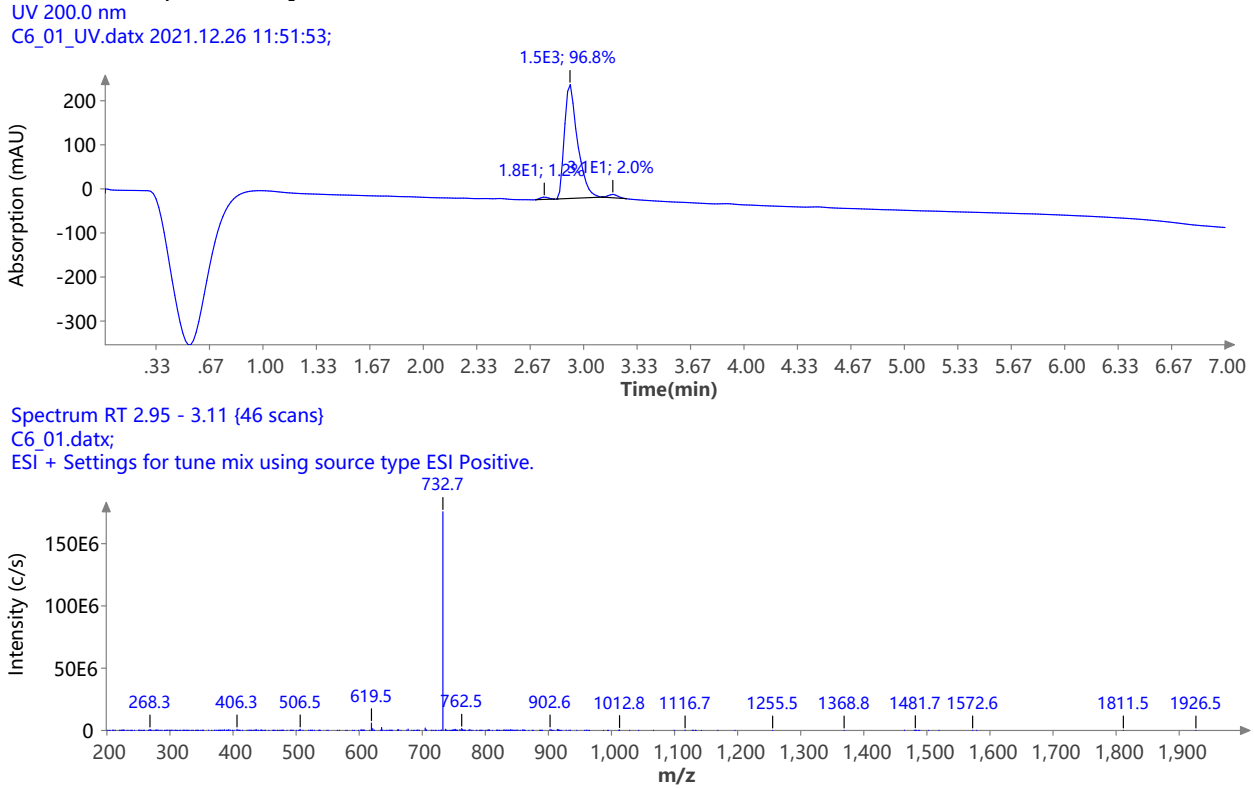

LCMS of compound **3-Glu(OMe)**[2]

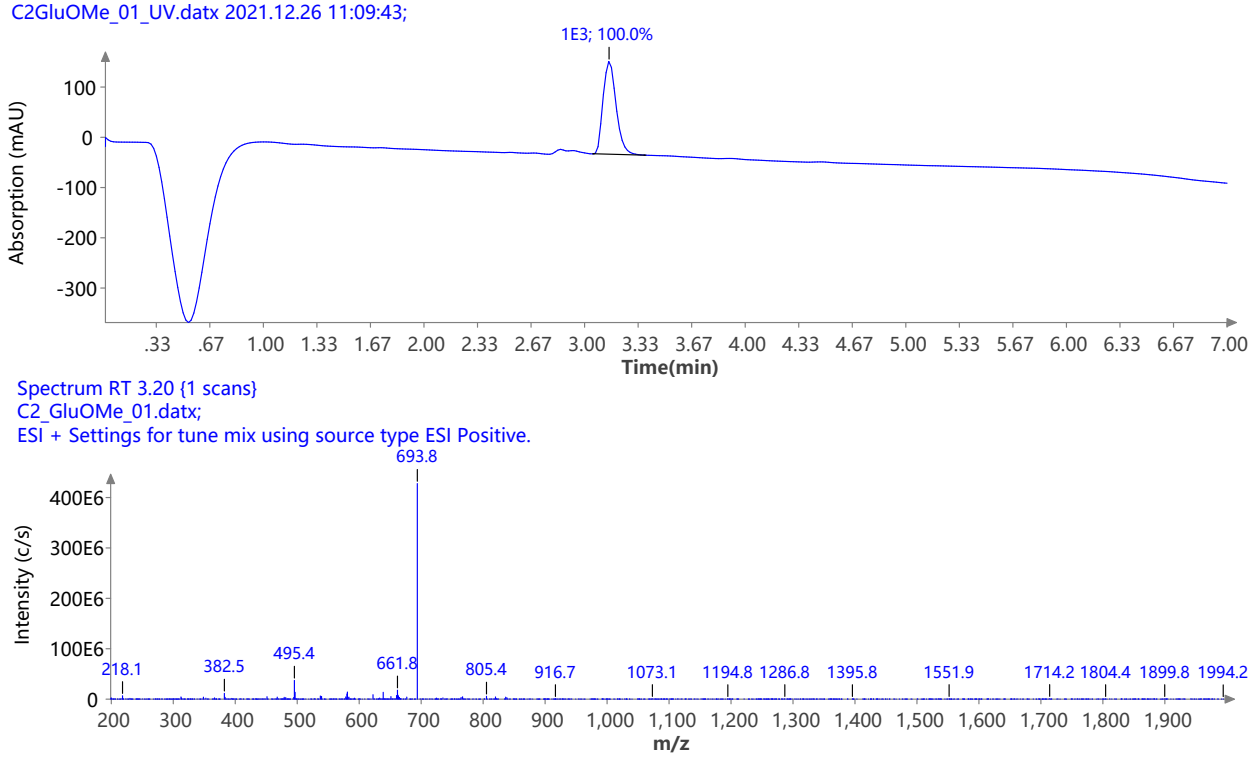

LCMS of compound **3-Gln(NMe$_2$)^2**

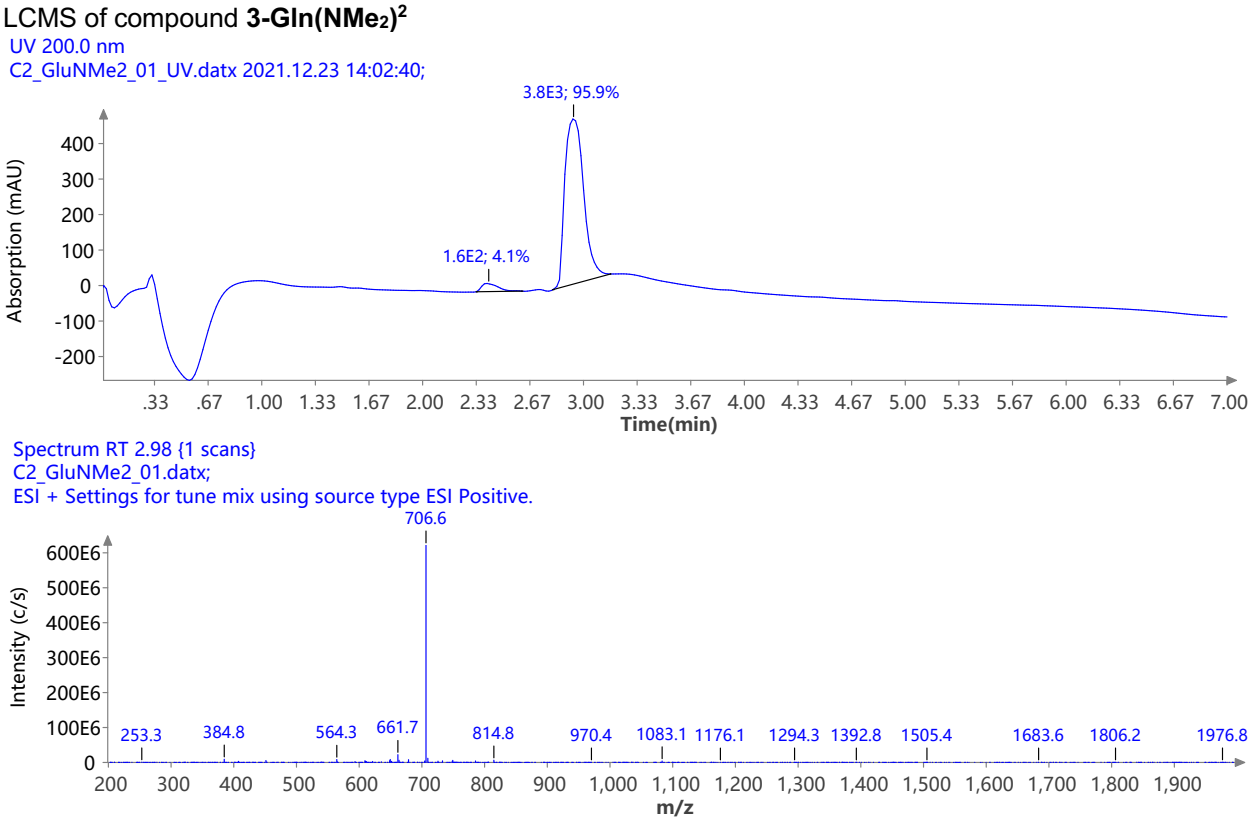

LCMS of compound **3-Asn(Pyr)^2**

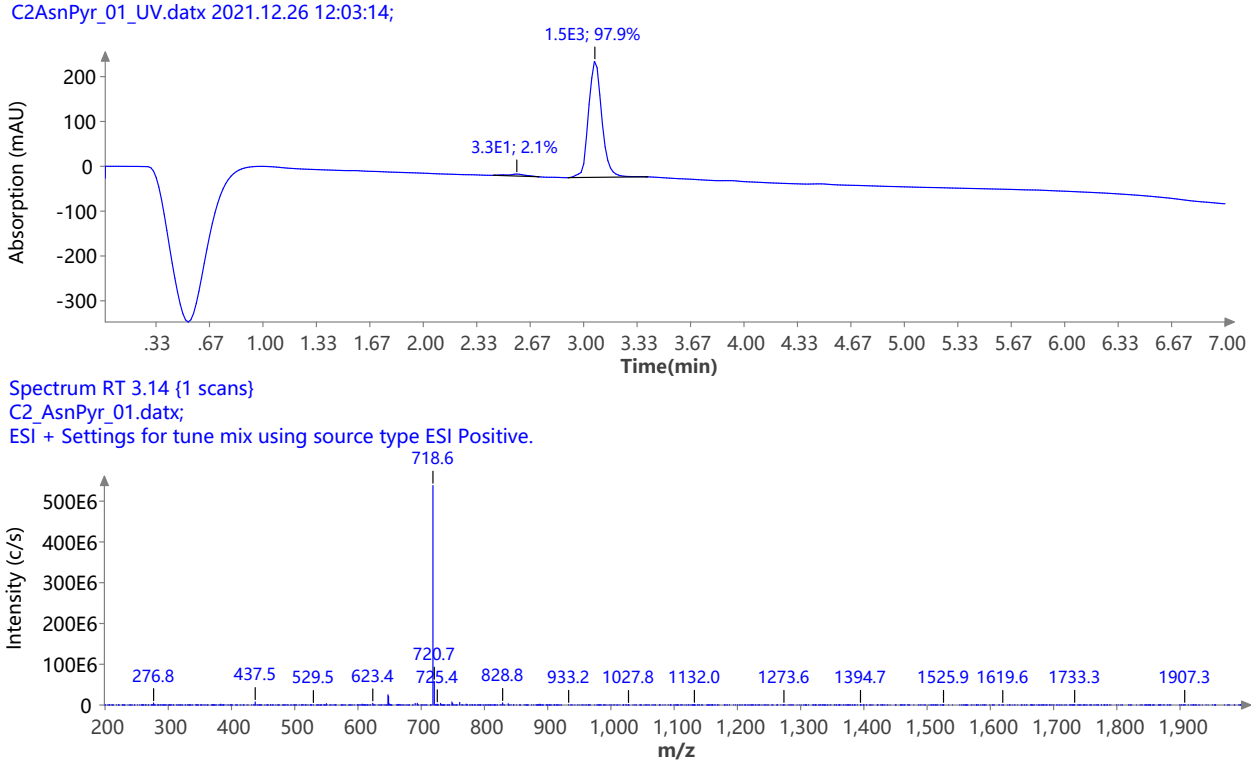

LCMS of compound **3-Asn(NMe$_2$)^2**

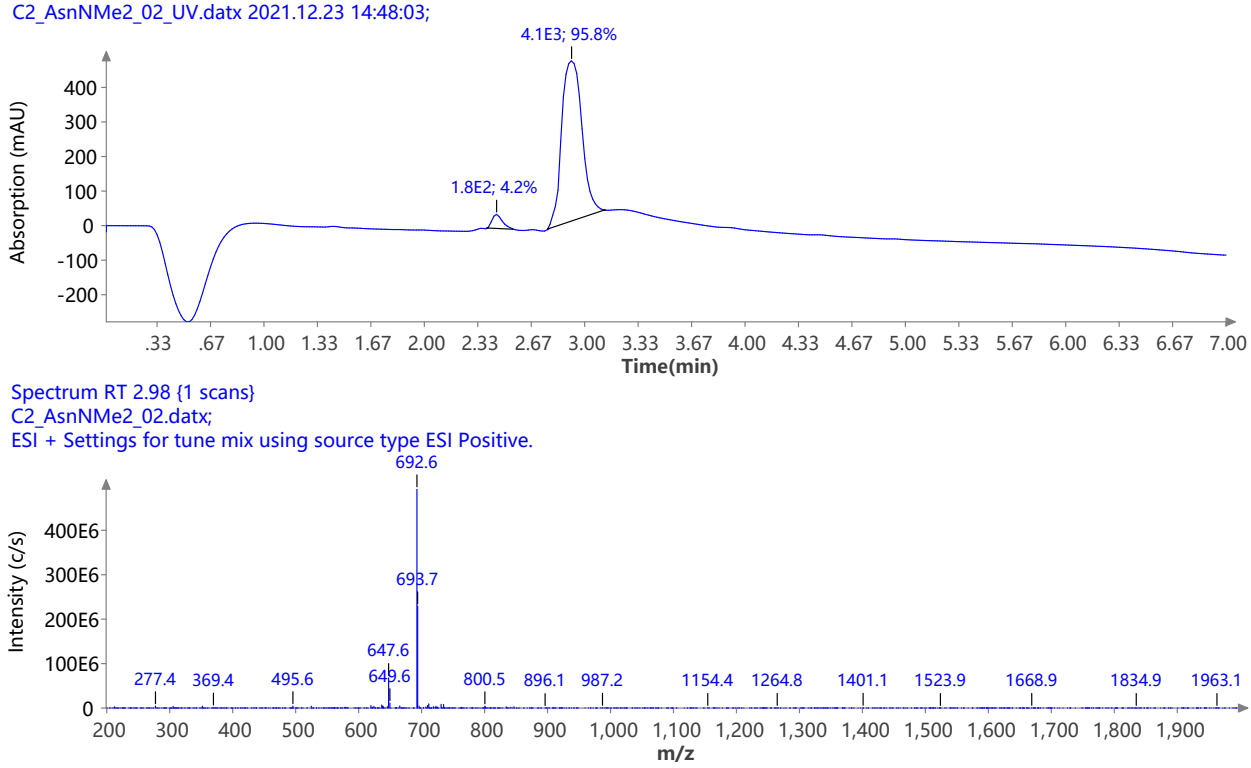

LCMS of compound **3-Pye^2(Ala^{3}Nal^5)**

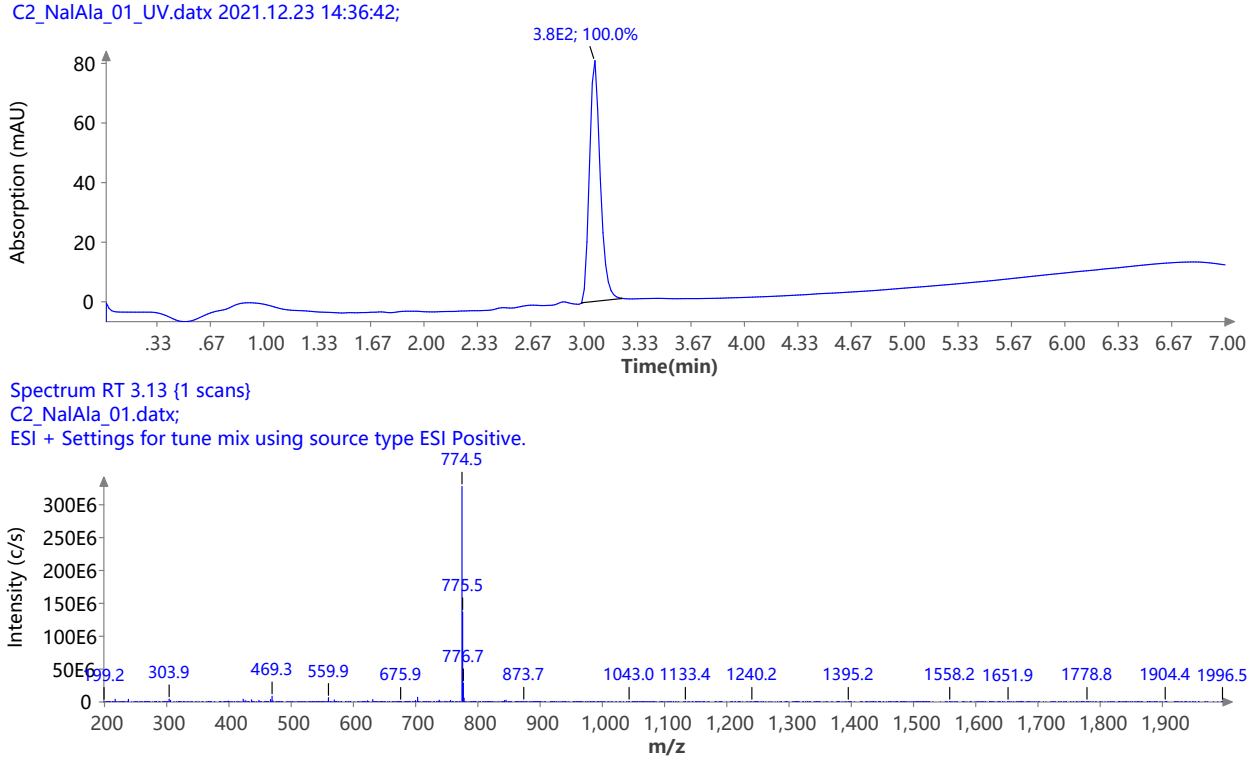

LCMS of compound **3-Pye^{2}(HPhe^{5})**

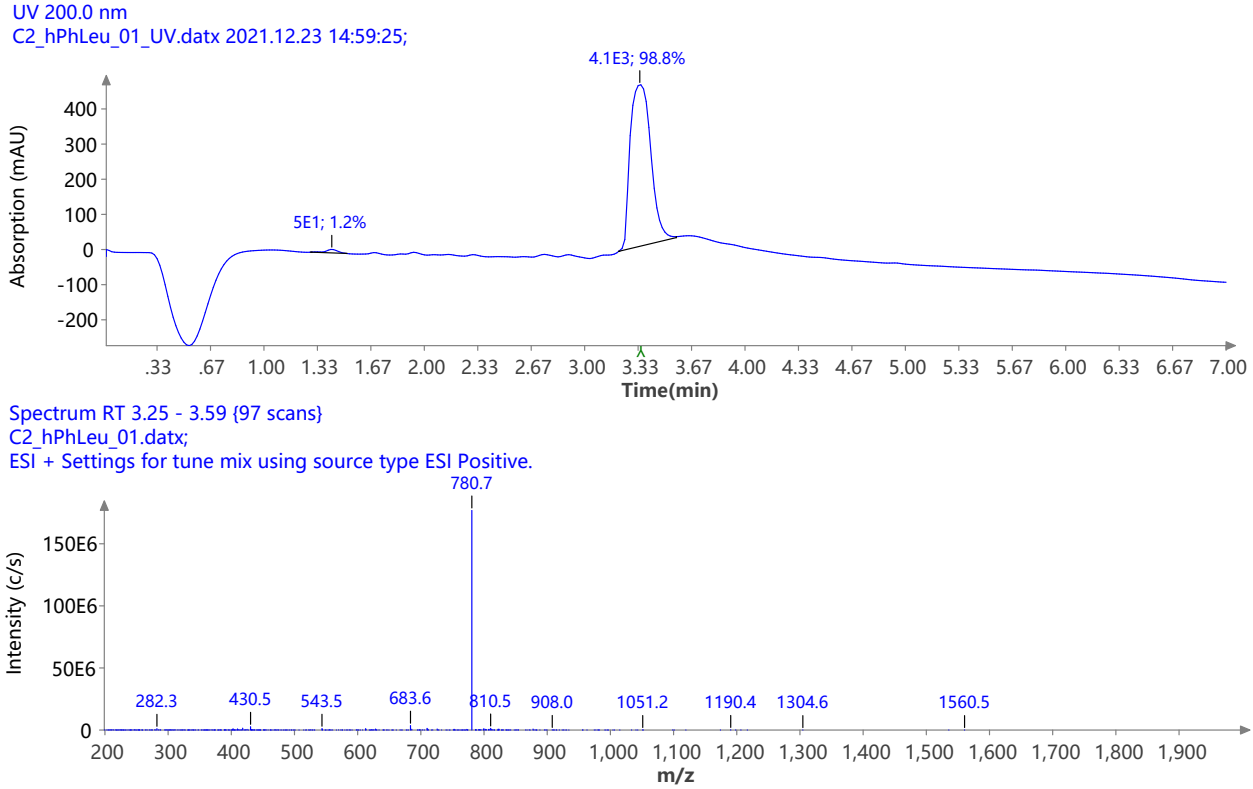

References

(1) Naylor, M. R.; Ly, A. M.; Handford, M. J.; Ramos, D. P.; Pye, C. R.; Furukawa, A.; Klein, V. G.; Noland, R. P.; Edmondson, Q.; Turmon, A. C.; Hewitt, W. M.; Schwochert, J.; Townsend, C. E.; Kelly, C. N.; Blanco, M. J.; Lokey, R. S. Lipophilic Permeability Efficiency Reconciles the Opposing Roles of Lipophilicity in Membrane Permeability and Aqueous Solubility. *J. Med. Chem.* **2018,** *61*, 11169-11182.

(2) Esposito, G.; Pastore, A. An alternative method for distance evaluation from NOESY spectra. *J. Magn. Reson. (1969)* **1988,** *76*, 331-336.

(3) Hu, H.; Krishnamurthy, K. Revisiting the initial rate approximation in kinetic NOE measurements. *J. Magn. Reson.* **2006,** *182*, 173-177.

(4) Butts, C. P.; Jones, C. R.; Towers, E. C.; Flynn, J. L.; Appleby, L.; Barron, N. J. Interproton distance determinations by NOE – surprising accuracy and precision in a rigid organic molecule. *Org. Biomol. Chem.* **2011,** *9*, 177-184.

(5) Begnini, F.; Poongavanam, V.; Atilaw, Y.; Erdelyi, M.; Schiesser, S.; Kihlberg, J. Cell Permeability of Isomeric Macrocycles: Predictions and NMR Studies. *ACS Med. Chem. Lett.* **2021,** *12*, 983-990.

(6) Rigaku Oxford Diffraction, CrysAlisPro software system, Rigaku Corporation, Wroclaw, Poland. **2020**.

(7) Sheldrick, G. SHELXT - Integrated space-group and crystal-structure determination. *Acta Crystallogr. A* **2015,** *71*, 3-8.

(8) Sheldrick, G. Crystal structure refinement with SHELXL. *Acta Crystallogr. C* **2015,** *71*, 3-8.

(9) Müller, P. Practical suggestions for better crystal structures. *Crystallogr. Rev.* **2009,** *15*, 57-83.